APPLIED COMPUTATIONAL ELECTROMAGNETICS SOCIETY (ACES)

NEWSLETTER

Vol. 16 No. 2

July 2001

TABLE OF CONTENTS

ACES NEWSLETTER STAFF

EDITOR-IN-CHIEF, NEWSLETTER
Bruce Archambeault
IBM
3039 Cornwallis Road, PO Box 12195
Dept. 18DA B306
Research Triangle Park, NC 27709
Phone: 919-486-0120
email:barch@us.ibm.com

ASSOCIATE EDITOR-IN-CHIEF
Ray Perez
Martin Marietta Astronautics
MS 58700, PO Box 179
Denver, CO 80201, U.S.A
Phone: 303-977-5845
Fax: 303-971-4306
email:ray.j.perez@lmco.com

EDITOR-IN-CHIEF, PUBLICATIONS
Andrew Peterson
Georgia Institute of Technology, ECE
777 Atlantic Drive
Atlanta, GA 30332-0250
Phone: 404-894-4697
Fax: 404-904-5935
email:peterson@ee.gatech.edu

MANAGING EDITOR
Richard W. Adler
Pat Adler, Production Assistant
Naval Postgraduate School/ECE Department
Code ECAB, 833 Dyer Road, Room 437
Monterey, CA 93943-5121, U.S.A.
Phone: 831-646-1111
Fax: 831-649-0300
email:rwa@attglobal.net

EDITORS

CEM NEWS FROM EUROPE
Pat R. Foster
Microwaves and Antenna Systems
16 Peachfield Road
Great Malvern, Worc, UK WR14 4AP
Phone: +44 1684 5744057
Fax: +44 1684 573509
email:prf@maasas1.demon.co.uk

MODELER'S NOTES
Gerald Burke
Lawrence Livermore National Labs.
Box 5504/L-156
Livermore, CA 94550, U.S.A.
Phone: (510) 422-8414
Fax: (510) 422-3013
email:burke2@llnl.gov

TECHNICAL FEATURE ARTICLE
Andy Drozd
ANDRO Consulting Services
PO Box 543
Rome, NY 13442-0543 U.S.A.
phone: (315) 337-4396
Fax: (314) 337-4396
email:andro1@aol.com

PERSPECTIVES IN CEM
Manos M. Tentzeris
Georgia Institute of Technology
ECE Dept.
Atlanta, GA 30332-0250
Phone: (404) 385-0378
email:eentze@ece.gatech.edu

THE PRACTICAL CEMIST
W. Perry Wheless, Jr.
University of Alabama
P.O. Box 11134
Tuscaloosa, AL 35486-3008, U.S.A.
Phone: (205) 348-1757
Fax: (205) 348-6959
email:wwheless@ua1vm.ua.edu

TUTORIAL
J. Alan Roden
IBM Microelectronics
Dept. OSXA
3039 Cornwallis Road
Research Triangle Park, NC 27709
Phone: (919) 543-8645
email:jaroden@us.ibm.com

ACES JOURNAL

EDITOR-IN-CHIEF
Ahmed Kishk
EE Department
University of Mississippi
University, MS 38677 U.S.A.University,
Phone: (662) 232-5385
Fax: (662) 232-7231
email:ahmed@olemiss.edu

ASSOCIATE EDITOR-IN-CHIEF
Allen Glisson
EE Department
University of Mississippi
MS 38677 U.S.A.
Phone: (662) 232-5353
Phone: (662) 232-7231
email:aglisson@olemiss.edu

NEWSLETTER ARTICLES AND VOLUNTEERS WELCOME

The ACES Newsletter is always looking for articles, letters, and short communications of interest to ACES members. All individuals are encouraged to write, suggest, or solicit articles either on a one-time or continuing basis. Please contact a Newsletter Editor.

AUTHORSHIP AND BERNE COPYRIGHT CONVENTION

President's Post

First, on behalf of the entire ACES membership, I wish to publicly thank Bruce Archambeault, Tony Brown, and Eric Michielssen for their three years of dedicated service to ACES, March 1998 – March 2001, as members of the Board of Directors. Bruce was just elected to a second term, and is presently serving as both the Society's Secretary and Editor-in-Chief of the *ACES Newsletter*. Ray Perez and Andrzej Krawczyk of Poland were also elected as Directors, and we welcome them to the BoD. Similarly, ACES extends its gratitude and congratulations to Ahmed Kishk and Allen Glisson for their efforts and successes as Editors-in-Chief for the *ACES Journal*, a privilege and responsibility that has now passed to Atef Elsherbeni. Atef is committed to solidifying the ACES move to electronic manuscript processing for the conference, *Newsletter*, and *Journal*. Please welcome Atef, and give him your active support in his initiatives. Last on this thank-you list, but first in our hearts, are the many who worked with Leo Kempel to produce an excellent **ACES 2001** conference!

>>> 2002 Conference Alert <<<

In the immortal words of Yogi Berra, "When you come to a fork in the road, take it!"

Ross Speciale (rspeciale@socal.rr.com) is Conference Chair for **ACES 2002**. I am pleased that Ross accepted this position, not only because he is exceptionally capable, but also because he is uniquely qualified to blend new technical session topics and content judiciously with historical ACES focus areas and priorities. One may rightfully argue that the conference content in recent years has been slowly drifting toward domination by academics (myself included), and we need to recognize that the work environment and influences in academia can inflict subconscious myopia on their professors/victims. The future health and vitality of the ACES conference depend upon refreshment and nourishment from CEM views and priorities of emerging importance outside academia, where the CEM "action" is often different and on a faster track to the future.

IEEE is an excellent organization, and most ACES members are also members of IEEE. When it comes to the fine specialization of applied computational electromagnetics, however, there remains the need for an alternative outlet for dissemination of significant and interesting technical information through conferences, short courses, and publications. ACES has a proud history of serving as a worthy, influential, and needed alternative. If ACES evolves toward becoming a "junior IEEE," neither organization is well served. It is incumbent upon ACES members to reflect on the differences, and contribute to strengthening the distinctive features that ACES can offer in the coming years. If we render to ACES our "coins" (i.e., the fruits of our labor) that fit ACES, the society will remain vibrant and progressively improve.

The punch line is ... if you wish to organize a session or short course on a subject that has been missing from our conference lineup in recent years, please contact Ross and make your desires known. I expect that he will find a way to put you to work productively! Similarly, prospective paper authors with a CEM story to tell are strongly encouraged to participate in **ACES 2002**. This is especially true if you feel your paper would enhance the breadth of the conference – consider **ACES 2002** as an old-fashioned "tent revival" opportunity! May we use this year well and to our advantage, embracing changes for the better. Further, may **ACES 2002** serve to invigorate and arouse new interest among our far-flung CEM colleagues in the military, government agencies, national laboratories, and private sector.

Perry Wheless
ACES President
25 May 2001

SECRETARY'S REPORT

ACES BOARD OF DIRECTOR'S MEETING MINUTES

The Applied Computational Electromagnetics Society's Board of Directors held its annual symposium business meeting 19 March 2001 at 1730, in 101A Spanagel Hall, Naval Postgraduate School. The meeting was called to order by President W. Perry Wheless, Jr.

Attendees were: W. Perry Wheless, Jr., Andrew Peterson, Bruce Archambeault, Ross Speciale, Leo Kempel, Dick Adler, Pat Adler, Atef Elsherbeni, Allen Glisson, Ahmed Kishk, Tapan Sarkar, Masanori Koshiba, Osama Mohammed, and Keith Lysiak.

Tapan Sarkar made a motion to accept the minutes of the fall 2000 ACES Board of Directors telecom meeting. The motion was seconded by Allen Glisson. Motion passed with all in favor.

Perry announced the winners of the recent BoD membership election. The three new BoD members elected for a three year term were: Ray Perez with 83 votes, Bruce Archambeault with 81 votes, and Andrzej Krawczyk with 56 votes.

Perry pointed out that after the recent election changes approved by the BoD, the nominations for the next year's election to the BoD will close on 1 May 2001. BoD member terms that will expire in March 2002 are Allen Glisson, Giuseppe Pelosi, and Perry Wheless.

Perry reported that Ping Werner wished to give up being the Elections committee chairperson, and recommended Rene Allard as her replacement. Perry approved the change.

Dick Adler presented the financial report. He discussed the difficulty he had converting from an old DOS-based version of Quicken to a newer version of Quicken. He believes the data transfer errors have all been found and corrected. Dick also presented a set of budget projections and reviewed the yearly expenses break out. Tapan Sarkar made a motion to accept the financial report. The motion was seconded by Allen Glisson. Motion passed with all in favor.

A discussion followed concerning reducing the ACES membership dues by $5.00. Tapan Sarkar made a motion to reduce the membership dues by $5.00. The motion was seconded by Allen Glisson with all in favor.

Perry discussed the need to have more members, and asked Tapan Sarkar, Masanori Koshiba, and Giuseppe Pelosi to make a plan to help make the ACES society better known, including an advertisement in the APS magazine.

Leo Kempel reported on the ACES 2001 Conference.
-- The total number of papers was slightly down to +/- 100.
-- About 150 people had registered so far, but the conference was not due to start until the following day.
-- He noted that the student papers were handled differently this year. All 10 were in one session, with no parallel sessions. Perry, Osama and Tapan were the judges for this year.
-- There were five vendors for Tuesday's vendor session.
-- There were 15 short courses in March 2000 with 4-5 cancelled. The number of days for short courses was reduced from three last year to two this year, and there were 10 scheduled. Two had been cancelled so far (on Monday). Which courses to offer was decided by a survey on the web site. The survey had 77 responses.
-- He made a few suggestions to Ross Speciale for next year's conference.
    -- use Co-chairs to 'ping' session chairpersons
    -- short courses which focus on broad topics seem to do best
    -- the student paper contest evaluation form should be on the web site
    -- the web site is extremely useful as a tool for the chairperson
    -- PDF files are not all the same, and more care is needed to make sure they include fonts and are useable. A pdf options file should be required
    -- there needs to be more quality control in the format of the papers
    -- should have a dedicated fax machine for copyright forms

Perry introduced Ross Speciale as the ACES 2002 Conference Chairman. Tapan Sarkar made a motion to appropriate $3000 for 2002 conference chairman expenses. The motion was seconded by Allen Glisson. Motion passed with all in favor.

Andy Peterson reported on the Publications Committee. Atef Elsherbeni is the new editor of the ACES Journal, and Bruce Archambeault is the new editor of the ACES Newsletter. It was noted that Ray Perez's many years as Newsletter editor was greatly appreciated, as well as Allen Glisson's and Ahmed Kishk's many years as Journal editors were greatly appreciated.

Andy noted that the November issue of the Journal was currently short on papers, but there was sufficient time yet (deadline is 1 September).

Electronic publication of the Newsletter was deferred to the fall BoD meeting telecon. Bruce Archambeault, Dick Adler and Atef Elsherbeni will try to have things worked out for this discussion. The need for QA was mentioned again.

Atef Elsherbeni reported on the ACES web page status. All agreed it was outstanding! Atef requested $9298 for the next year's web work. Tapan Sarkar made a motion to allocate the $9298 for the ACES web site improvements. The motion was seconded by Allen Glisson. Motion passed with all in favor.

The software exchange agenda item was withdrawn. The company making the original proposal is having difficulty with some processors made in third world countries.

Tapan Sarkar made a motion to allocate the funds necessary to pay for the publications committee and BoD dinners. The motion was seconded by Allen Glisson. Motion passed with all in favor.

Osama gave a demonstration of web based courses at Florida International University. Some discussion about using this type of seminar for ACES Conference short courses was held, and the subject is tabled for future discussion.

The meeting was adjourned at 1945.

Respectfully submitted by Bruce Archambeault

ACES UK CHAPTER ANNUAL REPORT, MARCH 2001

The UK Chapter has held steady this year with 15 corporate and 8 individual members. Financially it is very stable, maintaining its non-profit-making status to the benefit of members.

The one-day meeting on December 20th, 2000, attracted around 30 attendees. The morning session consisted of an FDTD-based talk from Melinda Picket-May, from the University of Colorado. The approach was delightfully refreshing with strong emphasis on educational issues, such as an open-ended approach to problem-solving. The most recent developments in ADI were contrasted with pseudo spectral methods, and many enlightening applications were shown, mostly in the field of IC packaging and multi-layer board stray coupling. As usual, this was followed by a wide-ranging set of members papers in the afternoon. The arrangements, provided by our hosts at Imperial College were splendid, as usual.

The ACES UK web site, hosted at Imperial College may be accessed at
http://www.me.ic.ac.uk/mechanical/.

C D Sillence,
ACES UK Chairman

PERMANENT STANDING COMMITTEES OF ACES INC.

COMMITTEE	CHAIRMAN	ADDRESS
NOMINATIONS	Adalbert Konrad	University of Toronto ECE Department 10 King's College Road Toronto, ON, CANADA M5S 1A4
ELECTIONS	Rene Allard	Penn State University PO Box 30 State College, PA 16804-0030
FINANCE	Melinda Piket-May	University of Colorado/Boulder Engineer Circle Boulder, CO 80309-0425
PUBLICATIONS	Andrew Peterson	Georgia Institute of Technology School of ECE Atlanta, GA 30332-0250
CONFERENCE	Doug Werner	Penn State University 211A EE East University Park, PA 16802
AWARDS	Pat Foster	MAAS 16 Peachfield Road Great Malvern, UK WR14 4AP

MEMBERSHIP ACTIVITY COMMITTEES OF ACES INC.

COMMITTEE	CHAIRMAN	ADDRESS
SOFTWARE VALIDATION	Bruce Archambeault	IBM 158 Lin Tilley Road Durham, NC 27712
HISTORICAL	Robert Bevensee	BOMA Enterprises PO Box 812 Alamo, CA 94507-0812

JOINT NOMINATIONS and ELECTIONS COMMITTEE REPORT

Adalbert Konrad, Nominations Chair, konrad@power.ele.utoronto.ca
Ping Werner, Elections Chair, plw7@psu.edu

ACES has nine directors, elected by the membership to a three-year term of office. The terms are staggered, with three expiring each year. Three new Directors are elected annually, and installed in office at the annual ACES conference in Monterey.

On 17 January 2001, the ACES Board of Directors voted to approved proposed changes in our annual election process. This report will serve as the required notification to the membership of these changes. A list of the changes, which was made effective immediately by the majority vote of the Board of Directors, follows:

1. The annual closing date for nominations will be May 1.
2. Candidate statements must be submitted by May 25 to ensure inclusion in the July Newsletter.
3. Ballots will be mailed in July. **Ballots will refer to the ACES Newsletter** for candidate statements. Candidate statements will appear in the July ACES Newsletter, regardless of whether the Newsletter is distributed in hardcopy or electronically in the future.
4. The deadline for the return of ballots will be August 31.
5. The votes will be counted by September 15, and announcements of the winners will appear in the next issue (nominally November) of the ACES Newsletter.
6. The three newly elected Directors will be installed in office at the next Annual Meeting of Members, which occurs at the annual conference.

Among other benefits, these changes will allow incoming new Directors to participate in the Fall Board of Directors meeting, which has been occurring recently in October by telephone conference call. Although they will not be voting members at that time, their participation should be informative and useful to them when they actively begin their three-year term.

2002 ELECTION FOR ACES BOARD OF DIRECTORS

CANDIDATES' STATEMENTS

GENERAL BACKGROUND

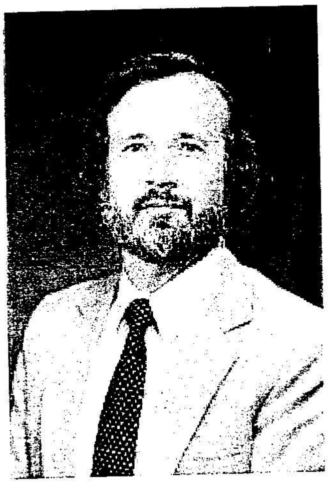

ALLEN W. GLISSON, Jr. received the B.S., M.S., and Ph.D. degrees in electrical engineering from the University of Mississippi, in 1973, 1975, and 1978, respectively. In 1978, he joined the faculty of the University of Mississippi, where he is currently Professor of Electrical Engineering. He was selected as the Outstanding Engineering Faculty Member in 1986 and again in 1996. He received a Ralph R. Teetor Educational Award in 1989. His current research interests include the development and application of numerical techniques for treating electromagnetic radiation and scattering problems, and modeling of dielectric resonators and dielectric resonator antennas. Dr. Glisson has been actively involved in the areas of numerical modeling of arbitrarily shaped bodies and bodies of revolution with surface integral equation formulations. He has also served as a consultant to several different industrial organizations in the area of numerical modeling in electromagnetics.

Dr. Glisson is a member of the Sigma Xi Research Society and the Honor Societies Tau Beta Pi, Phi Kappa Phi, and Eta Kappa Nu. He is a Senior Member of the IEEE and is a member of several professional societies within the IEEE, a member of Commission B of the International Union of Radio Science, and a member of the Applied Computational Electromagnetics Society. He was a U.S. delegate to the 22nd, 23rd, and 24th General Assemblies of URSI. Dr. Glisson has received a best paper award from the SUMMA Foundation and twice received a citation for excellence in refereeing from the American Geophysical Union. Since 1984, he has served as the Associate Editor for Book Reviews and Abstracts for the *IEEE Antennas and Propagation Society Magazine*. He is currently a member of the IEEE Antennas and Propagation Society Administrative Committee and IEEE Press Liaison Committee. He is also currently Co-Editor-in-Chief of the *Applied Computational Electromagnetics Society Journal* and serves on the Board of Directors of the Applied Computational Electromagnetics Society. Dr. Glisson has also served as an Associate Editor for *Radio Science* and as the secretary of Commission B of the U.S. National Committee of URSI, and he is the incoming Editor-in-Chief of the *IEEE Transactions on Antennas and Propagation*.

PAST SERVICE TO ACES

Dr. Glisson has been a member of ACES for many years and has attended numerous ACES conferences, presenting papers and chairing sessions. He has published several papers in the ACES Journal and contributed to the first ACES collection of canonical problems. He has also served as guest co-editor of a special issue of the ACES Journal. He currently serves on the Board of Directors of ACES, is the Treasurer of the Society, and is Co-Editor-in-Chief of the *ACES Journal.*

CANDIDATE'S PLATFORM

The use of computational electromagnetics has expanded dramatically since the founding of ACES. The scope of ACES has likewise expanded from a largely method of moments and NEC emphasis to include a wide variety of techniques for the solution of electromagnetics problems. ACES must continue to support the use of various computational methods and to encourage a dialogue between users of these methods. ACES must also continue to stress the importance providing useful information to potential users of computational electromagnetic tools, including information on the expected accuracy of the tools and validation information. Finally, while the emphasis of ACES is 'applied' computational electromagnetics, ACES must strive to maintain a healthy balance that includes some theoretical aspects of the use and development of the various computational tools.

GENERAL BACKGROUND

JIN-FA LEE has received the B.S. degree from National Taiwan University, in 1982 and the M.S. and Ph.D. degrees from Carnegie-Mellon University in 1986 and 1989, respectively, all in electrical engineering. From 1988 to 1990, he was with ANSOFT Corp., where he developed several CAD/CAE finite element programs for modeling three-dimensional microwave and millimeter-wave circuits. His Ph.D studies resulted in the first commercial three-dimensional FEM package for modeling RF/Microwave components, HFSS. From 1990 to 1991, he was a post-doctoral fellow at the University of Illinois at Urbana-Champaign. From 1991 to 2000, he was with the Department of Electrical and Computer Engineering, Worcester Polytechnic Institute. Currently, he is an Associate Professor with the Department of Electrical Engineering, ElectroScience Lab, The Ohio State University.

He was a Co-Chair for the 1996 ACES meeting, and the secretary for the 5th FEM Workshop for Microwave Engineering. He was a guest editor for a special session for CMAME on Computational Electromagnetics, a guest editor for a special issue of *Electromagnetics*, and a guest editor for an upcoming special issue of the *ACES Journal.* He has taught short courses for the APS/URSI Symposium, PIERS conferences and the ACES meeting on PDE-related topics. He has served on the editorial boards of the *IEEE Transactions on Microwave Theory and Techniques*, the Biennial IEEE Conference on Electromagnetic Field Computation (CEFC) and the Compumag conferences. He is currently a member of IEEE and SIAM and an associate member of URSI.

PAST SERVICE TO ACES

The candidate was Co-Chair for the 1996 ACES meeting. He organized and taught short courses and organized and chaired many sessions for ACES meetings over the years. He has written a tutorial paper on vector finite element methods for the ACES Newsletter, and is a guest editor for an upcoming special issue of the ACES Journal.

CANDIDATE'S PLATFORM

Entering the 21st century, great challenges and opportunities lie ahead for Computational Electromagnetics (CEM). Many breakthroughs and technologies developed over the past few decades have made it possible for us to solve a variety of electromagnetic problems more efficiently and accurately. However, there are still major technical issues remaining and new difficulties surface when we expand the capabilities of CEM. To properly address and consequently circumvent these difficulties, I believe, requires close and frequent collaboration between engineering and mathematical communities. Furthermore, traditional CEM research work has focused almost entirely on formulation, mathematical modeling, and solving the resulting matrix equations or the time domain marching equations. Little attention has been paid to the development of Computer Graphics, Computational Geometry, Advanced Graphical User Interfaces (GUIs), and Preand Post Processings that are integral parts of solving the electromagnetic problems using numerical methods. As we move into the era of using computer simulation tools to synthesize electromagnetic devices, these subjects, I believe, will take on the center stage.

I believe that ACES is in a unique position to advance the research and development of CEMs to analyze and design electromagnetic devices and electronics. As a Board member of ACES, I will promote activities that bridge the gap between engineering and mathematical communities, and stimulate interests in non-traditional CEM subjects that are necessary in a complete electromagnetic CAD/CAE tool.

OTHER UNIQUE QUALIFICATIONS

I was one of the first software developers to make the first commercial finite element package to solve electromagnetic problems. The company, Ansoft, has now evolved into one of the most successful CAD/CAE software company in providing electromagnetic solutions to industries. Being involved with the software development from top to bottom puts me in a unique position to gear research activities in the ACES community toward developing and enhancing real-life and versatile electromagnetic CAD tools.

GENERAL BACKGROUND

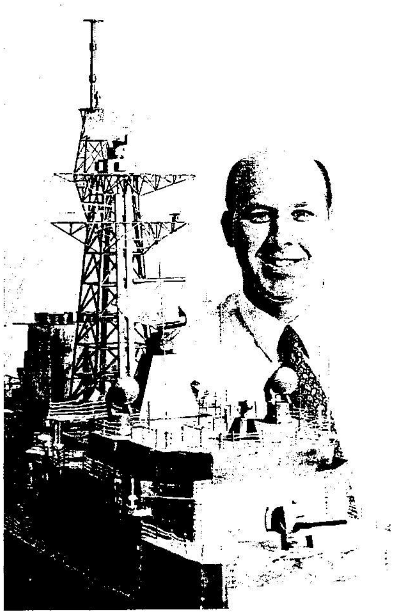

KEITH LYSIAK has earned a bachelors degree in electrical engineering (B.S.E.E) from The Ohio University in 1983, a masters degree in electrical engineering (M.S.E.E) from The Johns Hopkins University in 1989, and a doctorate in electrical engineering (Ph.D.) from The Pennsylvania State University in 1995. Both under-graduate and graduate studies concentrated in the area of electromagnetics with his doctorate thesis focused on a 2D hybrid method of moments / finite difference time domain approach to very accurate propagation over terrain.

Keith joined the U.S. Air Force as an enlisted member in 1980 and began his military career with the Strategic Air Command in flightline maintenance of communication, navigation, and electronic countermeasure systems on FB-111 fighter/bomber aircraft. He earned his undergraduate degree through the Airman's Education and Commissioning Program and became a commissioned officer in 1986. He spent three years in the Electronic Security Command at Ft. Meade where he performed research on High Frequency Direction Finding systems. He earned his masters degree during this assignment. During this period, he began using NEC under the supervision of Dr. Herbert Kobyashi to model direction finding antenna arrays. In 1989 he was reassigned to the Strategic Air Command with 49th Test Squadron performing Follow-on Test and Evaluation on strategic weapons and worked with instrumentation on the FB-111 fighter/bomber, B1-B bomber and the B2 bomber.

Upon leaving the Air Force in 1993, Keith attended Penn State to earn his Ph.D. He studied under Dr. Raymond Luebbers and worked on a project for the USAF to validate the use of FDTD for modeling Air Force vehicles. He also studied under Dr. James Breakall and Dr. Douglas Werner on U.S. Navy projects in the area of propagation and developed a hybrid MoM/FDTD approach for propagation model validation. During his research he became proficient in the application of MoM, UTD/GTD, and FDTD. He graduated in 1996 and joined the Southwest Research Institute in San Antonio, Texas. He is a principal engineer in the Radiolocation Systems Section of the Signal Exploitation and Geolocation Division. His primary responsibility is the numerical modeling of direction finding arrays on ships, aircraft, and land-based systems to predict DF performance, design arrays and develop calibration data.

PAST SERVICE TO ACES

Keith has been a member of ACES since the 4th Annual Review of Progress in 1988. He has presented papers at the annual reviews, has chaired sessions on NEC modeling for each of the past three years and has been the Publicity Chair for the conferences for the past two years.

CANDIDATE'S PLATFORM

Keith has been an ACES member for 13 years beginning shortly after the inception of the society. He has seen the evolutionary change from a NEC working group to a prestigious, international, technical society. He sees the viability of ACES in keeping it a unique organization focused on "Applied Computational Electromagnetics" as its name states. He would like to see the Society focus on real world application with numerical results compared to established codes and measurements. He would also like to see more emphasis placed on codes and algorithm developments that are readily available and not proprietary or restricted by intellectual property.

OTHER UNIQUE QUALIFICATIONS

Keith is uniquely qualified through varied experience in computational electromagnetics in DoD, academia, and research. He has also had unique experiences using general-purpose electromagnetic codes such as MoM, FDTD, and UTD/GTD to investigate propagation and the analysis of complex direction finding systems. He has leadership experience through 14 years of military service as both an enlisted and commissioned officer.

GENERAL BACKGROUND

ERIC MICHIELSSEN received his M.S. in Electrical Engineering (Magna Cum Laude) from the Katholieke Universiteit Leuven (KUL, Belgium) in 1987, and his Ph.D. in Electrical Engineering from the University of Illinois at Urbana-Champaign (UIUC) in 1992. He served as a research and teaching assistant in the Microwaves and Lasers Laboratory at KUL and the Electromagnetic Communication Laboratory at UIUC from 1987 to 1988 and from 1988 to 1992, respectively. He joined the Faculty of the Department of Electrical and Computer Engineering at the University of Illinois as a Visiting Assistant Professor in 1992, was appointed Assistant Professor of Electrical and Computer Engineering in 1993, and promoted to Associate Professor in 1998. Since 1994, he also has held an Affiliate Position in the Beckman Institute, and since 1995 he serves as Associate Director of the Center for Computational Electromagnetics.

Eric Michielssen directs a group of ten graduate students and post-docs conducting research in the area of computational electromagnetics, in particular fast wave/Maxwell equation solvers, and the application of stochastic optimizers to electromagnetic system design. Eric Michielssen authored or co-authored over 80 papers and book chapters and over 130 papers in conference proceedings. He received a Belgian-American Educational Foundation Fellowship in 1988 and a Schlumberger Fellowship in 1990. Furthermore, he was the recipient of a 1994 Union of Radio Scientists International (URSI) Young Scientist Fellowship, a 1995 National Science Foundation CAREER Award, and the 1998 Applied Computational Electromagnetics Society (ACES) Valued Service Award. Recently, he was named 1999 URSI – United States National Committee Henry G. Booker Fellow and selected as the recipient of the 1999 URSI Koga Gold Medal. In 2001, he received a UIUC Senior Xerox Awards for Faculty Research and during 2001-2002, he will be appointed Beckman Associate in UIUC's Center for Advanced Studies. His name appeared six times on the University of Illinois' "Incomplete List of Excellent Teachers". From 1997 to 1999, he served as an Associate Editor for Radio Science, and currently he is an Associate Editor for the IEEE Transactions on Antennas and Propagation. Eric Michielssen is a Senior Member of the IEEE and a member of URSI Commission B.

PAST SERVICE TO ACES

Eric Michielssen served as the Co-Chair and Conference Proceedings Editor for the 1996 Annual Review of Progress in Computational Electromagnetics (ACES '96). He served as the Technical Chair for ACES'97. Eric Michielssen's past service to ACES also includes the organization of special sessions at the 1995, 1996, 1997, 1998 and 2001 ACES Symposia on topics ranging from electromagnetic optimization to fast solvers. Finally, from 1998 to 2001, he served on the ACES Board of Directors, in 1999 as ACES Secretary and in 2000 as ACES Vice-President.

CANDIDATE'S PLATFORM

During the past several years, the science of computational electromagnetics has been revolutionized through a series of exciting developments. A partial list of recently introduced techniques strongly biased towards my own research interests includes efficient integral and differential based Maxwell equation solvers relying on fast multipole and wavelet techniques, new boundary conditions for finite element and transient simulators, novel optimization and model reduction techniques, etc. In the past, the applicability of CEM tools has often been restricted to the analysis of electrically small subsystems. However, it is now recognized by many in the CEM community that these recent developments may eventually lead to CEM tools capable of simulating and synthesizing large-scale electromagnetic devices in a multidisciplinary design setting. These next generation CEM tools will impact disciplines ranging from antenna design, to RCS analysis, the analysis of EMC phenomena, and the design and verification of interconnect and optoelectronic systems.

ACES is in a unique position to take the lead in (i) disseminating novel scientific techniques beyond the library archives towards application oriented CEM practitioners, (ii) facilitating the incorporation of these methods into existing CEM software packages, and (iii) promulgating standards that permit cross-platform and cross-disciplinary interoperability. As an ACES Board member, I will strive to achieve these goals by organizing and promoting events that bring together CEM tool developers, users, and scientists in an effort to produce a useful and productive dialogue between these often too disjoint communities. The active dissemination of novel science relevant to the CEM practitioner can be achieved not only by encouraging the publication of in depth review articles in the ACES Journal, but also through online/CD-ROM education initiatives. The incorporation of novel techniques into available tools can be facilitated through the organization of round table discussions at ACES symposia or through on-line discussion groups. Finally, ACES stimulated cross-disciplinary involvement and collaboration will ensure the relevance of future CEM tools in a multi-disciplinary environment. As an ACES Board member, I will aggressively pursue these goals with a view to further strengthening the unique position of ACES as the facilitator of the transition of CEM tools from developers to users.

GENERAL BACKGROUND

OMAR M. RAMAHI received the BS degrees in Mathematics and Electrical and Computer Engineering from Oregon State University, Corvallis, OR in 1984. He received his M.S. and Ph.D. in Electrical and Computer Engineering in 1986 and 1990, respectively from the University of Illinois at Urbana-Champaign. From 1990-1993, Dr. Ramahi held a visiting fellowship position at the University of Illinois at Urbana-Champaign. From 1993 to 2000, he worked at Digital Equipment Corporation (presently, Compaq Computer Corporation), where he was member of the alpha server product development group. In August of 2000, he joined the faculty of the James Clark School of Engineering at the University of Maryland at College Park, where he is also a faculty member of CALCE Electronics Products and Systems Center.

Dr. Ramahi served as a consultant to several companies. He was instrumental in developing computational techniques to solve a wide range of electromagnetic radiation problems in the fields of antennas, high-speed devices and circuits and EMI/EMC. His interests include experimental and computational EMI/EMC studies, high-speed devices and interconnects, biomedical applications of electromagnetics, novel optimization techniques, interdisciplinary studies linking electromagnetic application with new materials. He has authored and co-authored over 80 journal and conference papers and presentations. He is a coauthor of the book *EMI/EMC Computational Modeling Handbook* (Kluwer Academic, 1998). Dr. Ramahi is a Senior Member of IEEE and a member of the Electromagnetics Academy.

PAST SERVICE TO ACES

The candidate's past service to ACES includes presentation of papers, organization of special sessions for the ACES Symposia and participation as short course instructor.

CANDIDATE'S PLATFORM

The field of electromagnetism (EM) is probably one of the very few fields in applied science that has reached a high level of maturity. Computational electromagnetics, which is considered the applied side of electromagnetism, has witnessed an explosive growth in the past fifteen yeears. Today, we have numerical algorithms that can characterize wave-matter electromagnetic interaction with a high degree of accuracy and with sufficient speed. Despite the maturity in both theoretical and computational electromagnetics, the application of computational EM to new technological frontiers remains in its infancy. For instance, in the emerging field of nanotechnology, electromagnetism is expected to play a significant role. For computational EM practitioners, the primary challenge is in the fact that these new technologies are driven by strong interdisciplinary research teams that are typically devoid of computational EM experts. Interestingly enough, the classical EM practitioner paradigm has changed. Instead of using computational EM to solve known problems, we need to look at applications that can be designed by harvesting the power of EM with the aid of computational EM.

Having the vantage point of working with mechanical, electrical, and aerospace engineers in the emerging technologies, I have the advantage of identifying new and significant applications of computational EM and bring these applications to the EM community through ACES.

GENERAL BACKGROUND

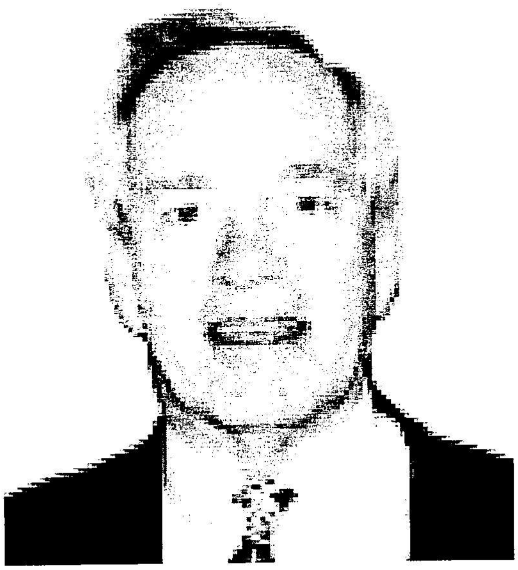

JOHN SHAEFFER has earned the Ph.D., M.S., and B.S. in Physics from St. Louis University (1971), Arizona State University (1965), and the University of Florida (1963). He is a Principal Scientist and founder of Marietta Scientific, Inc. He has specialized in electromagnetic phenomena, particularly electromagnetic scattering and radar cross-section. He has developed a three-day radar cross-section reduction short course that is offered through Marietta Scientific and was one of the principal developers of the Georgia Tech RCSR course. He is a co-author of the text ***Radar Cross Section***, 1st and 2nd editions.

MARIETTA SCIENTIFIC, Inc. was formed to provide Radar Cross Section services and software development to government and industry. He has helped lead NASA into visualization of complex electromagnetic effects through animation and imaging. He presently is leading an effort to develop PC based electromagnetic visualization software. He is also a heretic in proposing the idea that just because we can solve Maxwell's equations does not necessarily mean that we understand Maxwell.

He has developed the theory for Bistatic k-Space imaging which allows one to compute one-, two- or three-dimensional images of radiation centers from a given current distribution with only one body current solution (an excitation frequency sweep is not required). This method is particularly applicable for MOM codes for both scattering and antenna applications. This technique is currently being adapted into the PC EM visualization software.

Prior to this he was with **DENMAR, Inc.**, a Radar Cross Section Consulting Services Company with government and aerospace clients providing training, analytical, project, measurement, and materials analysis support.

At the **Lockheed-Georgia Possum Works,** he was a Low Observables Engineering Program Manager. He organized, hired, and trained a staff of RCS engineers and was responsible for Internal and Contract Research and Development (IRAD and CRAD) Programs in LO, for inter-company work, for LO Technology Development, and for staffing programs with LO engineers. The LO Department was organized with groups for analysis, test, materials, and project support.

At the **Georgia Tech Research Institute** he was a co-developer of the first Radar Cross Section Short Course, which eventually led to the published text. At GTRI he was a project leader in RCS and general electromagnetic modeling efforts including the HAVE SCATTER program for the measurement and data reduction of aircraft store RCS signatures. He also was a lecturer in several other radar related short courses. He developed unique numerical methods to model the magnetic fields of Naval vessels.

At the **McDonnell Douglas Research Laboratory** he worked on techniques and methods for analytically modeling electromagnetic behavior of complex shapes and structures. He formulated a strong coupling analysis for computer codes based on the method of moments, and developed electrostatic codes for analysis of multiple conductors described by potential or net charge immersed in an external electric field. From 1974 to 1977, he was associated with the Gas Dynamics Laboratory and developed computer codes for the analysis of swirling, turbulent radiative arc heater flow fields. These codes involved numerical techniques for solving coupled systems of nonlinear, parabolic, partial differential equations. From 1971 to 1974, he was associated with the Electronic Systems Technology Group of **McDonnell Aircraft,** investigating the interaction of lightning and other electrostatic phenomena with aircraft and for investigating electromagnetic EMI/EMC shielding properties of advanced graphite and boron epoxy composite materials and structures. From 1966 to 1968 he was involved in the design and diagnostics of radio frequency generated plasmas.

He has authored BOR, PATCH, BOR-PATCH, and BOR-WIRE-JUNCTION method of moments solutions of Maxwell's integral equations. He has developed the theoretical basis for the bistatic k-space image technique, which requires only a single frequency excitation of the body.

He has tinkered with electromagnetics since junior high school when he first became involved with ham radio, W4ALB and K8GIH.

PAST SERVICE TO ACES

Past service includes being a presenter and co-presenter of ACES papers over the last six years and has been a short course presenter for three different courses for the last several years. He was the ACES Short Course Chair for 2001 and will do this job again for ACES 2002.

CANDIDATE'S PLATFORM

The word "**APPLIED**" of our title is the key in guiding and directing ACES endeavors. Real world problems and developing technologies drive computational code and theory development. One only needs to look at the EM problems of the late 1960's that drove the development of MOM.

As a member of ACES BoD I will focus on those activities that bring together users, code developers and theorists. A key part of "APPLIED" is to better identify current areas that require EM computational efforts. Our Society activities need to further focus on activities that can bring together people and companies who require EM analysis for their products to interact with engineers who develop computational codes and theory.

MODELER'S NOTES

Gerald J. Burke

Under Modeler's Notes for this issue we have a contribution from Larry Laitinen updating his timing data for running NEC on some newer PCs and also a note by J. B. Knorr and B. Neta on plotting circularly polarized field patterns.

I was hoping to have some data to add to Larry's for the latest P-4s, but did not get the computer in time. Several of us at work have ordered 1.7 GHz Dell Dimension 8100s with 1 GB of 800 MHz RDRAM. That should make an interesting comparison with the P-IIIs with slower RAM. The reason for the delay was that we wanted to get them with Windows 98-SE to avoid the greater administrative load of Windows NT or 2000 (although many people, including Dick Adler and Larry Laitinen, would take exception with that statement.) We also wanted DVD drives, and Dell does not have a DVD drive that is compatible with Windows 98. We finally decided to get them with a CD-RW drive in bay 1 and a basic CD drive in bay 2. We then plan to trash the CD drives and replace them with DVD drives from a third party that should be compatible with Windows 98. Anyway, while we have been waiting the speed of the P-4s has edged up from 1.5 GHz to 1.7 GHz and the price has come down substantially. As I am writing this Dell does not show the 1.7 GHz system under the "consumer" page, but for "higher education" the price is $2991.95 for a 1.7 GHz P-4 with 1 GB of RDRAM, no monitor and the other items at default settings.

There are no new bugs in NEC to report. However, it is worth mentioning again the change recommended in the last Modeler's Notes of July 2000. Mike Morgan had encountered spikes in the magnetic field over a Sommerfeld ground. This was the result of small glitches in the electric field being magnified by taking differences to get the magnetic field. The fix, given in the July 2000 issue, was to disable four lines in subroutine EFLD. In April of this year John Grebenkemper sent results showing a problem with a vertical dipole lowered toward a ground of seawater with the Sommerfeld solution. When the top and bottom of the dipole bracketed a half wavelength height the input resistance was in error by a factor of nearly two. Above or below that height it was OK. This problem turned out to be the result of the same lines in EFLD that caused Mike's problem. For a short dipole the matrix elements were nearly imaginary. The "time saving" switch in EFLD put a small error in the small real part of the matrix elements, and that resulted in a large error in the input resistance. After Mike's problem I had made the change in NEC4D but not NEC4S, so a number of codes with the problem went out before April 9, 2001. For those who may have missed the July 2000 issue, the change is to comment out the four lines shown below in subroutine EFLD:

```
C       IF((ZIJS.GT.ZZMX1).OR.(-ZIJS.GT.ZPMX1).OR.(RHO.GT.RHMX1))THEN
C         IMAGF=2
C         GO TO 17
C       END IF
```

If anyone can contribute modeling-related material for future newsletters, they are encouraged to contact our editor Bruce Archambeault or Jerry Burke, Lawrence Livermore National Lab., P.O. Box 808, L-154, Livermore, CA 94550, phone: 925-422-8414, FAX: 925-423-3144, e-mail: burke2@llnl.gov.

PC NEC-4.1 PERFORMANCE DATA

Larry Laitinen, University of Oregon

Intel Pentium CPU clock frequencies now exceed 1-GHz, with workstation PCs based on slightly slower 800 to 900 MHz P-III CPUs costing approximately $1000 to $1500. Two 850 MHz PC workstations and one 933 MHz server PC were recently purchased and thus presented the opportunity to evaluate their floating point number crunching performance with LLNL's NEC-4.1 MoM antenna analysis code. NEC-4.1 performance data for various processors has been previously published over the years in the ACES Newsletter and on the NEC-list.

As CPU clock frequencies continue to increase, the fundamental question is what incremental increase in performance are we getting relative to two to three year old PCs with slower CPUs? Interest in PC upgrading seems to intensify when new PCs have clock frequencies about double those of PCs currently in use. It was only about two years ago that a 500 MHz P-III was considered "fast."

The recently purchased 850 MHz PC workstations replaced older/slower PCs in word processing, web and database office applications. The 933 MHz PC server will be replacing a 333 MHz server PC running Windows-NT and Exchange Server (a department level mail server). Thus these new machines were not configured specifically for number crunching.

The 850 MHz workstation PC tested has a Gigabyte GA-BX2000 (Intel 440BX chipset) motherboard, Intel Pentium-III CPU with 256-KB "on die" full-speed L2 cache, 256-MB ECC PC100 SDRAM, 30-GB IBM DeskStar disk drive (7200-RPM, 2-MB buffer/cache), ATI 32-MB video card, Windows-NT SP6, etc.

The 933 MHz server PC has a Gigabyte GA-6VXD7 (Apollo VIA chipset) motherboard, Intel Pentium-III CPU with 256-KB "on die" full-speed L2 cache, 1-GB ECC PC133 SDRAM, duplexed IBM 35-GB Ultra-160 SCSI disk drives, etc. The cost of this server PC was under $4500, including hot-swappable redundant power supplies and hot-swappable duplexed disk drives.

With Windows-NT V4 SP6A running on these machines, the base memory usage was approximately 59-MB, leaving the balance available for NEC execution. For the 1200-segment test problem, total memory usage was about 84-MB. Thus the NEC-4.1 test application used about 25-MB of RAM for 1200-segments in the double-precision mode. For the 600-segment DP test the total memory usage was about 66.8-MB.

A one year old 500 MHz Dell Inspiron-7500 Notebook PC with 128-MB of PC100 SDRAM was also tested for those interested in notebook PC performance. [I have added results for my Dell Inspiron-5000e that operates at 650 MHz on AC but cuts back to 500 MHz on the battery to save power — Jerry Burke]

As in the past, NEC-4.1 was compiled by Jerry Burke of LLNL using the DEC (now Compaq) Visual Fortran compiler.

The test results for these three machine types were added to previously compiled test data shown in Table 1. Estimated MFLOPS ratings are included, based on the approximation provided by Jozef R. Bergervoet: $((8/3) * N^3)/(\text{Matrix Factor Time})$ where N is the number of segments and $N > 1000$.

As can be seen from Table 1, the fastest matrix factor time (47.4-seconds) was on the 850 MHz workstation PC – approximately 4.3% faster than the 933 MHz server PC. Which is interesting since the 933 MHz server PC also has faster PC133 memory compared to the PC100 memory on the workstation PC. Matrix fill time, however, was faster on the 933 MHz PC by approximately the ratio of the clock frequencies, or about 9%. Thus the combination of

Table 1. Double-precision execution times in seconds for the TEST1200.NEC 1200-segment input file for various processors. NEC4.1 was compiled with the DEC Visual Fortran compiler. The OS is Windows-NT V4.

CPU/Motherboard	L2 Cache	RAM	Matrix Fill	Matrix Factor	Total exec.	MFLOPS (est.)	Norm./clock[1] M-Fill	M-Fact.
P-III 850 MHz Gigabyte GA-BX2000	256KB	256MB PC100	7.881	47.408	56.120	97.19	1.337	0.792
P-III, 933 MHz Gigabyte GA-6VXD7	256KB	1GB PC133	7.250	49.453	57.453	93.18	1.324	0.691
P-III AC, 650 MHz	512KB	256MB	11.310	47.790	60.690	96.42	1.216	1.025
Battery, 500 MHz Dell Inspiron5000e[2]	512KB	256MB PC100	14.280	52.730	68.500	87.39	1.252	1.207
P-III 500 MHz Dell Inspiron7500[2]	512KB	128MB PC100	12.829	55.539	69.791	82.97	1.397	1.149
P-III 450 MHz Gigabyte GA-686BA	512KB pburst	128MB 8-ns	14.100	69.831	85.453	65.99	1.015	1.085
P-II 450 MHz XPS D300	512KB pburst	256MB (Dell Dimension)	14.901	73.045	89.488	63.08	1.336	0.971
P-II 400 MHz Gigabyte GA-686BA	512KB pburst	128MB 8-ns	16.563	71.543	89.839	64.41	1.352	1.115
P-II 350 MHz Gigabyte GA-686BA	512KB pburst	128MB 8-ns	17.985	76.150	96.078	60.51	1.420	1.194
P-II 333 MHz Gigabyte GA-686DL2	512KB pburst	265MB 10-ns	18.967	92.743	113.814	49.69	1.031	1.099
P-II 300 MHz Gigabyte GA-686LX	512KB pburst	128MB 10-ns	21.101	95.867	119.251	48.07	1.412	1.107
P-II 300 MHz Dell Dimension	512KB pburst	96MB ??	21.251	102.778	126.271	44.83	1.402	1.032
P-II 266 MHz Gigabyte GA-686LX	512KB pburst	64MB 10-ns	23.574	104.009	130.107	44.30	1.424	1.149
P-II 266 MHz Gigabyte GA-686KX	512KB pburst	64MB 60-ns FPM	24.895	119.302	146.972	38.62	1.348	1.002
P-MMX 200 MHz Gigabyte GA-586HX	512KB pburst	64MB 60-ns FPM	38.205	202.311	244.982	22.78	1.171	0.788
Pentium 133 MHz Gigabyte GA-586HX	512KB pburst	64MB 60-ns FPM	66.636	275.587	348.941	16.72	1.007	0.867
Pentium 133 MHz Hitachi MX-133T[2]	256KB pburst	80MB 60-ns EDO	79.965	307.412	394.998	14.99	0.838	0.777
Pentium 100 MHz Intel P54C-PCI	256KB pburst	64MB 60-ns	89.869	319.900	418.512	14.40	0.996	0.996
Pentium 90 MHz Intel P54C-PCI	256KB pburst	64MB 60-ns	99.333	353.708	462.865	13.03	1.000	1.000

[1] Fill and Factor times normalized by clock speed with the 90 MHz Pentium as a reference.

[2] Notebook PC.

the 850 MHz Intel P-III CPU and 440BX chipset on the Gigabyte GA-BX2000 motherboard outperforms the more expensive Gigabyte GA-6VXD7 motherboard and 933 MHz CPU with the VIA Apollo chipset – at least for FP number crunching. Estimated DP MFLOPS were 97.19 (850 MHz workstation PC) and 93.18 (933 MHz server PC).

Now look at the excellent DP performance on the one year old Dell Inspiron-7500 Notebook PC in Table 1: 55.5-seconds matrix factor time for about 83-MFLOPS [and the 650 MHz Inspiron 5000e beating the 933 MHz GA-6VXD7 in factor time — J.B.].

Single-precision tests were also performed on the new machines, and ranged from 127.7 to 162.1-MFLOPS, or 54% to 71% faster than DP.

The last two columns of Table 1 show the fill and factor times relative to the 90 MHz Pentium and normalized by the ratio of their clock speed to 90 MHz. Normalized ratios less than one indicate poorer performance that has not kept up with the increased clock frequency. While normalized ratios greater than one indicate better than expected performance based on the increased clock frequency. Points of interest include the switch from the P-I to the P-II CPU and from FPM memory in the GA-686KX motherboard to the faster SDRAM memory in the GA-686LX motherboard. After that the waters are somewhat muddied by the lack of test data in the 450 MHz to 850 MHz range with motherboards designed specifically for the then newer P-III CPUs. However, we can see that the Dell 500 MHz P-III based Inspiron-7500 [and 650 MHz Inspiron-5000e] provided excellent performance relative to the two 450 MHz desktop PCs tested, one of which was also a Dell.

As shown by the normalized matrix factorization ratios 0.792 and 0.691, the respective 850 MHz and 933 MHz PC performance did not keep up with their faster clock frequencies relative to the referenced 90 MHz Neptune PC. Similar results were obtained using the 266 MHz P-II with GA-686LX motherboard.

The normalized performance ratios were converted to effective MHz ratings in Table 2 with the 266 MHz GA-686LX as a reference. If you have a 266 MHz PC now and are looking to upgrade to a faster PC, Table 2 gives you some guidance on what to expect in "effective" MHz ratings for faster PCs. Note that the 850 MHz P-III tested has an effective speed of 585 MHz in DP relative to the GA-686LX at 266 MHz, or about a 2.19X improvement for a 3.5X clock ratio. Thus about 60% of the increased clock frequency is useful. Note that the Dell Inspiron-7500 scaled nearly 1:1 in MFLOPS:MHz. Nevertheless, the 933 MHz server PC with Ultra-160 SCSI type disk drives makes Windows-NT execute noticeably faster than on a 500 MHz PC with a UDMA/IDE type disk drive.

If you are currently running NEC-4.1 on a 450 MHz PC and are interested in upgrading to a faster PC, then Table-3 provides some guidance on what to expect. For the 850 MHz test case the clock frequency increased 88.9% over the 450 MHz reference, but the effective DP speed is equivalent to a 662.8 MHz PC – well short of the 850 MHz you might expect. For the 933 MHz test case the results are even worse, yielding only 635.4 MHz effective speed for NEC-4.1 matrix factorization DP floating point.

Keep in mind that the floating point hardware in these Pentium based systems may perform up to 3 to 4 times faster by incorporating the Intel Pentium optimized Math Kernel Library with the LAPACK linear algebra library into the NEC-4.1 code, as suggested by Jozef Bergervoet a few years ago and Tom Wallace in the March 2000 Newsletter.

Finally, the data presented here shows, again, that CPU clock frequency is often an over rated and misleading performance metric for PC based FP applications. The supporting chipset, memory and motherboard designs are important factors that must be considered to realize the highest level of CPU FP performance.

–Larry, W7JYJ

Table 2. Effective MHz ratings of the Pentium-II and III CPUs and motherboards for 300 and 1200-segment matrix factorization tests. The 266 MHz Pentium-II in a Gigabyte GA-686LX motherboard is the reference. Effective speed ratings are relative to this reference.

CPU Clock	Motherboard	RAM SPEED	Effective CPU clock speed (MHz) 300-Seg.	1200-Seg.	
933 MHz P-III	GA-6VXD7	PC133	441.6	560.9	
850 MHz P-III	GA-BX2000	PC100	452.5	585.0	
650 MHz P-III	Dell I5000e	PC100		579.8	
500 MHz P-III	Dell I7500	PC100	389.2	499.4	
450 MHz P-III	GA-686BA	8-ns	423.6	396.8	
450 MHz	Dell R450	??	375.6	379.3	
400 MHz	GA-686BA	8-ns	398.6	387.7	
350 MHz	GA-686BA	8-ns	371.3	363.8	
333 MHz	GA-686DL2	10-ns	292.5	298.8	
300 MHz	GA-686LX	10-ns	284.7	289.0	
300 MHz	Dell D300	??	268.6	269.6	
266 MHz	GA-686LX	10-ns	266.4	266.4	(ref)
266 MHz	GA-686KX	60-ns	216.0	232.2	

Table 3. Effective MHz ratings of the Pentium-II CPUs and motherboards for 300 and 1200-segment matrix factorization tests. The 450 MHz P-III Gigabyte GA-686BA motherboard is the reference. Effective speed ratings are relative to this reference.

CPU Clock	Motherboard	RAM SPEED	Effective CPU clock speed (MHz) 300-Seg.	1200-Seg.	
933 MHz P-III	GA-6VXD7	PC133	468.6	635.4	
850 MHz P-III	GA-BX2000	PC100	480.1	662.8	
500 MHz P-III	Dell I7500	PC100	413.0	565.8	
450 MHz P-III	GA-686BA	8-ns	450.0	450.0	(ref)
450 MHz P-II	Dell Dimension		398.9	430.2	

Input data used in the tests for 1200 segments follows. For 300 segments the second GM command was `GM0,2,...`.

```
CE Timing test - Multiple parallel wires,  1200 segments
GW0,10,0.,0.,0.,0.,0.,1.,.001,
GM0,9,0.,0.,0.,.2,0.,0.,
GM0,11,0.,0.,0.,0.,.2,0.,
GE
EX0,0,5,0,1.,
XQ
EN
```

Plotting Circularly Polarized Field Patterns Using Processed NEC 4 Output Files

J. B. Knorr
Naval Postgraduate School
Monterey, California

B. Neta
Naval Postgraduate School
Monterey, California

I. Introduction

NEC4 computes E_θ and E_φ, the linearly polarized components of the far field radiated by an antenna. Software packages such as GNEC, which are built around the NEC4 engine [Ref. 1], allow the user to plot far field patterns for E_θ and E_φ from the data in the NEC4 output file. When the far field of an antenna is elliptically polarized, the NEC4 output file indicates the sense of polarization, right or left hand. While this information is useful, antennas that radiate a field that is basically circularly polarized are better characterized by their right and left hand circularly polarized field patterns. The cavity backed spiral, for example, is an antenna that is used in applications where circular polarization is desired and one would prefer to see the far field patterns of the right and left hand components, E_{right} and E_{left}. This note describes a simple approach to plotting the patterns for E_{right} and E_{left} by processing the data in the standard NEC4 output file.

II. Approach

The standard NEC4 output file provides the user with the magnitude and angle of E_θ and E_φ. Most user interfaces simply allow the user to access this data to plot the far field patterns for E_θ and E_φ. The current version of GNEC is an example. If the NEC4 output file is processed and E_θ and E_φ are replaced with E_{left} and E_{right}, then any plotter designed to extract data from the NEC4 output file can be used to display left and right hand circularly polarized field patterns instead of the usual linearly polarized field patterns. The required processing is straightforward. A Matlab program is provided in Appendix 1.

III. Field Decomposition

The linearly polarized field components E_θ and E_φ can be decomposed quite simply into left and right hand circularly polarized components. Write

$$\mathbf{E} = E_\theta \mathbf{a}_\theta + E_\varphi \mathbf{a}_\varphi \quad \text{or}$$

$$= \underbrace{0.5E_\theta[\,\mathbf{a}_\theta + j\mathbf{a}_\varphi\,]}_{\text{(LHC)}} + \underbrace{0.5E_\theta[\,\mathbf{a}_\theta - j\mathbf{a}_\varphi\,]}_{\text{(RHC)}} \underbrace{- j0.5E_\varphi[\,\mathbf{a}_\theta + j\mathbf{a}_\varphi\,]}_{\text{(LHC)}} + \underbrace{j0.5E_\varphi[\,\mathbf{a}_\theta - j\mathbf{a}_\varphi\,]}_{\text{(RHC)}}.$$

In the above expressions, bold type denotes vector quantities, **a** is the unit vector, LHC indicates left hand circular and RHC indicates right hand circular polarization. Now write

$$\mathbf{E} = \mathbf{E}_{left} + \mathbf{E}_{right}$$

where

$$\mathbf{E}_{left} = 0.5[E_\theta - jE_\varphi][\mathbf{a}_\theta + j\mathbf{a}_\varphi] \text{ and}$$

$$\mathbf{E}_{right} = 0.5[E_\theta + jE_\varphi][\mathbf{a}_\theta - j\mathbf{a}_\varphi].$$

IV. Field Patterns of an Eight Arm Cavity Backed Spiral

The eight arm cavity backed spiral is an interesting antenna that is often used in applications requiring broad bandwidth and circular polarization. The spiral can be excited to produce a sum beam (mode 1) or a difference beam (mode 2). This antenna serves as a good example for illustrating the difference between linearly and circularly polarized field patterns.

A. Mode 1

To produce a sum beam, the eight arms of the spiral are excited with a 45 degree

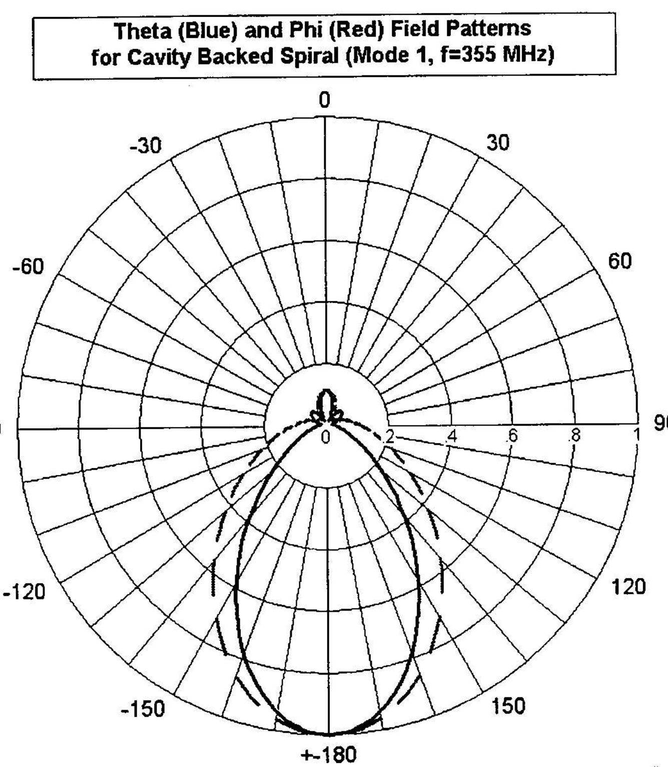

Figure 1. Linearly polarized field patterns for mode 1 excitation of an eight arm cavity backed spiral antenna. Patterns are in a plane containing the axis of the spiral (normal to plane of spiral). E_θ solid line, E_φ dashed line.

phase shift from one arm to the next. This results in opposing arms being excited in phase. Figure 1 shows the linearly polarized field pattern and Figure 2 shows the circularly polarized field patterns.

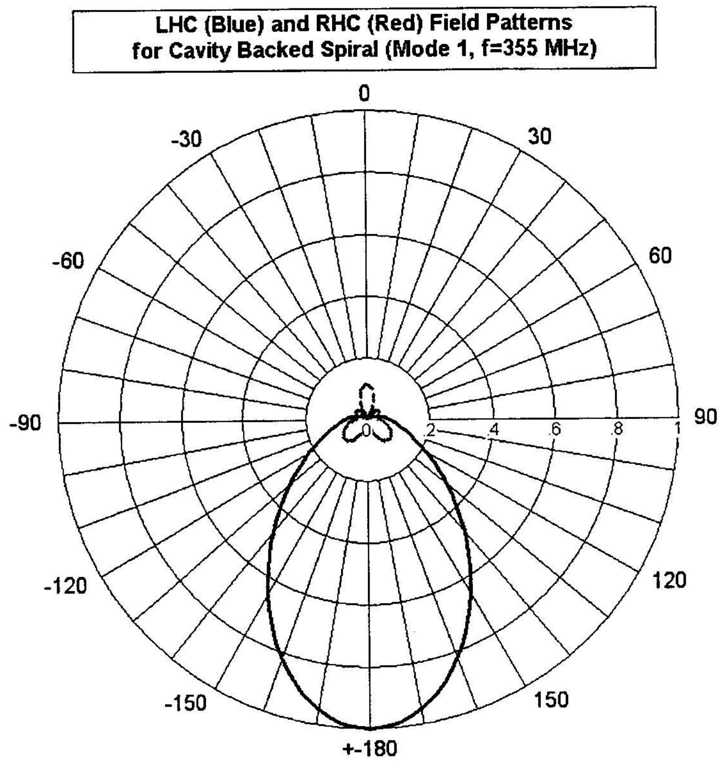

Figure 2. Circularly polarized field patterns for mode 1 excitation of an eight arm cavity backed spiral antenna. Patterns are in a plane containing the axis of the spiral (normal to plane of spiral). E_{left} solid line, E_{right} dashed line.

An inspection of Figures 1 and 2 reveals the patterns for the linearly and circularly polarized fields are very different. One can determine the relative magnitudes of the linearly polarized field components from the patterns displayed in Figure 1 but without phase information, any other field pattern is impossible to deduce.

B. Mode 2

To produce a difference beam, the eight arms of the spiral are excited with a 90 degree phase shift from one arm to the next. This results in opposing arms being excited 180 degrees out of phase so that in a plane normal to the plane of the spiral and containing the axis of the spiral, the far field contributions of the opposing arms will cancel, producing a null in the pattern. Figure 3 shows the linearly polarized field patterns and Figure 4 shows the circularly polarized field patterns. Again, the difference between the patterns for the linearly polarized field components displayed in Figure 3 and the circularly polarized field

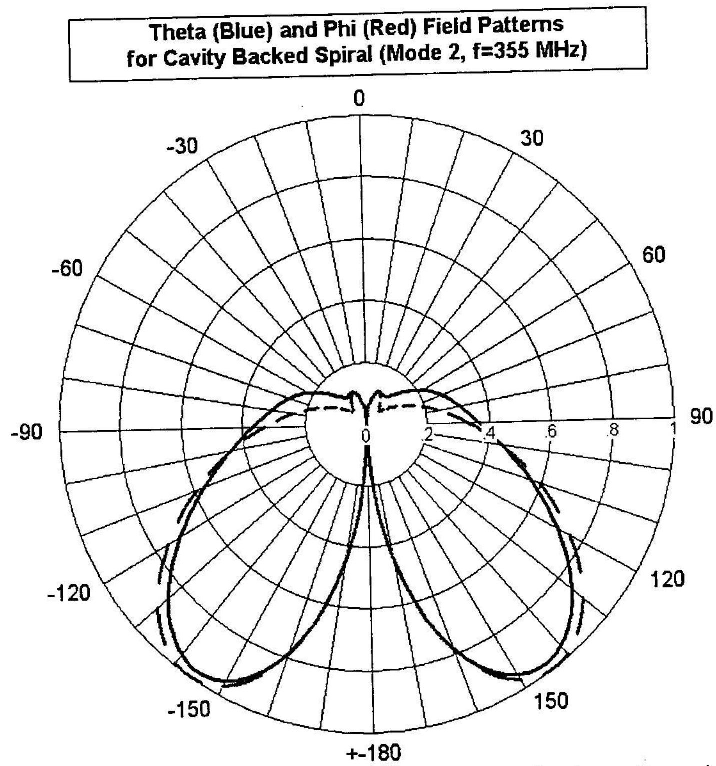

Figure 3. Linearly polarized field patterns for mode 2 excitation of an eight arm cavity backed spiral antenna. Patterns are in a plane containing the axis of the spiral (normal to plane of spiral). E_θ solid line, E_φ dashed line.

components displayed in Figure 4 are evident. One could not deduce the patterns in Figure 4 from the patterns in Figure 3.

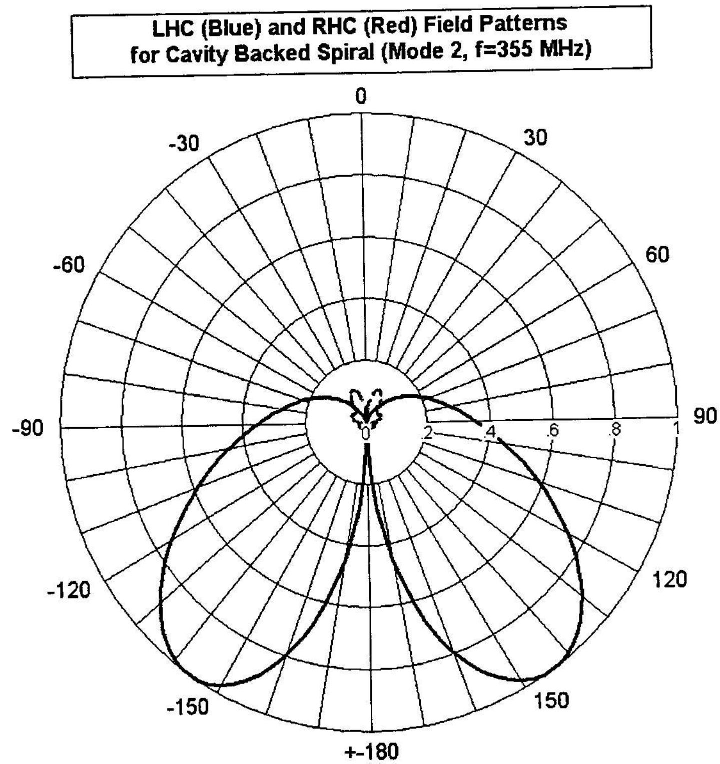

Figure 4. Circularly polarized field patterns for mode 2 excitation of an eight arm cavity backed spiral antenna. Patterns are in a plane containing the axis of the spiral (normal to plane of spiral).

V. Conclusions

A simple approach to displaying the circularly polarized field patterns of an antenna analyzed using NEC4 has been presented. Equations have been provided for decomposition of the linearly polarized field into left and right hand circularly polarized components. If the normal NEC4 output file is processed and E_{left} and E_{right} are substituted for E_θ and E_φ in the output data file, then any plotter capable of extracting data from the normal NEC4 output file can be used to display the left and right hand circularly polarized field patterns of the antenna. Work is under way to implement this display capability in a future release of GNEC.

References

[1] GNEC, Nittany Scientific, http://www.nittany-scientific.com/.

Appendix 1. Matlab Code

```
% This matlab program
% (1) reads a NEC4 output file,
% (2) computes left and right hand circularly polarized fields from the linearly polarized
% theta and phi components and
```

```
% (3) replaces E theta with E left and E phi with E right.
% The program prompts the user for an input file name (NEC4 output file).
% The program also asks the user for the output file name (it overwrites the file).
% For each of these there is a default which is taken if the question is not answerd.
% The number of Thetas will be given on the screen at the end of the run.
clear
help lrnec;
% Input the default values in the variables below:
default_infile=('PSAT_PAT.nou');
default_outfile=('psatpat.nou');
% Prompt user for input values. The default value is used
% If carriage return is selected without inputting data.
disp(' '); % Line Space on screen
infile=input('Type in the input file name: ','s');
if isempty(infile)
  infile = default_infile;
end
disp(' '); % Line Space on screen
outfile=input('Type in the output file name: ','s');
if isempty(outfile)
  outfile = default_outfile;
end
disp(' '); % Line Space on screen
% Display selected values. Comment out after debugging:
infile
outfile
% open file to write
%
fid_out=fopen(outfile,'w')
%
% open the file to read
%
fid_v=fopen(infile,'r')
if fid_v > 0
 sprintf('v file opened:')
end
%    Read the file
%         ... read each text header line
while 1
%         ... This WHILE LOOP to READ EACH DATA LINE is an
%             infinite loop, since "while 1" is always true.
%             The way to exit from the loop is with an if, break.
%             IF length(line) == 0  Break out of loop!!
%             The "isstr" function will test if line is a character
%             string. The if ~isstr(line) logic means if line is
%             NOT (~) a string. So if ~isstr(line) is TRUE when
```

```
%            line is NOT a string, and is the end-of-file.
%            When end of file is reached, "break" exits the WHILE Loop.
 line = fgetl(fid_v);
 fprintf(fid_out,'%s\n',line);
%  length(line)
 if length(line) > 72
  if line(55:72) == 'RADIATION PATTERNS'
   line(55:72)
   last =1
   break
  end
 end
end
% end of "while 1" loop, which reads the header lines
%         ... initialize a line counter
iline=0;
% read the empty line after RADIATION PATTERNS header
%
line=fgetl(fid_v);
fprintf(fid_out,'%s\n',line);
% read 3 lines of headers after that
line=fgetl(fid_v);
fprintf(fid_out,'%s\n',line);
line=fgetl(fid_v);
fprintf(fid_out,'%s\n',line);
line=fgetl(fid_v);
fprintf(fid_out,'%s\n',line);
j=0;
% line
while 1
  line=fgetl(fid_v); % line of data
%         ... Check for the effective "end-of-file"
  if feof(fid_v), break, end
%         ... Increment line counter. This is the index for each
%             data array
  if length(line) > 0
      if line(2:9) == 'RUN TIME'
        fclose(fid_out);
        break
      end
    if line(4:21) == 'AVERAGE POWER GAIN'
     fprintf(fid_out,'%s\n',line);
     while 1
      line=fgetl(fid_v); % line of data
      fprintf(fid_out,'%s\n',line);
      if length(line) > 2
```

```
      if line(2:9) == 'RUN TIME'
%           fclose(fid_v); % --- end of v file
         fclose(fid_out);
         break
       end
      end
    end    % end of while
   else

     j=j+1;
     etm=str2num(line(77:87));
     etp=str2num(line(90:96));
     epm=str2num(line(101:111));
     epp=str2num(line(114:120));
     vet=etm*cos(etp*pi/180)+i*etm*sin(etp*pi/180);
     vep=epm*cos(epp*pi/180)+i*epm*sin(epp*pi/180);
     ver=.5*(vet-i*vep);
     vel=.5*(vet+i*vep);
     erm=sqrt(real(ver)^2+imag(ver)^2);
     erp=atan2(imag(ver),real(ver))*180/pi;
     elm=sqrt(real(vel)^2+imag(vel)^2);
     elp=atan2(imag(vel),real(vel))*180/pi;
        ab=[erm erp elm elp];
     fprintf(fid_out,line(1:72));
     fprintf(fid_out,'%15.5e%9.2f%15.5e%9.2f\n',ab);
    end
  end
end
```

MODELING VERY THIN LOSSY SURFACES IN THE PRESENCE OF INCIDENT FIELDS USING ANSOFT HFSS VERSION 8.0

Vicente Rodríguez and Kefeng Liu
ETS-Lindgren
2205 Kramer Ln
Austin, TX 78758
Vicente.Rodriguez@emctest.com

Abstract- Ansoft HFSS is a very complete package for the solving of electromagnetic (EM) problems. It includes a large set of numerical tools for the simulation of geometries in the presence of EM fields. Among these tools it includes the usage of impedance boundary conditions (IBC) for the modeling of thin lossy surfaces. Unfortunately the IBC does not work when the excitation of the problem is an incident field. For very highly conductive surfaces the software user may get around this by simulating these thin highly conductive structures as perfect electric conductor (PEC). For Surfaces with lower losses the authors suggest simulating the two-dimensional (2D) surface with a surface resitivity as a three-dimensional structure with an equivalent finite thickness and volumetric conductivity. Results show good agreement between using the thick slab approach when compared with equivalent problems excited with ports where the IBC can be used.

I. Introduction

The authors became aware of a bug in version 8.0 of Ansoft HFSS. This bug is in the implementation of the IBC. There is no apparent problem with the IBC when applied to structures that are excited by ports (where ports are 2D surfaces where a static solution of the fields is found and this solution is used as the excitation for the problem). But when the problem requires an incident plane wave to be the excitation the IBC does not work correctly. If the surface is highly conductive it may be desirable to model the thin lossy surface as a PEC. However for thin lossy dielectric materials where PEC is not an accurate model we suggest the use of a thin slab. It is understandable that this approach uses more memory and therefore longer computational time. But the *a priori* knowledge of the skin depth of the lossy material being used should help the user to decide on the thickest possible slab that will behave as closely as possible to the 2D material that was to be modeled by the IBC. Ansoft is aware of this problem and expects the release of a patch to its customers sometime in the future. In the meantime we would like to present this alternate approach that may be useful in getting around the problem for users that need to solve problems that require the use of IBC in the presence of incident fields prior to the release of the patch.

II. Selecting the Thickness of the Slab

The problem under study contained a thin coat with losses in the order of 1KΩ/ . Using the IBC capabilities provided by Ansoft HFSS this would have been really easy to model. The user can simply choose the surface and then select the type of boundary and the reactance and resistance of it. Since the IBC does not provide correct results when used with incident fields it was decided to model the surface as a slab of certain thickness. The volume losses of this material should be equivalent to the losses of the 2D coat.

To obtain this equivalent lossy material we can start with the definition of Resistance:

$$R = \rho \frac{L}{S} \qquad (1)$$

Where S is the cross section surface and L is the length of the conductor. Equation (1) can be rewritten by separating the cross section if the conductor in to width (w) and thickness (t).

$$R = \frac{\rho}{t}\frac{L}{w} = \rho_s \frac{L}{w} \qquad (2)$$

The first term in equation (2) is the surface resistance (ρ_s) given in Ohms per square (Ω/). Two obtain an equivalent volume conductivity from this surface resistance the following equation is used:

$$\sigma = \frac{1}{\rho} = \frac{1}{\rho_s t} \qquad (3)$$

This conductivity is used in defining the material of which the slab is made. A slab made of this material has the same resistance as the original 2D lossy sheet. As an example, let us assume that the surface resistance of 500Ω/ . A slab with a thickness of 1mm would have to be made of a material with a conductivity of 2S/m. This procedure is, of course, a low frequency/static approach and the skin effects must be taken in to account.

While it is possible to draw a slab as thin as desired within HFSS to model the thin 2D coat, a very thin slab would require a very large number of tetrahedra to be discretized. At the same time a very thick slab will have the problem that at certain angles of incidence it may be electrically too different from the 2D surface. The user should choose a thickness that is thin enough to approach the desired 2D lossy sheet while not too thin as to require large amounts of memory to be solved. Once a thickness is chosen it is necessary to check whether at the required frequency range the skin effects for the given lossy slab will affect the static approach used in defining those volumetric losses. Also studying the skin depth of the equivalent material of the slab for the frequency range of interest

may show that a thicker slab may be used without affecting the equivalent resistance of the slab.
The skin depth is given by the following equation [1]:

$$\delta = \frac{1}{\alpha} = \frac{1}{\omega\sqrt{\mu\varepsilon}\sqrt{\frac{1}{2}\left[\sqrt{1+(\sigma/\mu\varepsilon)^2}-1\right]}}\ \mathrm{m} \qquad (4)$$

The study of the skin depth provides an idea of how thick the slab can be without affecting the use of an equivalent volume conductivity.
Figure 1 shows the skin depth for a given material with a conductivity of 2S/m which is equivalent to our lossy sheet of around 500Ω/ used in some of the numerical experiments conducted. The graph shows that for all the frequencies the skin depth is larger than 20mm. As a rule of thumb it can be stated that as long as the thickness of the slab is within a tenth of the thickness of skin depth the static approach for the equivalent material definition should hold.
Hence, a slab with a thickness of 1mm would be thick enough without affecting the volumetric conductivity.

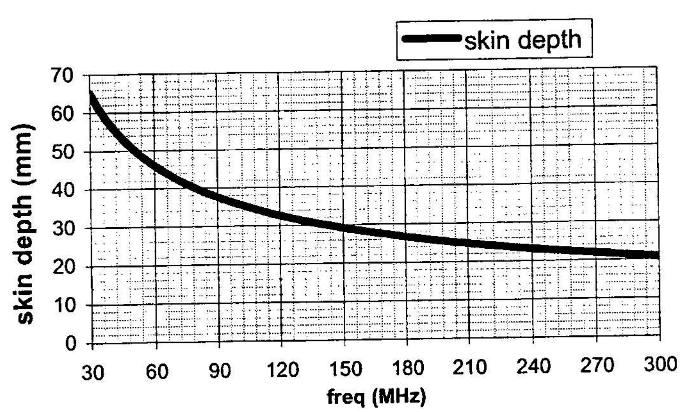

Figure 1. Skin depth vs frequency for a material with rel. permitivitty of 2.17 and a conductivity of 2S/m

III. Numerical Experiments

To check the validity of the slabs a series of numerical experiments where performed. Some of the results where also compared with measured data. A model containing IBC and excited by a port was compared with a similar geometry where the IBC where substituted by slabs and excited by an incident field. Figure 2 shows the general idea of the two different approaches.

In the cases excited by a port, the geometry is inserted in a waveguide. This waveguide has walls that have been set to PEC and Walls that have been set to PMC. This gives "incident" fields at the port that have x or y components. By selecting which walls are set to be PMC and which ones PEC and incident Ex field or Ey field can be selected as the excitation. For the incident field excitation an $E\varphi$ or and $E\theta$ is selected with an incidence at θ_{inc} = 0 and φ_{inc} =90 or 0. This provides an equivalent excitation for the problem.
While analyzing some absorber for EMC anechoic chambers the authors became aware that these two different excitation although equivalent where providing different results. While searching for the reason for the discrepancy ferrite tile (ε_r=10.9, μ_r=101.2 , magnetic tan(δ)=1.541 at 30MHz) 0.677cm thick backed by wood (ε_r=2.2 ,tan(δ)=0.027) 1.33cm thick. This is a typical EMC anechoic chamber absorber treatment. The reflectivity results where the same with either excitation. The results agree with the analytical solution for this geometry as shown in Table A.

Table A. Reflectivity from ferrite tile .667cm thick backed by wood 1.33cm thick mounted on PEC.

	Analytical	Port Excitation	Inc. field Excitation
Reflectivity in dB	-9.983	-9.982	-9.991

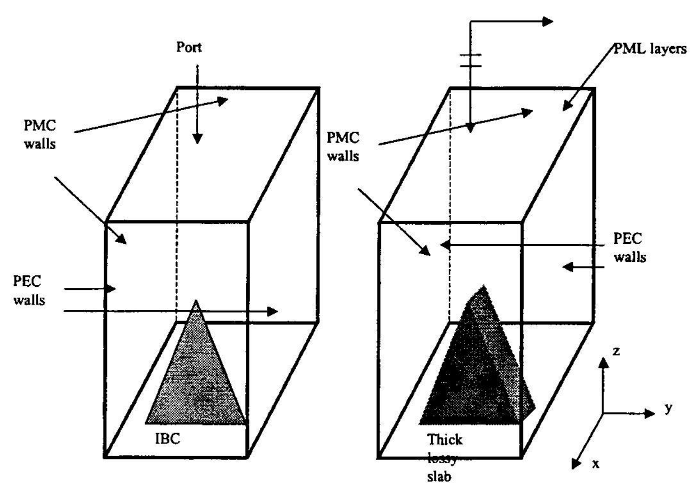

Figure2. The two equivalent problems being investigated

The results in Table A show that as expected these two excitations are equivalent. When a IBC was defined somewhere within the problem region the results from the two equivalent excitations were different. Ansoft confirmed this finding by notifying us that they too have found this bug in the implementation of the IBC in the presence of incident field excitation. Since our project required us to solve a structure with very thin lossy surfaces the idea of using the thick slabs to model the 2D lossy sheets was used.

Figure 3 shows the results obtained when analyzing one of these structures using IBC to model the thin sheets excited by a port, and the results of exciting them with an incident field using thick slabs to model the thin sheets. The structure being analyzed is new absorber for EMC applications developed by ETS-Lindgren. The size of the problem region was 30cm by 15cm and the height of 1m, the thickness chosen for the slabs was 1mm. As the figure shows there is good agreement between both solutions. Over the entire range the largest difference is less than 1.2dB. The main reason for using an incident field is that it allowed us to study the behavior of the absorber at oblique incidences. For the oblique incidence cases periodic boundary conditions where used.

IV. Conclusions

The use of the thick slabs of equivalent loss is a simple way to get around the error in Ansoft HFSS. The technique presented to convert from a surface resistance to a volume conductivity has been presented and proved. It has been shown that by checking the skin depth the user can be sure that the static approximation used is valid for a given range of frequencies. The results show good agreement between the use of IBC with port excitation and the use of an incident field with the thick slabs. This allows the user of Ansoft HFSS to explore the effects of oblique incidence on structures containing thin lossy coats.

V. References

[1] Balanis, C. A. *Advanced Engineering Electromagnetics,* John Wiley & Sons: New York, NY, 1989.

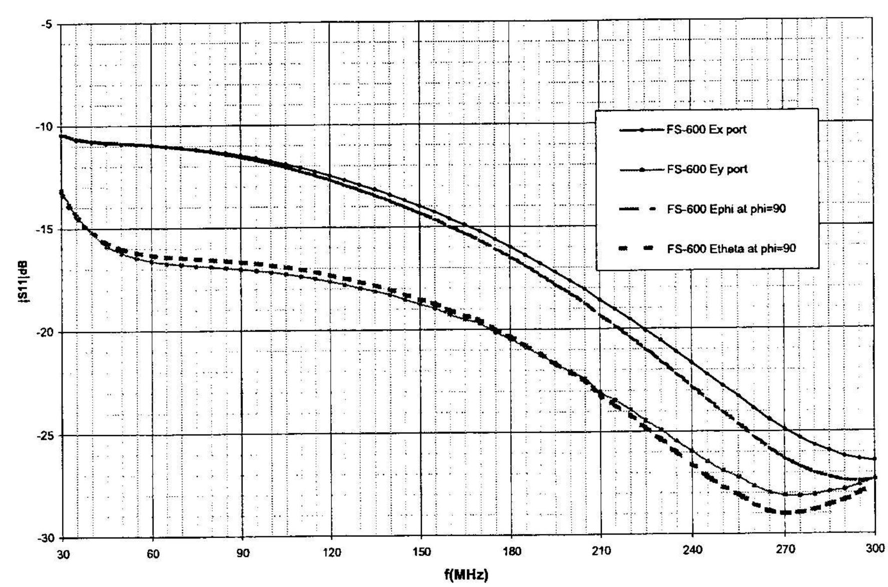

Figure 3. Normal incidence on FS-600 absorber using a port excitation with IBC and an incident field with thick slabs.

The Practical CEMist: Eight-Band HF Wire Antenna Impedance Characteristics

Perry Wheless and Mike Fanning

Abstract— **Both measured and computer-predicted impedance characteristics of a multiband horizontal off-center-fed hf wire antenna are presented. This antenna is effective for communications in the eight amateur hf bands about 3.8, 7.2, 10.1, 14.2, 18.15, 21.3, 24.95, and 28.5 MHz. Impedances are found to be amenable for matching to 50Ω transmitters by most available Tee, Pi, and L-network tuning units. A dual coax feed, with a 4:1 balun located at the transmitter end of the system, is practical. Feed-point impedances were measured with a laboratory grade impedance analyzer, and these are compared with impedances based on Numerical Electromagnetics Code (NEC) results.**

Keywords— **Multiband HF antennas, Windom, HF wire antennas.**

I. Introduction

The wire antenna under discussion is a modification of the traditional "Windom" [1] antenna, similar to Figure 1 below. For best impedance compromise behavior about 3.9, 7.2, 14.2, and 28.5 MHz, the historical Windom configuration would be one continuous horizontal wire approximately 36.6 meters long, overall (L), with a single-wire feeder connected 0.36L from one end. Because the wire feeder is part of the antenna in the classical version, considerable rf levels occur at the transmitter location. When a dual coax feed and transmitter-end balun, illustrated in Figure 2, replace the single-wire feeder, negligible stray rf currents at the transmitter are observed in practice even at 1 kW transmit power. Note that the approach path of the coax feed lines is perpendicular to the wire antenna axis (for the greatest distance possible) to ensure minimal undesired interaction.

For this study, the overall length has been increased to 46.9 meters as a consequence of empirical observations. Using the historical guideline of 0.36L, the feed point placement would separate the antenna into parts 16.9 and 30.0 meters, respectively. Results for a minor feed point variation resulting in side lengths of 18.9 and 28.0 meters, in accord with Figure 1, are presented here.

The abstract cites eight discrete frequencies. For reference, the band limits corresponding to these cases are 3.5 - 4.0, 7.0 - 7.3, 14.0 - 14.35, 18.069 - 18.168, 21.0 - 21.45, 24.89 - 24.99, and 28.0 - 29.7 MHz. There are approximately 400,000 licensed radio amateurs in the United States, many of whom must erect antennas in limited space and/or under restrictive neighborhood covenants. Hence, a single wire antenna capable of competitive performance on all the currently allocated hf amateur bands is of considerable interest. The height above ground, 1.96 meters, is also not coincidental, but was chosen to be typical of fence height (a convenient mechanical wire antenna support) in many residential developments.

P. Wheless is with the Electrical and Computer Engineering Department at The University of Alabama. E-mail: wwheless@coe.eng.ua.edu .

M. Fanning is now with Adtran, Huntsville, AL.

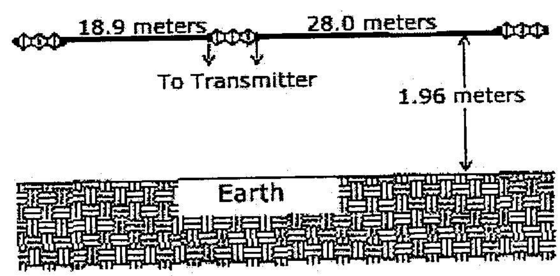

Fig. 1. Asymmetric HF multiband hf antenna.

II. Moment Method Predicted Impedances

Computer predictions of the various antenna feed-point impedances were made using NEC2-PC software. More powerful versions of NEC are now readily available, but NEC2 is adequate for the simple wire antenna configuration under consideration here. The wire radius was taken to be 3.43 mm in all cases. As a matter of academic interest, computations were made both in a free space environment and in the present of non-ideal (real) earth. From local AM broadcast station data and consulting Figures 6.1 and 6.2 of Hagn [2], the ground conductivity σ and dielectric constant ϵ_r values used for computer modeling were those given in Table I. The impedances in Table I are those at the antenna feed-point terminals.

Table I
Feed-Point Impedances Computed by NEC

Freq. MHz	σ mS/m	ϵ_r	Ground Present	Ground Absent
3.80	2.3	19	$181 + j437$	$198 + j441$
7.20	3	15	$1324 + j1257$	$1371 + j1147$
10.1	3.8	15	$1291 + j473$	$1207 + j642$
14.2	4.8	14	$557 + j893$	$619 + j852$
18.15	5.5	13	$177 - j366$	$137 - j402$
21.3	6.0	13	$1154 - j642$	$1185 - j778$
24.95	6.6	13	$377 - j395$	$328 - j419$
28.5	7.0	13	$198 - j53$	$157 - j59$

In practical applications, the impedances of most interest are those at the transmitter end of the feed line, rather than those directly at the antenna terminals. Therefore, hereafter in this report impedances at the antenna feed point have been transformed to the transmitter end, assuming an intervening transmission line length of 15.25 meters (50 feet). Transmission line loss was taken into account, with 0.205 dB loss at 3.8 MHz, 0.28 dB loss at 7.2 MHz, 0.34 dB loss at 10.1 MHz, 0.385 dB loss at 14.2 MHz, 0.44 dB loss at 18.15 MHz, 0.49 dB loss at 21.3 MHz, 0.51 dB loss at 24.95 MHz, and 0.60 dB loss at 28.5 MHz. Even if SWR remains essentially constant along the transmission line, the specific numerical impedance values change with distance, and commercially available reactive Antenna Tuning Units (ATU's) frequently have bounds on the values of impedance that can be matched successfully to the 50Ω transmitter output impedance.

In addition to a commercial 4:1 balun, individual $\lambda/2$ coax baluns were used instead for comparison purposes. For completeness, note that smaller coaxial cable was used to fabricate the coax baluns (see Figure 2). This smaller cable had loss per hundred feet of 0.80 dB at 3.8 MHz, 1.2 dB at 7.2 MHz, 1.5 dB at 10.1 MHz, 1.7 dB at 14.2 MHz, 2 dB at 18.15 MHz, 2.2 dB at 21.3 MHz, 2.35 dB at 24.95 MHz, and 2.5 dB at 28.5 MHz. Because the transformation calculations with lossy line components is tedious, the computer program TAME [3] was employed for this task.

III. Measured Impedances

All measured impedances were recorded with a Hewlett Packard 4191A rf impedance analyzer, with performance specifications which can be seen in H-P equipment catalogs of the early 90s vintage. The single measurement port on this instrument is an unbalanced coaxial connector input.

IV. Predicted and Experimental Results

Recall that Table I shows NEC predicted impedances, both in the presence and absence of real ground, at the antenna feed-point terminals. The reader is reminded that all impedances hereafter are at the transmitter end of the 15.25 m transmission line section.

Figure 2 depicts the preferred mode of antenna feed/operation. In practice, the balun is a commercial "broadband" 4:1 balun. However, such baluns are not well behaved and predictable except when terminated in the design load impedance. It was deemed more reliable and accurate, for an archival experimental study, to use $\lambda/2$ coax baluns that are more amenable to deterministic electrical characterization. To illustrate the potential discrepancies, measured Z_{in} with a coax balun is compared in Table II to Z_{in} measured at the unbalanced input side to the commercial 4:1 balun contained in an available MFJ Model MFJ-941D antenna tuner. The differences at 14.2 and 24.95 MHz are particularly conspicuous.

In Tables III through V, computer model Z_{in} values for three cases are compared to experimentally measured Z_{in} numbers. To quantify agreement (or absence of agreement) between theory and experiment, it is useful to define an error function U by

$$U = \sum_{i=1}^{8} \left[\left(R^i_{theory} - R^i_{meas.} \right)^2 + \left(X^i_{theory} - X^i_{meas.} \right)^2 \right] \tag{1}$$

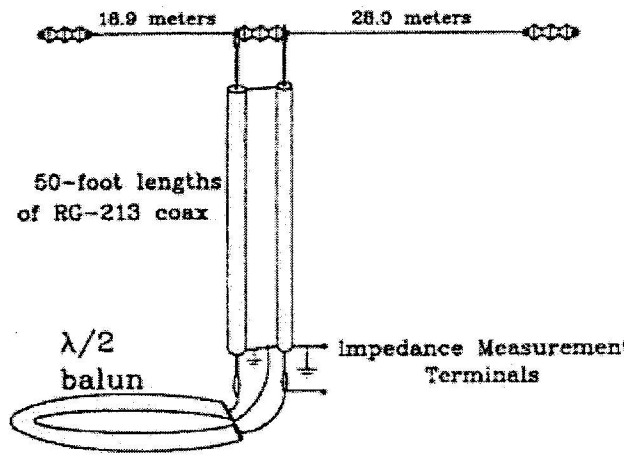

Fig. 2. Principal measurement configuration.

Table II
Comparison of Measured Z_{in} for Monoband Coax Balun versus Commercial 4:1 Balun

Frequency	Coaxial Balun	Broadband Balun
MHz	Z_{in} Ω	Z_{in} Ω
3.8	$9.8 + j4.8$	$2.7 + j12.3$
7.2	$37.2 - j53.7$	$11.5 - j23.3$
10.1	$4.3 + j22.1$	$3.3 + j25.8$
14.2	$7.2 - j27.3$	$64.2 - j80.3$
18.15	$48.2 + j39.2$	$71.7 + j24.4$
21.3	$5.3 - j2.1$	$5.7 + j5.8$
24.95	$35.8 + j73.1$	$150 + j1.3$
28.5	$7.9 + j10.2$	$13.1 + j32.8$

Error function U is a fundamental indicator of difference between the two quantities. The focus for Table III is predicted impedances for the antenna in a free-space environment. Table IV is similar, but with antenna impedances predicted in the presence of non-ideal ground. Tables III and IV both employ the network of Figure 2. It is interesting to note that, in the context of the Figure 2 configuration, the differences between computer modeling of the antenna system in a free-space environment and in the presence of real ground are small.

Table V addresses the first of two alternative configuration proposals that naturally arise. Namely, the balun is placed at the antenna terminals rather than at the transmitter, as illustrated in Figure 3. This reduces the transmission line requirement to one cable, and presumably minimizes extraneous rf currents flowing on the outer conductor of that single cable. On the other hand, one rightfully would expect that placing the balun at the antenna feed terminals changes the current distribution so that NEC2 predictions will be less accurate. The data of Table V substantiate that concern, as the error function value zooms in this case.

Table III
Predicted versus Measured Impedance
Measurement Circuit of Figure 2
Ground Absent

Frequency MHz	Theoretical Z_{in} Ω	Measured Z_{in} Ω
3.8	$3.6 + j0.9$	$9.8 + j4.8$
7.2	$23.8 - j70.2$	$37.2 - j53.7$
10.1	$3.2 + j0.9$	$4.3 + j22.1$
14.2	$14.2 - j46.2$	$7.2 - j27.3$
18.15	$11.9 + j37.7$	$48.2 + j39.2$
21.3	$8.8 - j28.4$	$5.3 - j2.1$
24.95	$12.9 + j33.3$	$35.8 + j73.1$
28.5	$15.8 - j5.8$	$7.9 + j10.2$
Error function $U = 5,813$		

Table IV
Predicted versus Measured Impedance
Measurement Circuit of Figure 2
Ground Present

Frequency MHz	Theoretical Z_{in} Ω	Measured Z_{in} Ω
3.8	$3.4 + j0.9$	$9.8 + j4.8$
7.2	$23.4 - j71.0$	$37.2 - j53.7$
10.1	$3.3 + j1.1$	$4.3 + j22.1$
14.2	$13.8 - j46.6$	$7.2 - j27.3$
18.15	$14.1 + j36.6$	$48.2 + j39.2$
21.3	$9.2 - j28.4$	$5.3 - j2.1$
24.95	$13.1 + j32.0$	$35.8 + j73.1$
28.5	$15.5 - j8.8$	$7.9 + j10.2$
Error function $U = 5,904$		

Table V
Predicted versus Measured Impedance
Measurement Circuit of Figure 3
Ground Present

Frequency MHz	Theoretical Z_{in} Ω	Measured Z_{in} Ω
3.8	$2.6 - j20.9$	$19.9 - j15.1$
7.2	$58.1 - j114$	$83.8 - j52.1$
10.1	$9.9 - j0.7$	$12.1 + j17.4$
14.2	$40.4 - j84.6$	$32.3 - j96.4$
18.15	$88.1 + j95$	$85.7 + j31.9$
21.3	$21.5 - j53.4$	$12 - j29$
24.95	$50.6 + j65$	$103 + j127$
28.5	$40.6 + j1.3$	$18.8 - j8.4$
Error function $U = 17,194$		

The second proposal is to measure antenna feed-point impedance directly at the terminals. Former AM broadcast antenna engineers, based on their earlier experience,

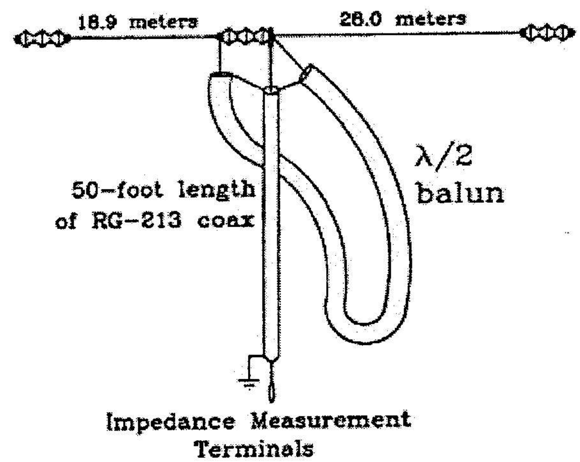

Fig. 3. Secondary measurement configuration.

will instantly view this as a highly dubious proposition for a nonresonant antenna. It is documented elsewhere, in [4] for example, that such measurement on an asymmetric antenna is not reliable. Stray reactance associated with the measuring equipment and physical connection can be highly problematic. Still, to illustrate the nature and scope of the numerical difficulties one may expect to encounter in such circumstances, we offer here a set of measured data as typical results. For this procedure, the impedance analyzer was supported in immediate proximity to the feed terminals on a wooden support. Because the impedance analyzer has only an unbalanced measurement port, it was necessary to connect one antenna feed point to instrument ground, and it was observed immediately that the "polarity" of instrument connection affects the observed impedance value. Thus, the impedance was actually measured twice, as shown in Figure 4, and the average of the two numbers is reported as the measured value. The results of this exercise are summarized in Table VI and show a measurement disturbance arising from direct connection to the antenna terminals. The error function $U = 3,693$ may appear moderate as a raw number, but one would expect a result closer to perfection ($U = 0$) for an inherently reliable measurement procedure.

Thus, the exercise described by Table VI's data suggests that the generally preferred impedance measurement configuration for (nonresonant/reactive) asymmetric antennas is to place the impedance analyzer remotely, through a section of transmission line, and then properly interpret the numbers by careful calculations that take into account the (lossy) transmission line.

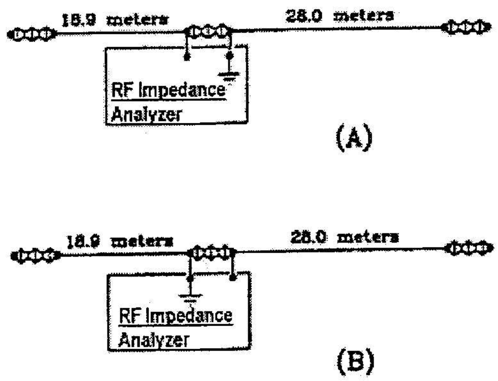

Fig. 4. Direct Z Measurement.

Table VI
Predicted Z_{in} Based on Impedances Measured Directly at Antenna Terminals

Frequency	Measured	Predicted*	Measured
MHz	Z_{ant} Ω	Z_{in} Ω	Z_{in} Ω
3.8	$237 + j376$	$4.6 + j0.8$	$9.8 + j4.8$
7.2	$639 - j840$	$15.7 - j51.6$	$37.2 - j53.7$
10.1	$404 - j653$	$3.3 + j4.5$	$4.3 + j22.1$
14.2	$676 - j595$	$10.7 - j33$	$7.2 - j27.3$
18.15	$94 - j118$	$50.2 + j25.9$	$48.2 + j39.2$
21.3	$344 - j261$	$12.3 - j21.2$	$5.3 - j2.1$
24.95	$231 - j347$	$15.8 + j36.1$	$35.8 + j73.1$
28.5	$290 - j197$	$9.3 - j11.3$	$7.9 + j10.2$
*Figure 2 configuration.			
Error function $U = 3,693$			

V. Concluding Remarks

Actual operational experience and experimentation with similar antenna geometries over an extended period of time, as well as results of this specific study, clearly indicate that the feed line/balun configuration of Figure 2 is preferable over that of Figure 3. Although the outer conductors of the coaxial feed lines are technically a system participant in the real-world implementation, it has been found that feed line involvement is negligible when the coax feed is directed away from the antenna feed point at a right angle. The communications link performance associated with the Figure 3 circuit has been found to be consistently inferior to that of the Figure 2 configuration, attesting to the effect of the altering the current distribution on the antenna by placing the balun directly at the feed point.

For determination of matching network component value requirements at the transmitter, it turns out that the results from Tables III and IV are equivalently acceptable. For the particular wire antenna geometry of this study, it is clear (in retrospect) that the extra time and effort to include non-ideal ground effects were not necessary when attention is restricted to impedance characteristics. Of course, real ground presence has a profound effect on radiation patterns and efficiency at the indicated low height above ground of Figure 1. Thus, accounting for real ground is essestial for NEC characterization of the antenna's radiation properties, a matter for separate investigation.

The antenna is mismatched (with respect to a 50Ω resistive transmitter output impedance) at all the target operating frequenices. The important fact, however, is that the antenna offers impedances in all eight hf bands that are easily matched by available commercial tuners such as the MFJ-941D and MFJ-989B. Furthermore, operating away from natural resonant frequencies, through a matching network, results in a relatively high-Q operating environment that serves to reduce the radiation of harmonic frequencies that may be present at significant levels in the output of certain transmitter types.

On-air operational experience has been that this multiband antenna type is suprisingly effective on the bands from 10.1 MHz through 28.5 MHz. At 7.2 MHz, the radiation angle is high due to the horizontal orientation in relatively close proximity to ground, and communications performance is therefore best at short to medium distances. The high angle radiation effect is more pronounced on the 3.8 MHz band, where the antenna is mostly useful for local groundwave and NVIS skywave contacts.

Where covenants and other residential constraints are absent, so that the antenna height above ground can be increased freely, the multiband off-center-fed antenna becomes quite competitive on all bands in comparison with the common alternatives of monoband quarter-wave ground mounted verticals and conventional half-wave center-fed dipoles. When elevated to a height of about 20 meters, for example, performance at 7.2 MHz becomes excellent and 3.8 MHz coverage improves substantially.

When a portable and quickly deployable multiband hf antenna is needed, or for restricted sites where only one wire antenna may be erected to cover all the hf amateur bands, the antenna described in this report is an attractive candidate worthy of serious consideration.

References

[1] American Radio Relay League, *The Radio Amateur's Handbook, 38th Edition*. Newington, Connecticut: ARRL, 1961, p.364.

[2] G.H. Hagn, "HF ground constant measurements at the Lawrence Livermore National Laboratory (LLNL) field site," *Applied Computational Electromagnetics Society Journal and Newsletter*, vol. 3, no. 2, Fall 1988.

[3] *TAME (Top Algorithms for Microwave Engineering)*, Dr. Stephen E. Sussman-Fort, Department of Electrical Engineering, State University of New York at Stony Brook.

[4] R.W.P. King, H.R. Mimno, and A.H. Wing, *Transmission Lines, Antennas and Waveguides*. New York: Dover Publications, 1965, p. 146.

A Review of the TLM Method and its Applications

David P. Johns, Fred J. German
Flomerics Inc., 257 Turnpike Rd., Southborough, MA 01772

Abstract: As the TLM method enters its thirtieth year, the authors review the development of the TLM method for electromagnetic analysis and its applications to EM design problems. Numerical results are provided for real world applications and benchmark problems.

I. INTRODUCTION

The solution of electromagnetic field problems by transmission-line networks is possible by the analogy that exists between wave propagation in a medium as described by Maxwell's equations and the wave propagation on transmission-lines. The TLM method uses this analogy to represent Maxwell's equations by a transmission-line matrix [1].

Consider the two-dimensional TLM node shown in Fig. 1 which consists of two ideal transmission lines crossed at a junction. If the inductance and capacitance per unit length for an individual line are L and C respectively, then the node can be represented by the lumped network shown in Fig. 2.

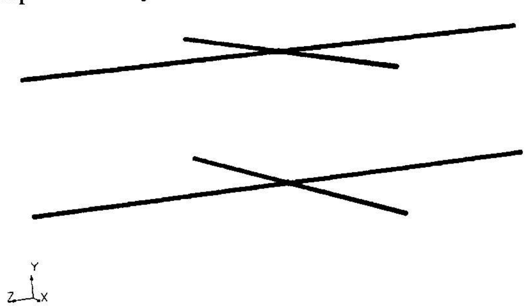

Fig. 1 Shunt Connected 2D TLM Node

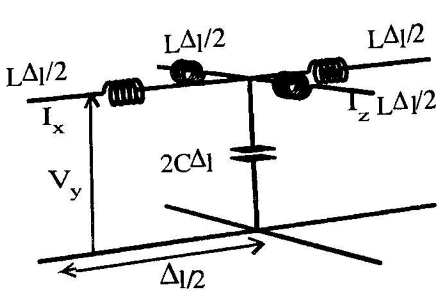

Fig. 2 Equivalent Circuit for Shunt Node

The transmission line equations which describe the voltage and current at this node are:

$$\frac{\partial V_y}{\partial x} = -L_i \frac{\partial I_x}{\partial t} \tag{0.1}$$

$$\frac{\partial V_y}{\partial z} = -L_i \frac{\partial I_z}{\partial t} \tag{0.2}$$

$$\frac{\partial I_x}{\partial x} + \frac{\partial I_z}{\partial z} = -2C_i \frac{\partial V_y}{\partial t} \tag{0.3}$$

These equations may be combined to give the wave equation:

$$\frac{\partial^2 V_y}{\partial^2 x} + \frac{\partial^2 V_y}{\partial^2 z} = 2LC \frac{\partial^2 V_y}{\partial^2 t} \tag{0.4}$$

A similar set of equations can be obtained from the expansion of Maxwell's Curl equations. For d/dy = 0 and a lossless medium (conductivity $\sigma = 0$), the set of equations (which represent the TE mode solution) are:

$$\frac{\partial E_y}{\partial x} = -\mu \frac{\partial H_z}{\partial t} \tag{0.5}$$

$$\frac{\partial E_y}{\partial z} = \mu \frac{\partial H_x}{\partial t} \tag{0.6}$$

$$\frac{\partial H_x}{\partial z} - \frac{\partial H_z}{\partial x} = \varepsilon \frac{\partial E_y}{\partial t} \tag{0.7}$$

where μ and ε are the permeability and the permittivity of the medium respectively. These equations may also be combined to give the wave equation:

$$\frac{\partial^2 E_y}{\partial^2 x} + \frac{\partial^2 E_y}{\partial^2 z} = \mu\varepsilon \frac{\partial^2 E_y}{\partial^2 t} \tag{0.8}$$

The following equivalencies between the transmission-line equations and Maxwell's equations can be established:

$$E_y \equiv V_y, \quad H_z \equiv I_x, \quad H_x \equiv -I_z \qquad \mu \equiv L, \quad \varepsilon \equiv 2C \tag{0.9}$$

Comparisons can also be made for the other set of field components Hy, Ex and E_z (TM mode) using the appropriate set of Maxwell's equations.

If voltage and current waves on each transmission-line propagate at the speed of light c then:

$$c = \frac{1}{\sqrt{L_i C_i}} \qquad \textbf{(0.10)}$$

In free space ($\mu = \mu_0$ and $\varepsilon = \varepsilon_0$):

$$c = \frac{1}{\sqrt{\mu_0 \varepsilon_0}} \qquad \textbf{(0.11)}$$

and from the previous comparisons, the complete network of intersecting transmission-lines represents a medium of relative permittivity twice that of free space. The velocity of waves on the lines Vn, is

$$V_n = \frac{c}{\sqrt{2}}. \qquad \textbf{(0.12)}$$

The ratio Vn/c deteriorates with frequency but it can be taken as constant at lower frequencies.

In TLM, a mesh is formed by connecting a large number of uniformly distributed transmission-lines. A delta-function, at time t=0, is excited at an appropriate point, then the pulses travel along the lines until they reach a junction taking one time interval ($\Delta t = \Delta l/c$) to do so. In becoming incident on the junction the pulses scatter as shown in Fig.3 according to the scattering matrices of the nodes.

The mesh as a whole consists of submatrices equivalent to the number of nodes in the mesh. The process is repeated in iterative form (each iteration = $\Delta l/c$) and the TLM solution is constructed by storing the total amplitudes at a point as the pulses arrive at that point. This output is a stream of impulses separated by a time interval $\Delta l/c$.

The output caused by any input signal, for example a digital pulse waveform, can be found by convolving the output impulse response by the shape of the input signal. In most engineering problems, it is useful to study the response of the system due to a sinusoidal waveform. This can be accomplished by taking the Fourier transform of the output impulse response.

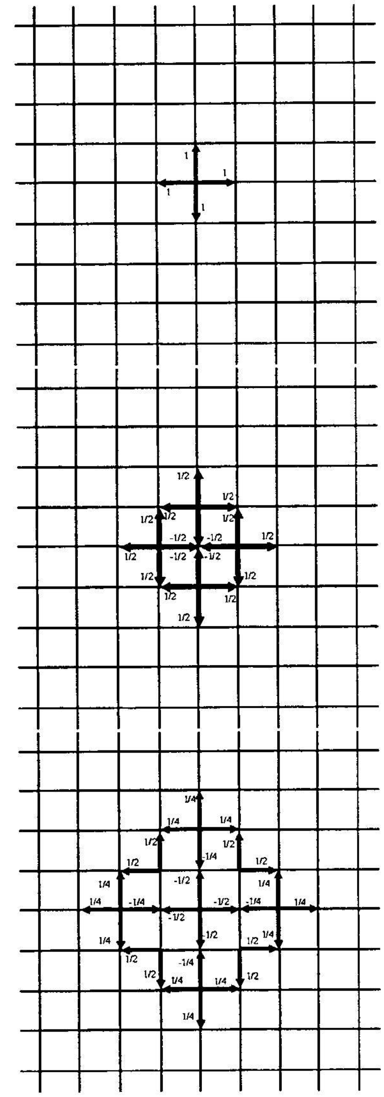

Fig. 3 Scattering and Connecting in 2-D TLM

Inhomogeneous problems require the introduction of additional capacitance at the nodes to represent an increase in permittivity. This is achieved by introducing an open-circuit stub of normalized characteristic admittance Y_0 [2]. Also the losses in the medium can be accounted for by the addition of an infinitely long stub of normalized characteristic admittance G_0. At each time step, part of the energy scatters into the loss stub and never returns, thus modeling a loss mechanism within the TLM mesh.

The use of shunt connected transmission-lines is not the only approach available. An alternative method would be to represent the fields with series connected nodes [3].

Solutions can be obtained, in this case, by comparisons between the transmission-line equations of the series node and Maxwell's equations. It can be seen that two meshes made up of thes two types of nodes can be used to represent both TE and TM wave propagation within the grid.

II. 3-D EXPANDED NODE TLM

The two nodes can be combined to form a total solution of Maxwell's equations in three-dimensions. One way to build up such a 3-D model is by having alternative shunt and series nodes separated from each other by $\Delta l/2$ [4]. 3-shunt and 3-series nodes connected as shown in Fig. 5 provides a complete solution.

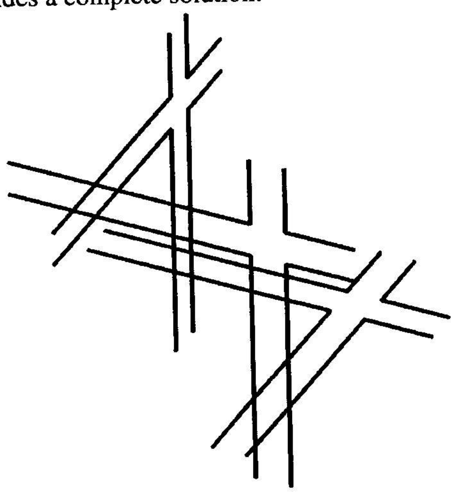

Fig. 4 3-D Expanded TLM Node formed from 2-D Shunt and Series Nodes

The six components of the electromagnetic field are available in the 3-dimensional nodes and are analogous to common voltage (E-field) or common currents (F- field) at the shunt or the series nodes. Also, it is important to see that μr, εr and σ of the medium represented by the 3-dimensional node may be made variable, simply by adjusting the values Z_0, Y_0 and G_0 respectively. Any complicated inhomogeneous medium may be described by a model made up of a large number of such 3-dimensional nodes.

In TLM the physical properties of a problem can be expressed directly in terms of transmission-line model parameters without the need to formulate the problem as a calculus model first. The simplicity in which problems can be formulated by the method and the ease in which the method is used are an advantage.

The TLM method has been developed so that it is possible to discretise the space irregularly using a graded mesh [5]. In that sense, the mesh can be crowded at the most intricate part of the geometry.

IV. CONDENSED NODES

As numerical methods in electromagnetics matured, a noted disadvantage was found in both the expanded TLM and the Yee Finite Difference methods. The six field components are spatially separated within a cell, which makes boundary conditions, mesh grading and the inclusion of sub-cell features such as wires complicated and difficult to apply. To alleviate this problem, P. B. Johns developed a new approach in 1987 and called it the Symmetrical Condensed Node (SCN) [6,7].

The basic Symmetrical Condensed Node (SCN) without stubs is depicted in Fig. 8. Each node has 12 transmission lines all having the same characteristic impedance Z_0. There are two pairs of transmission- lines in each direction of propagation to carry the two orthogonal polarisations. The field components are all referenced to the cell-center, and fields are also available at the cell boundaries.

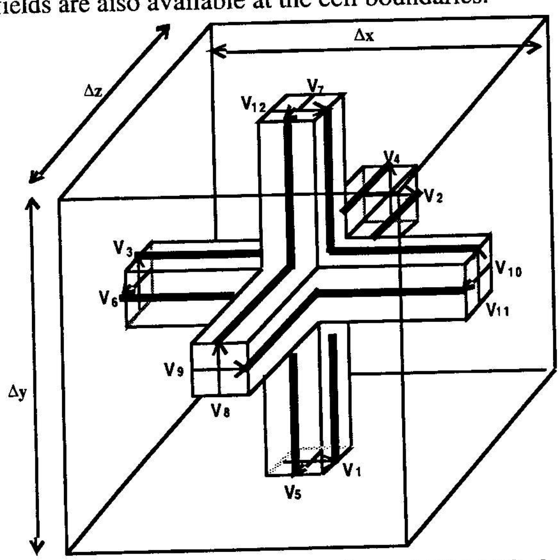

Fig. 5 3-D Symmetrical Condensed TLM Mesh

The terms in the 12-port scattering matrix are developed by writing the field coupling in Maxwell's equations in terms of the voltage and currents associated with each line. The scattering coefficients are then found by applying energy conservation rather than formulating equivalent electrical circuits. The result is a "remarkably simple" [6] formulation.

$$
[S] = 1/2 \begin{bmatrix}
 & 1 & 1 & & & & & & 1 & & -1 & \\
1 & & & & & 1 & & & & -1 & & 1 \\
1 & & & 1 & & & & 1 & & & & -1 \\
 & & 1 & & 1 & & -1 & & & & 1 & \\
 & & & 1 & & 1 & & -1 & & 1 & & \\
 & 1 & & & 1 & & 1 & & -1 & & & \\
 & & & -1 & & 1 & & 1 & & 1 & & \\
 & & 1 & & -1 & & 1 & & & & 1 & \\
1 & & & & & -1 & & & & 1 & & 1 \\
 & -1 & & & 1 & & 1 & & 1 & & & \\
-1 & & & 1 & & & & 1 & & & & 1 \\
 & 1 & -1 & & & & & & 1 & & 1 &
\end{bmatrix}
$$

Fig. 6 SCN scattering Matrix

Extensive studies have been made to compare the accuracy of the SCN with the expanded node and FDTD formulation. In particular, German et al have documented the dispersion of waves travelling over a 3D irregular mesh [8].

The SCN has the advantage of exhibiting less dispersion than the expanded node and FDTD for both regular and graded meshes. This is particularly noticeable when using a graded mesh that has an abrupt change in cell size [8].

Simons et al have made a comparison of SCN TLM and the Yee formulation of FDTD for a problem containing a sharp metallic edge [9]. The authors have found that "in order to achieve the same accuracy, the FDTD mesh must be 1.49 times as fine as the TLM mesh." Including the computational costs of the algorithms, the FDTD algorithm requires 1.65 times as much memory, and 3.84 times as much computational effort in order to achieve the same accuracy as the corresponding TLM simulation for problems with sharp metal edges.

It should be noted, that Chen, Ney and Hoefer, recognizing the needs for improved resolution and accuracy, proposed a new condensed formulation of the FD-TD method [10]. In addition, a condensed frequency-domain Finite-Difference approach has been put forth [11].

V. ADVANCED TLM TECHNIQUES

While a detailed theoretical presentation of advanced TLM modeling techniques is beyond the scope of this paper, it is appropriate to at least mention several improvements that have dramatically improved the modeling efficiency of the TLM method.

Over the last decade, the SCN has been improved further resulting in the Hybrid Node [12] and Super- Condensed Node [13], resulting in greater computation efficiency and improved accuracy.

Multi-grid formulations of SCN have been developed to enable the mesh to be refined in a truly local manner, thereby saving huge computation resources [14].

A Frequency-Domain formulation of TLM based on the SCN has also been introduced to compliment the time-domain technique [15].

It is possible to model single [16] or multi-wires [17], thin slots [18] and thin non-perfectly conducting panels [19] in the SCN TLM mesh. These 'sub-cell' models which permit small features to be modeled within a coarse mesh completely account for all field interactions and coupling. The resulting computational savings can be enormous.

Models are also available to model frequency-dependent materials [20] in the SCN TLM mesh.

VI. APPLICATIONS of TLM

3D TLM has found applications in many engineering problems; microwave design, optics, heat diffusion, to name a few. In this section we present two representative TLM application examples: one in the area of electromagnetic compatibility (EMC) and the other in antenna design.

The characterization of radiated emissions from slots and apertures in electronic equipment enclosures is a very important problem in EMC design and this problem is well suited to the TLM method. The time domain nature of the method insures that no resonances are missed in the frequency domain, and the sub-cell slot model capability allows very small seams, or gaps, in equipment enclosures to be modelled quickly and with a high degree of accuracy.

An aluminum chassis of dimensions 30 x 22 x 14 cm was modeled. The enclosure was fed with a wire connected to the top of the box by a 50-ohm coax line and terminated at the bottom of the box with a 47-ohm surface mount resistor. The enclosure contained a small slot cut into the bottom of the front panel as shown in Figure 21. The slot had dimensions 12 x 0.1 x 0.05 cm and was modelled using the sub-cell slot model. Results for the power delivered by the source and for the electric field at a point 3 m in front of the box are shown in Figures 22 and 23, respectively. Comparison with measurements from Reference [21] is observed to be excellent.

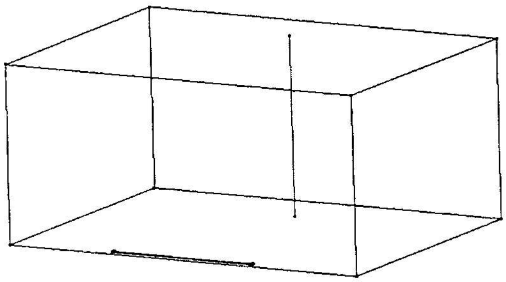

Fig. 7. Box with slot for emissions model.

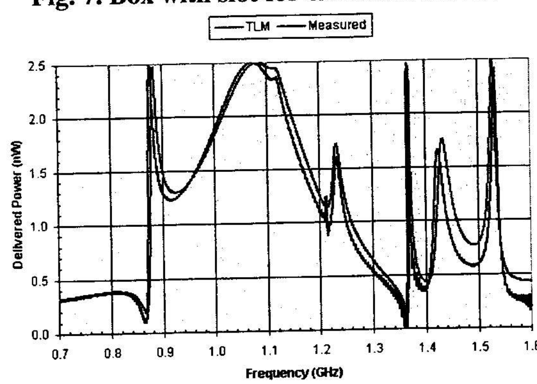

Fig. 8. Delivered power for box with slot.

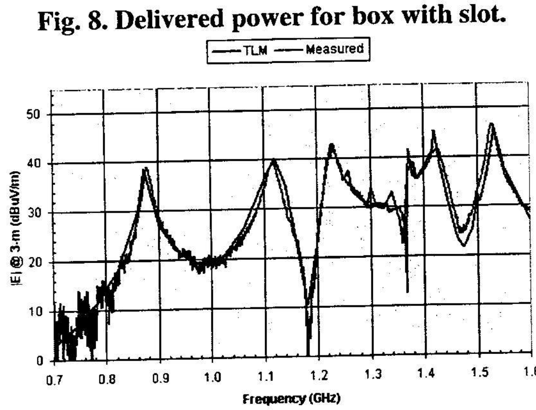

Fig. 9. Magnitude of E field 3m in front of box with slot.

The next example demonstrates the application of TLM to an antenna analysis problem. TLM is ideal for simulating antenna structures, since the analysis is performed in the time-domain. Fourier transformation leads to wideband VSWR, return-loss and radiation results. Antenna simulations usually exhibit short time-domain responses, since the input power is radiated and absorbed by the mesh absorbing boundary conditions. The bandwidth of a microstrip patch antenna can be widened by introducing U-shaped slots [22]. An example of such an antenna is shown in Fig. 10. The dimensions are W=35.5mm, L=26.0mm, Ws=12.0mm, Ls=19.5mm, a=2.2mm, b=4.3mm, c=2.1mm and F=15.0mm. The substrate is air and h=5.0mm.

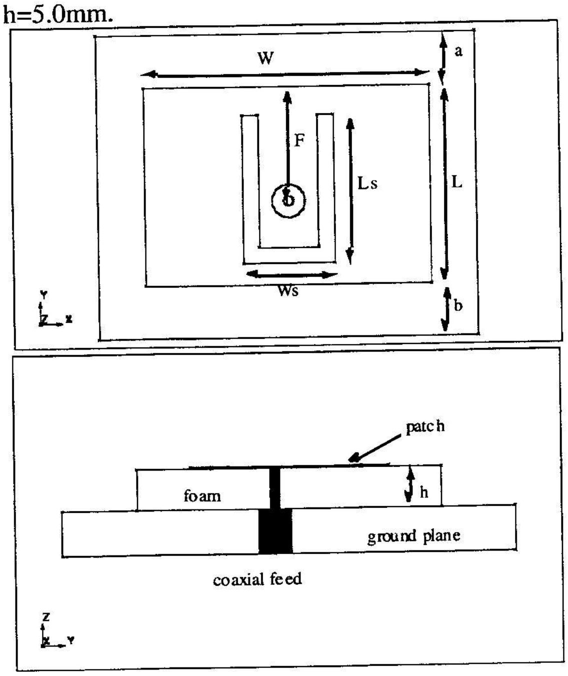

Fig. 10 Geometry of a coaxially fed patch with a U- shaped slot

The simulated and measured VSWR (Reference 22) is compared in Fig. 11 and shows excellent agreement.

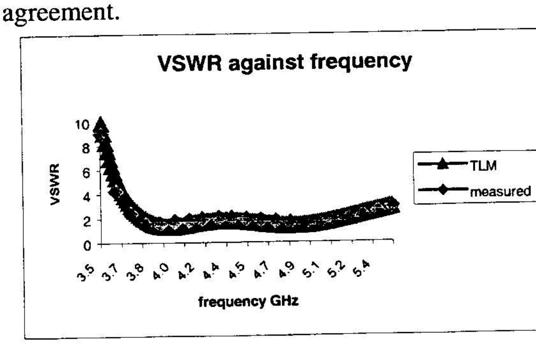

Fig. 11 VSWR against frequency for u-slot patch

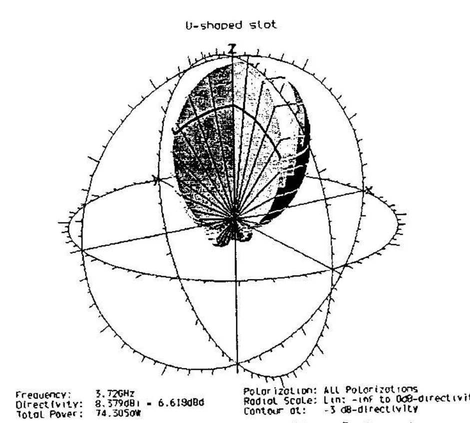

Fig. **12 Radiation pattern of u-slot antenna at 3.72 GHz**

VII. CONCLUSIONS

TLM has matured into a powerful method for electromagnetic analysis. Its beauty lies in its simplicity and direct relationship to physical processes. This has attracted many research workers to develop and apply TLM to a wide variety of problems.

It may be argued that the TLM method lends itself to EMI analysis, since it inherently employs transmission-lines and circuits to model the electromagnetic fields, concepts used widely in EMC engineering. It is relatively straightforward to include wires and lumped circuits in TLM, since these components can be represented directly by transmission-lines. The high accuracy and stability associated with condensed node TLM formulations is also attractive for antenna design engineers who increasingly rely on electromagnetic modeling.

REFERENCES

[1] Johns P. B. & Beurle R. L., ' Numerical Solution of 2-Dimensional Scattering Problems Using a Transmission-Line Matrix', Proce. IEE, Vol. 118, No. 9, Sept 1971.

[2] Akhtarzad S. & Johns P. B., ' Generalised Elements for TLM Method of Numerical Analysis', Proc. IEE, Vol. 122, No. 12, Dec 1975.

[3] Akhtarzad S. & Johns P. B., ' Three-Dimensional Transmission-Line Matrix Computer Analysis of Microstrip resonators', IEEE Trans MTT, Dec 1975.

[4] Akhtarzad, S. and Johns, P. B., 'The solution of Maxwell's equations in three space dimensions and time by the TLM method of numerical analysis', Proceedings IEE 122, 12, p.1344-1348, December 1975.

[5] Mukhtar A. & Sitch J. E., 'Transmission-Line Matrix Method with Irregularly Graded Space', IEE Proc., Vol. 128, Pt. H, No. 6, Dec 1981.

[6] Johns P. B., 'A symmetrical condensed node for the TLM method', IEEE Trans. Microwave Theory and Techniques, Vol. MTT-35, No. 4, pp. 370-377, 1987.

[7] Allen, R et al., 'Numerical results for the symmetrical condensed TLM node', IEEE trans. Microwave Theory and Techniques, Vol. MTT-35, No. 4, p.378-382, 1987.

[8] German F., Svigelj J & Mittra R., 'A Numerical Comparison of Dispersion in Irregularly Graded TLM and FDTD Meshes', Proc. Applied Computational Electromagnetics Society (ACES), Monterey, 270-279, Mar 1996.

[9] Simons N. R. S. et al., 'Comparison of the Transmission-Line Matrix and Finite-Difference Time-Domain Methods for a Problem Containing a Sharp Metallic Edge', IEEE Trans MTT, Vol. 47, No. 10, Oct 1999.

[10] Chen Z. et al., 'New Finite-Difference Time-Domain Formulation and its Equivalence', IEEE Trans on Microwave Theory and Techniques, Vol. 39, No. 12, December 1991.

[11] Afande M. M., et al., 'A Finite Difference Frequency-Domain Method that Introduces Condensed Nodes and image Principle';, IEEE Trans MTT, Vol. 43, No. 4, April 1995.

[12] Scaramuzza R. & Lowery A.,'Hybrid symmetrical condensed node for the TLM method ', I.E.E. Electronics Letters, Vol. 26, No. 23, 8th November 1990, pp. 1947-1948.

[13] Trenkic V., Christopoulos C. & Benson T. M., 'New symmetrical super-condensed node for the TLM method', I.E.E. Electronics Letters, Vol. 30, No. 4 , 17th February 1994, pp. 329-330.

[14] Wlodarczyk A. J., 'New Multigrid Interface for the TLM Method', IEE Electronics Letters, Vol. 32, No. 12, June 1996.

[15] Johns D. P. et al., 'New TLM technique for steady- state field solutions in three dimensions', I.E.E. Electronics Letters, Vol. 28, No. 18, 27th August 1992, pp. 1692-1694.

[16] Wlodarczyk, A.J.; Johns, D.P.,'New wire interface for graded 3-D TLM, IEE Electronics Letters , Volume: 28 Issue: 8 , 9 April 1992, Page(s): 728 -729.

[17] Trenkic V.,et al.., 'Modelling of coupling between transient electromagnetic field and complex wire structures', International Journal of Numerical Modelling, vol. 12, 257-273, 1999.

[18] Mallik A., Johns D. P. & Wlodarczyk A. J., 'TLM Modelling of Wires and Slots', Proc. International EMC Conf., Zurich 1993.

[19] Johns D. P. et al., 'New TLM models for thin structures', IEE Proc. Int. Conf. on Computation in Electromagnetics, Conf. Publ. No. 350, pp. 3335-338, Nov. 1991.

[20] Paul, J et al.,' Generalized material models in TLM .I. Materials with frequency-dependent properties', Antennas and Propagation, IEEE Transactions on , Volume: 47 Issue: 10 , Oct. 1999, Page(s): 1528 -1534.

[21] Li, M., 'EMI from Shielding Enclosures - FDTD Modelling and Measurements', Electromagnetic Compatibility Laboratory, University of Missouri-Rolla

[22] Lee K. F et al., 'Experimental and simulation studies of the coaxially fed U-slot rectangular patch antenna', IEE Proc. Microw. Antennas Propag., Vo. 144, No. 5, Oct 1997.

Editor's note: this issue of the ACES newsletter starts a new column on CEM for commercial EMI/EMC applications. Colin Brench will be providing these articles of topics of interest to commercial CEMists.

Computational Electro-Magnetics in Commercial EMC Design

Colin Brench
Compaq Computer Corp.

Home electronic devices have reached very high levels of sophistication. For example, home computers are now available with computational power that would have pleased everyone involved in computational electromagnetics (CEM) just a few years ago. Along with these advances in digital electronics have come far more sophisticated electromagnetic compatibility (EMC) challenges. The first PC's had clock frequencies of 4.7 MHz; today they approach 2 GHz, and there is little reason to expect them to stop here. This is almost a one thousand-fold increase, and the EMC design rules used 20 years ago are really not up to the task of designing these faster computers.

This ever increasing product complexity is making the use of CEM more popular with EMC engineers than it has ever been. Over the years, EMC engineers have continued to develop their own design rules. Usually, these rules are very specific to a particular type of product, and are additions to the basic rules in general use. To be used properly, any design rule must be fully understood; when can it be applied and when not? More importantly, what were the assumptions behind the original rule, and what are its limitations? This is where CEM can be especially beneficial; CEM can expand and clarify an engineer's understanding of the problem. When the EMC design rules are understood they can provide an excellent starting point for those EMC engineers who wish to begin using CEM.

One challenge in effectively using CEM for EMC design is in learning how to define the problem that has to be addressed. Unfortunately, EMC issues usually have to be considered at the system level, and this can make it hard to break the problem into practical parts for modeling. A second challenge is to obtain valid source data. The characteristics that greatly influence electromagnetic interference (EMI) are usually considered to be parasitics or stray effects, and therefore are not defined. The characteristics of concern include: signal rise times, low levels of stray coupling, imperfect signal routing, and similar effects.

Today, while the numbers are growing, there are still relatively few EMC engineers who use CEM as a regular part of their design work. One reason for this is the relatively steep learning curve that must be faced, which is in direct conflict with the need to finish the design within a strict time-table. To this end, organizations such as ACES and the IEEE EMC Society are actively providing much needed introductory training. Training is needed in the various numerical techniques and in how to apply them to practical problems. In many cases, a greater depth of electromagnetic theory is also very beneficial.

There are many ways to apply CEM tools to EMC that fall along traditional design lines, such as the prediction of the radiated field strength from a shielded enclosure or from connecting cables. There are also non-traditional applications that open a wider view of EMC design, such as predicting induced voltages across slots that can be measured on a lab bench. There is a great potential for CEM to be used to develop other diagnostic tests.

For CEM to be more accepted in the EMC world, there are a number of related considerations that must be addressed. It is well known within the EMC field that measurement accuracy is not high; indeed, measurement uncertainty is a major topic of interest. This naturally leads to questions of accuracy in modeling. There is great comfort in measurements, even with the associated uncertainty, and the question asked is always how well the model compares to the measurements. While these problems are more emotional than technical, they are still very much in people's minds when evaluating the use of CEM.

In addition to the measurement and modeling uncertainty, other concerns include measurement and modeling correlation, starting data, and how CEM is used in EMC design. These issues and others will be covered in future articles in this Newsletter. There is no doubt that modeling is a powerful tool for the EMC engineer; however, its full potential is still to be realized.

THIS PAPER IS REPRINTED FROM THE MARCH ISSUE, IN CORRECTED FORM

TECHNICAL FEATURE ARTICLE

POWER SERIES ANALYSIS OF WEAKLY NONLINEAR CIRCUITS

Donald D. Weiner[1]
Andrew L. Drozd[2]

ABSTRACT

This is the third in a series of articles that explores the analysis and modeling of nonlinear behaviors in circuits, devices, and receiver systems. Analytic and numerical methods can be developed to readily analyze complex nonlinearities from elemental formulations such as the weakly nonlinear series. The topics discussed are quite general and have application to such diverse areas as automatic control, broadcasting, cable television, communications, EMC, electronic devices, instrumentation, signal processing, and systems theory. The previous articles in this series discussed the nonlinear effects of intermodulation, spurious responses, desensitization, cross modulation, gain compression/expansion as well as the concepts of average power, available power and/or exchangeable power [1-3]. In this article, we discuss in greater depth the various nonlinear modes and mechanisms that may arise in practical systems and components that incorporate nonlinear devices.

INTRODUCTION

All circuits containing electronic components are inherently nonlinear. Nevertheless, the preponderance of analyses dealing with electronic circuits assumes linear behavior. This paradox exists because (1) linear circuits are characterized by linear equations that are relatively easy to solve, (2) many nonlinear circuits can be adequately approximated by equivalent linear circuits provided the input signals are sufficiently small, and (3) closed-form analytical solutions of nonlinear equations are not ordinarily possible.

One model of a nonlinear circuit that is readily analyzed is shown in Figure 1. Observe that this model consists of a zero-memory nonlinearity preceded and followed by isolated linear filters. Use of this model is referred to as the power series approach. The nonlinearity is characterized in the time domain by its power series coefficients $\{a_1, a_2, \ldots, a_N\}$ and is said to be weakly nonlinear when only the first few terms of the power series are needed to represent the nonlinear behavior. Typically the linear filters that model the linear circuits preceding and following the nonlinear portion of the electronic device are characterized in the frequency domain by their linear transfer functions H(f) and K(f).

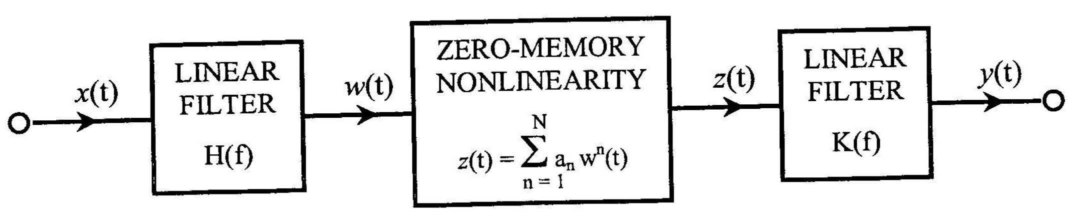

Figure 1. Power Series Model for a Nonlinear System With Memory

[1]Syracuse University, Link Hall, Syracuse, NY 13244, DDWEINER@ecs.syr.edu
[2]ANDRO Consulting Services, Beeches Technical Campus, Bldg. 3, Ste. 4, Rte. 26N, Turin Rd., Rome, NY 13440, androcs@borg.com

A system is said to have memory when the output at time t depends upon values of the input prior to time t. The nonlinearity in Figure 1 has zero memory because its output at a specific instant of time depends upon its input only at the same instant. Circuits containing energy storage elements have memory while purely resistive circuits have zero memory. Since the linear filters in Figure 1 are intended to be frequency selective, they contain energy storage elements. As a result, their outputs depend upon the past history of their inputs and the nonlinear system, as a whole, possesses memory.

The power series model is readily analyzed because the individual blocks shown in Figure 1 can be treated as isolated segments. Specifically, given the input $x(t)$, the output $w(t)$ of the first linear filter is readily obtained using conventional linear analysis. The output $z(t)$ of the zero-memory nonlinearity is then determined by substitution of $w(t)$ into the power series representation of the nonlinearity. Finally, the circuit output $y(t)$ is easily obtained as the response of the second linear filter to the known input $z(t)$. Thus, analysis of the power series model readily proceeds from input to output.

Although the power series model is an adequate representation for many electronic circuits, the reader is cautioned that this model is not universally applicable. A more general model is based upon the Volterra series or nonlinear transfer function approach [1]. However, the power series model does provide insight into the many nonlinear effects that occur in weakly nonlinear circuits [2].

Response of First Linear Filter

Allowing for the presence of interfering signals in addition to the desired signal, assume Q sinusoidal signals to be present at the input to the power series model shown in Figure 1. Hence,

$$x(t) = \sum_{q=1}^{Q} |E_q| \cos(2\pi f_q t + \theta_q). \qquad (1)$$

By introducing the complex amplitude

$$E_q = |E_q|\, e^{j\theta_q} \qquad (2)$$

and defining

$$E_{-q} = E_q^{*},\ E_0 = 0,\ f_{-q} = -f_q, \qquad (3)$$

the excitation can be expressed as

$$x(t) = 1/2 \sum_{q=1}^{Q} \left[E_q e^{j2\pi f_q t} + E_q^{*} e^{-j2\pi f_q t} \right]$$
$$= 1/2 \sum_{q=-Q}^{Q} E_q e^{j2\pi f_q t}. \qquad (4)$$

The transfer function of the first linear filter in Figure 1 is denoted by

$$H(f) = |H(f)| e^{j\psi(f)}. \qquad (5)$$

Because the filter is linear, superposition applies. Consequently, its response is a sum of sinusoids at the same frequencies as those contained in the input. Each sinusoidal output magnitude at a particular frequency equals the corresponding input magnitude multiplied by the magnitude of the transfer function at that frequency while each output phase angle equals the corresponding input angle plus the phase angle of the transfer function at that frequency. In particular,

$$w(t) = \sum_{q=1}^{Q} |E_q|\, |H(f_q)| \cos\left[2\pi f_q t + \theta_q + \psi(f_q)\right] \qquad (6)$$

For real circuits the transfer function has the property that

$$H(-f) = H^*(f) = |H(f)|e^{-j\psi(f)}. \qquad (7)$$

As a result, $w(t)$ can be written as

$$w(t) = 1/2\sum_{q=1}^{Q} [E_q H(f_q)\, e^{j2\pi f_q t} + E_q^* H^*(f_q)\, e^{-j2\pi f_q t}]$$

$$= 1/2 \sum_{q=-Q}^{Q} E_q H(f_q)\, e^{j2\pi f_q t}. \qquad (8)$$

Response of Zero-Memory Nonlinearity

The output of the zero-memory nonlinearity is

$$z(t) = \sum_{n=1}^{N} a_n w^n(t). \qquad (9)$$

The n^{th} term in this sum is said to be of n^{th} degree because it involves $w(t)$ raised to the n^{th} power. Focusing on the n^{th}-degree portion of $z(t)$,

$$a_n w^n(t) = a_n/2^n \left[\sum_{q=-Q}^{Q} E_q H(f_q)\, e^{j2\pi f_q t} \right]^n =$$

$$a_n/2^n \sum_{q_1=-Q}^{Q} \cdots \sum_{q_n=-Q}^{Q} E_{q_1} \cdots E_{q_n} H(f_{q_1}) \cdots H(f_{q_n})\, e^{j2\pi (f_{q_1}+\ldots+f_{q_n})t}. \qquad (10)$$

Consequently, Equation (9) can be written as

$$z(t) = \sum_{n=1}^{N} \sum_{q_1=-Q}^{Q} \cdots \sum_{q_n=-Q}^{Q} A_n(q_1,\ldots,q_n)\, e^{j2\pi(f_{q_1}+\ldots+f_{q_n})t} \qquad (11)$$

where

$$A_n(q_1,\ldots,q_n) = a_n/2^n E_{q_1} \cdots E_{q_n} H(f_{q_1}) \cdots H(f_{q_n}). \qquad (12)$$

Response of Second Linear Filter

Having obtained $z(t)$, the final step in the analysis is determination of $y(t)$, the output of the power series model. Note that this is also the response of the second linear filter whose transfer function is

$$K(f) = |K(f)|\, e^{j\phi(f)}. \qquad (13)$$

As was the case with the first linear filter, superposition applies and

$$y(t) = \sum_{n=1}^{N} \sum_{q_1=-Q}^{Q} \cdots \sum_{q_n=-Q}^{Q} B_n(q_1,\ldots,q_n)\, e^{j2\pi(f_{q_1}+\ldots+f_{q_n})t} \qquad (14)$$

where

$$B_n(q_1,\ldots,q_n) = A_n(q_1,\ldots,q_n)\, K(f_{q_1}+\ldots+f_{q_n}). \qquad (15)$$

Observe that the magnitude of $B_n(q_1,\ldots,q_n)$ is

$$|B_n(q_1,\ldots,q_n)| = a_n/2^n\, |E_{q_1}| \cdots |E_{q_n}|$$

$$|H(f_{q_1})| \cdots |H(f_{q_n})|\, |K(f_{q_1}+\ldots+f_{q_n})| \qquad (16)$$

while its angle is given by

$$\angle B_n(q_1,\ldots,q_n) =$$

$$\theta_{q_1}+\ldots+\theta_{q_n} + \psi(f_{q_1}) +\ldots+ \psi(f_{q_n}) + \phi(f_{q_1}+\ldots+f_{q_n}). \qquad (17)$$

The most striking feature concerning the response, as given by Equation (14), is the presence of new frequencies not contained in the input. Terms involving these new frequencies are referred to as intermodulation components. Their complex amplitudes depend upon the complex input amplitudes, the power series coefficients, and the linear transfer functions of the two filters evaluated at the appropriate frequencies.

Because $E_0 = 0$, each sum in the n-fold summation of Equation (10) contains 2Q terms. Consequently, the total number of terms in the n^{th}-degree portion of $z(t)$ is $(2Q)^n$. This number grows rapidly with increasing values of Q and n. The number of terms in $y(t)$ is identical to that of $z(t)$. As a result, evaluation of all of the terms in Equation (14) is extremely tedious. Simplification of this expression is discussed next.

Total Response for a Particular Frequency Mix

Intermodulation components whose frequencies fall well outside of the system passband are usually not troublesome because they are greatly attenuated by the frequency selectivity of the system. Thus, with regard to Equation (14), it is necessary to focus only on those terms whose frequencies fall either within or close to the system passband.

For example, consider a system tuned to 50 MHz with a 1 MHz bandwith. Assume the input to consist of two interfering sinusoids at $f_1 = 46$ MHz and $f_2 = 48$ MHz. If the system contains a nonlinearity, an intermodulation component at $2f_2 - f_1 = 50$ MHz may be generated. This falls at the tuned frequency and may cause significant interference with the desired signal when the amplitudes of the interfering tones are sufficiently large. On the other hand, the intermodulation component whose frequency is $2f_1 + f_2 = 140$ MHz falls will outside of the system passband and may be ignored.

Therefore, the first step in evaluating Equation (14) is to determine which intermodulation frequencies are of concern. Having done this, the second step is to determine the manner by which the pertinent intermodulation frequencies are generated. For this purpose, the concept of a frequency mix is introduced.

A frequency mix is characterized by the number of times the various frequencies appear in the frequency sum $(f_{q_1}+\ldots+f_{q_n})$ of Equation (14). For example, consider a power series model for which N = 5. Focus on the intermodulation frequency given by $2f_2 - f_1$. Corresponding to n=3, $2f_2 - f_1$ is produced by the single frequency mix $(f_2 + f_2 - f_1)$. Corresponding to n=5, $2f_2 - f_1$ is produced by the two frequency mixes $(f_2 + f_2 + f_2 - f_2 - f_1)$ and $(f_2 + f_2 + f_1 - f_1 - f_1)$.

As far as frequency mixes are concerned, the order in which the frequencies appear is unimportant. For example, $(f_2 - f_1 + f_2)$ represents the same mix as does $(-f_1 + f_2 + f_2)$ and $(f_2 + f_2 - f_1)$. What is important is the number of times each frequency appears in the mix. Note that $(f_2 + f_2 - f_1)$ involves $-f_1$ once and f_2 twice, $(f_2 + f_2 + f_2 - f_2 - f_1)$ involves $-f_2$ once, $-f_1$ once, and f_2 three times, while $(f_2 + f_2 + f_1 - f_1 - f_1)$ involves $-f_1$ twice, f_1 once, and f_2 twice.

The concept of a frequency mix has been introduced in order to clarify the manner by which an intermodulation frequency is produced. To avoid confusion, frequency mixes, such as $(f_2 + f_2 + f_1 - f_1 - f_1)$, are enclosed in parentheses while intermodulation frequencies, such as $2f_2 - f_1$, are not.

To aid in the representation of a frequency mix, let the number of times that the frequency f_k appears be denoted by m_k. Considering negative frequencies, recall that $f_{-k} = -f_k$. Therefore, for an excitation consisting of Q sinusoidal tones, as given by Equations (1) and (4), the input frequencies are $f_{-Q},\ldots,f_{-1}, f_1,\ldots,f_Q$. It follows that any possible frequency mix can be represented by the frequency mix vector

$$\underline{m} = (m_{-Q},\ldots,m_{-1}, m_1,\ldots,m_Q). \quad (18)$$

By way of example, assume Q = 2 corresponding to the four input frequencies f_{-2}, f_{-1}, f_1, f_2 and the frequency mix vector

$$\underline{m} = (m_{-2}, m_{-1}, m_1, m_2). \quad (19)$$

The frequency mix $(f_2 + f_2 - f_1)$ is represented by $\underline{m} = (0, 1, 0, 2)$ while $\underline{m} = (1, 1, 0, 3)$ represents the frequency mix $(f_2 + f_2 + f_2 - f_2 - f_1)$ and $\underline{m} = (0, 2, 1, 2)$ represents the frequency mix $(f_2 + f_2 + f_1 - f_1 - f_1)$.

In general, the nth-order frequency mix $(f_{q_1}+\ldots+f_{q_n})$, as appears in Equation (14), can be expressed as

$$f_{\underline{m}} = \sum_{\substack{k=-Q \\ k\neq 0}}^{Q} m_k f_k$$

$$= m_{-Q}f_{-Q}+\ldots+m_{-1}f_{-1} + m_1f_1+\ldots+m_Qf_Q. \quad (20)$$

Since exactly n frequencies are involved in an nth-order frequency mix, it follows that

$$\sum_{\substack{k=-Q \\ k\neq 0}}^{Q} m_k = m_{-Q}+\ldots+m_{-1} + m_1+\ldots+m_Q = n. \quad (21)$$

With regard to the n indices $q_1,\ldots,q_n$ of Equation (14), observe that $B_n(q_1,\ldots,q_n)$ and $(f_{q_1}+\ldots+f_{q_n})$ are unchanged by a permutation of the indices. Consequently, many of the terms in Equation (14) are identical. Corresponding to a particular frequency mix vector $\underline{m}$, it can be shown that the number of identical terms is given by the multinomial coefficient

$$(n; \underline{m}) = (n!)/[(m_{-Q}!)\ldots(m_{-1}!)(m_1!)\ldots(m_Q!)]. \quad (22)$$

For example, consider the frequency mix $(f_2 + f_2 + f_2 - f_2 - f_1)$ for which n = 5 and $\underline{m} = (1, 1, 0, 3)$. Using Equation (22), the number of identical terms in Equation (14) contributing to this mix is

$$(5; 1, 1, 0, 3) =$$

$$(5!)/[(1!)\,(1!)(0!)(3!)] = 20. \quad (23)$$

Combining all of these terms, the resulting intermodulation component is given by

$$y_5\,(t; 1, 1, 0, 3) =$$

$$20a_5/32[E_2^*E_1^*E_2^3\, H^*(f_2)\, H^*(f_1)H^3(f_2)\, K(2f_2 - f_1)\, e^{j2\pi(2f_2 - f_1)t}]. \quad (24)$$

In general, let the sum of identical terms corresponding to a particular frequency mix vector $\underline{m}$ of order n be denoted by $y_n(t; \underline{m})$. It follows that $y_n(t; \underline{m})$ can be expressed as

$$y_n\,(t; \underline{m}) =$$

$$\frac{(n; \underline{m})\, a_n}{2^n} (E_Q^*)^{m_{-Q}} \ldots (E_1^*)^{m_{-1}} (E_1)^{m_1} \ldots (E_Q)^{m_Q}$$

$$\left[H^*(f_Q)\right]^{m_{-Q}} \ldots \left[H^*(f_1)\right]^{m_{-1}} \left[H(f_1)\right]^{m_1} \left[H(f_Q)\right]^{m_Q}$$

$$K(f_{\underline{m}})e^{j2\pi f_{\underline{m}} t} \quad (25).$$

Although $y_n(t; \underline{m})$ is complex, $y(t)$ is real. Therefore, terms in Equation (14) exist in conjugate pairs.

Characterization of a nonlinear electronic circuit by the power series model requires specification of the prefilter transfer function H(f), the postfilter transfer function K(f), and the power series coefficients $\{a_1, a_2,\ldots,a_N\}$. When accurate predictions of the nonlinear responses are desired, one might expect that accurate modeling of the power series coefficients is the most critical task. Equation (25) reveals that this is not the case. The prefilter transfer function H(f) appears as a factor n times whereas the power series coefficient a_n and the postfilter transfer function K(f) appear only once. As a result, errors in the modeling of H(f) may be much more serious than similar errors in the modeling of a_n and K(f). Because of the accuracy to which H(f) must be known in order to stay within a prescribed output error, it may be exceedingly difficult to make accurate predictions of nonlinear responses when n is large.

SUMMARY

This article discussed the characterization of weakly nonlinear electronic circuits by the power series modeling approach. This approach requires the specification of prefilter and postfilter transfer functions, and the power series coefficients. The responses of the first and second linear filters, zero-memory nonlinearities, and the total response for a particular frequency mix were mathematically described. It was shown that because of the accuracy to which the prefilter transfer function must be known in order to stay within a prescribed output error, it may be exceedingly difficult to make accurate predictions of nonlinear responses when the number of terms, n, to be considered is large. In the next article in this series, we will continue to discuss the various nonlinear modes and mechanisms that arise in practical systems. The series will conclude with a presentation on new findings of research and development to add nonlinear analysis and prediction capabilities to existing CEM tools that are used to determine detailed interference rejection requirements for large, complex systems.

REFERENCES

1. D. D. Weiner and J. F. Spina, "*Sinusoidal Analysis and Modeling of Weakly Nonlinear Circuits*", Van Nostrand Reinhold Company, New York 1980, ISBN 0-442-26093-8.
2. D. D. Weiner, A. L. Drozd, K. V. Sunderland, and I. Popitich, "*Analysis and Modeling of Weakly Nonlinear Systems*", Newsletter Technical Feature Article for the Applied Computational Electromagnetics Society, Vol. 15, No. 1, ISSN 1056-9170, March 2000, pp. 9-15.
3. D. D. Weiner and A. L. Drozd, "*Power Considerations for the Measurement of Nonlinear Effects*", Newsletter Technical Feature Article for the Applied Computational Electromagnetics Society, Vol. 15, No. 2, ISSN 1056-9170, July 2000, pp 13-18.

Book Review

Book: Electromagnetic Field Measurements in the Near Field
Author: Hubert Trzaska
Publisher: Noble Publishing, 2001, 216 pages

Measurements are an essential part of electromagnetics and I thought this book could be of use to many of us. Though most electromagnetic standards address measurements in the far field, it turns out that many of the diagnostics done in electromagnetic field measurements (e.g antennas, radars, etc) are done in the near field. I have come across other texts that deal with electromagnetic field (EMF) measurements in the near field but this is a new book and addresses such near field measurements from a general approach.

The book is divided in ten chapters and their titles are as follows: Chap. 1:Introduction, Chap. 2:The Principles of Near Field EMF Measurements, Chap. 3: EMF Measurements Methods, Chap 4: Electric Field Measurements, Chap 5: Magnetic Field Measurement, Chap 6: Power Density Measurements, Chap 7: Directional Pattern Synthesis, Chap 8: Other Factors Limiting Measurements Accuracy, Chap 9: Photonic EMF Measurements, and Chap 10:Final Comments.

EMF measurements in the far field (Fraunhofer zone) is one of the less accurate measurements of physical quantities. Hazardous exposure to EMF requires field measurements in the primary and secondary field sources as well as fields disturbed by the presence of materials and the transmission media. The attention of this book is in the near field (Fresnel region). The near field conditions cause farther degradation of the near-field EMF measurements accuracy as compared to those in the far field. These difficulties bring frustration to the designers of EMF measurement equipment. The problem of EMF standards is to address the accuracy of field measurements. According to the author the accuracy of good EMF standards does not exceed +/- 5%. The book is devoted to the specific problems of EMF measurements in the near field and to the analysis of the main factors limiting the measurement accuracy, especially in the near field. Chapter 1 addresses the numeric limits and frequencies in some of the known standards. Chapter 2 provides essential information for practical metrology including a brief summary of the near field properties as well as the basic equations and formulas related to fields generated by simple radiating sources.

In order to determine the best method for EMF measurements in the near field, it is first necessary to determine which quantities best characterize the field. These quantities will then be the subject of measurements. Chapter 3 addresses the measurement of E, H and S in the near field. From the point of view of shielding, absorbing, or EMF-attenuating materials, investigations of the E, H and S measurements are sufficient. For protection from unwanted EMF, the measurement of specific absorption rate (SAR) is added to the needed measurements. The SAR is calculated based on temperature-rise measurements. The chapter also addresses the measurements of induced currents in the body. Electric field measurements are discussed in Chapter 4. The basic method of electric field measurements, within a wide frequency range, involves the use of a charge induction in a body illuminated by the field. Field averaging by a measuring antenna is discussed in the chapter and error of E-field measurement resulting from averaging of the measured field by the measuring antenna is calculated. The possibility of the field spatial distribution measurement , especially under conditions of multipath propagation and interference, and the measurement of the maximal and minimal magnitudes of the field strength requires the use of probes equipped with antennas whose sizes are much longer than the wavelengths. Dipoles are normally used for such measurements and the measurement error vs. kh of the dipole antenna is calculated. It is important to know the precise frequency response of E-field measuring probes. In order to achieve this, the schematic representation of an E-field probe is studied (for low and high frequencies), as well as the schematic representation of such probes with different types of filtering. Chapter 4 also addresses the interactions of the measuring antenna and the field source and the sources of errors that such interactions introduce. This work is also extended to include errors from antenna input impedance changes. The chapter also addresses the changes to the probe's directional pattern. The magnitudes of the calculated directional pattern irregularities versus kh are presented. This consideration is related to the electrical length of the dipoles, which is of special concern when resonant antennas are used (for shorter antennas the error vanishes). The chapter ends with comparison of E-field probes.

Chapter 5 is very similar to Chapter 4 in its approach to addressing magnetic field measurements. This chapter discusses probe properties for RF magnetic field measurements and in particular, the factors limiting measurement accuracy. The approach is limited to a probe consisting of a circular loop antenna loaded with a detector of a shaped frequency response. The majority of the presented estimations are fully applicable for Hall-cell probes, magneto-optic probes, magneto-diode probes, and for other designs, especially when considering the averaging of the measured field upon the surface of the measuring antenna. As was done in Chapter 4, the frequency response of the probe is modeled using circuit analysis by representing the probe in its electrical schematic representation. The error in the accuracy of the measurement is made as a function of the distance between the source of radiation and the antenna. The effect of antenna input impedance is also addressed in the calculations.

Power density measurements are discussed in Chapter 6. The power density measurements in the near field (especially in proximity to electrically small sources), using the electric or magnetic field measurement, are burdened with an error. The value of the error is dependent upon the type and the structure of the source and the measured EMF component as well as the distance between the source and a point of observation. Based on error measurements as a function of kR , as well as assuming the smallest distances from a field source in which the measurements should be performed, it is possible to estimate the minimal frequency at which the measurement may be applied without the necessity of using additional correction factors. Because of the deterministic character of the error, the factors may be analytically estimated for a known source type, measured EMF component, propagation geometry and distance. Widely applied methods of electromagnetic power density measurement were presented and analyzed in this chapter. The considerations are purely theoretical in character and they are concerned with the field relations only. The source of the accuracy limitation of the measurement, the error of the method, was demonstrated in the chapter and the magnitude of the error for different combinations of source and measurement was estimated. Then, a certain improvement of the accuracy, as a result of simultaneous measurements of E and H fields, and calculation of an arithmetic or geometric mean was proposed. Chapter 7 addresses the detailed considerations of the polarization problem resulting from the need to understand and apply the omni-directional probes as well as their design and construction. These needs are the result of: (1) the specificity of the polarization intricacies, especially in the near field; (2) the necessity of understanding the polarization phenomena in order to select optimal procedures when measurements are planned and for interpretation of their results and (3) the development of the ability to select an appropriate probe and meter for specific measurements conditions.

In the previous chapter, the most typical and frequent factors limiting EMF measurement accuracy were discussed. They resulted mainly from the type of antenna applied in the EMF probe, its size and mutual coupling between the antenna and the radiation source. In Chapter 8 a brief discussion is presented on the influence of thermal drift on probe parameters, the role of its dynamic characteristics and the deformation of the measured field by a person performing the measurements by the meter, by resonant phenomena and by other factors.

Chapter 9 addresses the issue of photonic measurements. There is considerable literature devoted to the field of opto-electronics elements used as sensors for a variety of physical measurements. Several publications discuss the use of opto-electronic transducers for EMF measurements. The principle of photonic transducers may be applied to the modulation of an optical beam. The subject of the modulation may be the signal's phase (which is a function of the light velocity of propagation in an electro-optic medium), its frequency, amplitude or polarization. The type of modulation as well as that of the electro-optic crystal are selected in such a way as to obtain the device's maximal sensitivity. Sensitivity is still a measurment issue with optical detectors. In Chapter 9 two approaches are followed: the direct interaction of the measured field onto the electro-optical crystal and a voltage induced by the field in an auxiliary antenna (playing the role of the measured field concentrator) impressed on the modulator. Apart from technological differences, the factors limiting measurements accuracy are, in the case of the photonic probes, similar or identical to those discussed in Chapter 8. Chapter 10 is dedicated to some final comments by the author.

INDEX TO COMPUTER CODE REFERENCES FOR VOL. 15 (2000) OF THE *ACES JOURNAL* AND THE *ACES NEWSLETTER*

This computer code index is usually updated annually and published in the second issue of each volume of the *ACES Newsletter.*

LEGEND:

AJ	ACES Journal
AN	ACES Newsletter
SI	Special Issue
*	Pre- or postprocessor for another computational electromagnetics code
**	Administrative reference only: no technical discussion (This designation and the index do not include bibliographic references)
Page No.	The first page of each paper in which the indicated code or technique is discussed

Special Issue Topics:

AJ No. 2 – Special Issue on Genetic Algorithms
AJ No. 3 – Special Issue on Computational Electromagnetic Techniques in Mobile Wireless Communications

NOTE: the inclusion of any computer code in this index does not guarantee that the code is available to the general ACES membership. Where the authors do not give their code a specific name, the computational method used is cited in the index. The codes in this index may not all be general-purpose codes with extensive user-oriented features – some may only be suitable for specific applications. While every effort has been made to be as accurate and comprehensive as possible, it is perhaps inevitable that there will be errors and/or omissions. We apologize in advance for any inconvenience or embarrassment caused by these.

Allen W. Glisson and Ahmed A. Kishk, Editors-in-Chief, *ACES Journal*
16 May 2001

ABSTRACTS OF *ACES JOURNAL* PAPERS

VOLUME 15, 2000

This compilation of abstracts is updated annually and is normally published in the second issue of the *ACES Newsletter* of the following year. Most of the abstracts below were extracted from the searchable abstract database on the ACES web site at aces.ee.olemiss.edu. A few of the abstracts were scanned. Minor editing and reformatting of the abstracts was done. As Editors-in-Chief, we accept full responsibility for any errors and/or omissions that appear in the text. We apologize in advance for any inconvenience or embarrassment caused by such errors. The full text of the papers is also available to ACES members on the ACES web site.

Allen W. Glisson and Ahmed A. Kishk, Editors-in-Chief, *ACES Journal*
15 May 2001

EMAP5: A 3D HYBRID FEM/MOM CODE

Y. Ji and T. Hubing

EMAP5 is a numerical software package designed to model electromagnetic problems. It employs the finite element method (FEM) to analyze a volume, and employs the method of moments (MoM) to analyze the region exterior to the FEM volume. The two methods are coupled by enforcing the continuity of the tangential fields on the interface. Dielectrics, lossy dielectrics, and metal objects can be modeled within the FEM volume. Metal objects can also be located exterior to, or on the surface of the FEM volume. A simple input file translator (SIFT) is provided with EMAP5 that allows users to define basic input configurations on a rectangular grid without a graphical interface. It is also possible to use commercial mesh generators to analyze more complex geometries of arbitrary shape. EMAP5 can model three types of sources: incident plane waves, voltage sources on metal patches and impressed current sources in the finite element region. This paper describes the implementation of EMAP5 and provides four examples to demonstrate the range of configurations that EMAP5 is capable of modeling using the SIFT translator. **[Vol. 15, No. 1 (2000), pp. 1-12]**

A HYBRID MOM/FEM TECHNIQUE FOR SCATTERING FROM A COMPLEX BOR WITH APPENDAGES

Andrew D. Greenwood and Jian-Ming Jin

A hybrid technique is developed to allow the scattering from small appendages to be approximately combined with the scatter from a large body of revolution (BOR). The hybrid technique thus enables the rotational symmetry of the large BOR to be exploited to solve the scattering problem with much less computational complexity than a fully three-dimensional (3-D) solution. The technique combines the finite element method (FEM) for BOR scattering with the method of moments (MoM) for small appendages. The hybrid formulation is discussed in detail, including an approximate Green's function which permits the decoupling of the solutions from the FEM and the MoM. Numerical examples are given to show the applicability and accuracy of the hybrid technique. **[Vol. 15, No. 1 (2000), pp. 13-19]**

IMPEDANCE OF A HALF-WAVE DIPOLE OVER A FINITE GROUND PLANE

P. R. Foster and R. A. Burberry

A study has been carried out on the impedance of a half-wave dipole above a finite ground plane. The Method of Moment code, NEC-4, has been used and it has been found that for ground planes which are greater than 1.0 by 1.0 wavelengths, the changes from the effect with an infinite plane are negligible. With very small planes, the current distribution across the ground plane and the impedance are substantially different from those with larger ground planes. **[Vol. 15, No. 1 (2000), pp. 21-25]**

THE DESIGN OF PLANAR SLOT ARRAYS REVISITED

J. C. Coetzee and J. Joubert

Design procedures for planar waveguide slot arrays have been known and used for years, but the inexperienced designer is often faced with a number of practical problems when trying to implement them, especially in the case of larger arrays consisting of sub-arrays. Some helpful hints concerning the numerical implementation are provided. These include an effective procedure to avoid the necessity of good initial guesses for the unknown dimensions and recommendations for the subdivision of the nonlinear equations into smaller groups. Other practical aspects which are not explicitly defined elsewhere in the literature, are also addressed. **[Vol. 15, No. 1 (2000), pp. 27-33]**

INTRODUCTION TO GENETIC ALGORITHMS IN ELECTROMAGNETICS

Randy L. Haupt

This special issue of the ACES Journal is devoted to new developments in Genetic Algorithm (GA) applications in computational electromagnetics. Genetic Algorithms have become extremely popular in the computational electromagnetics literature. The papers included in this special issue are very arcane, so I decided to include an unreviewed tutorial overview at the last minute as an introduction for those of you who are at a more basic level. GAs model natural selection and genetics on a computer to optimize a wide range of problems. **[Vol. 15, No. 2 (2000)]**

A GENETIC ALGORITHM OPTIMIZATION PROCEDURE FOR THE DESIGN OF UNIFORMLY EXCITED AND NONUNIFORMLY SPACED BROADBAND LOW SIDELOBE ARRAYS

Brian J. Barbisch, D. H. Werner, and P. L. Werner

This paper presents a systematic methodology for designing uniformly excited broadband low sidelobe linear and planar antenna arrays by varying interelement spacings. In the past, attempts to develop a robust array broadbanding design technique have been only marginally successful because of the large number of possible spacing combinations involved, coupled with the theoretical limitations surrounding the problem. The genetic algorithm (GA) has recently proven to be a very effective design tool for nonuniformly spaced low sidelobe antenna arrays with uniform excitation intended for operation at a single frequency. This paper introduces an approach for extending previous applications of GA to include the design of optimal low sidelobe arrays that operable over a band of frequencies. In addition, it will be demonstrated that designing for low sidelobe operation over a bandwidth adds significant array steerability that can be described as a simple mathematical relation. Finally, it will be shown that the GA objective function is no more complicated to evaluate for broadbanding purposes than it is in the single frequency case. Several examples of GA-designed broadband low sidelobe arrays will be presented and discussed. **[Vol. 15, No. 2 (2000), pp. 34-42]**

APPLICATION OF EVOLUTIONARY OPTIMIZATION ALGORITHMS IN COMPUTATIONAL OPTICS

Daniel Erni, Dorothea Wiesmann, Michael Spühler, Stephan Hunziker, Esteban Moreno, Benedikt Oswald, Jürg Frölich, and Christian Hafner

The spatial and spectral treatment of electromagnetic fields express an essential operation regarding, e.g., the functionality of dense integrated optical devices. Such molding of fields can hardly be handled without sophisticated heuristic optimization tools. By means of five design examples we have demonstrated that evolutionary algorithms (EA) are highly qualified to solve "real world" inverse problems considering various applications in the field of planar integrated optics, optical communication technology, and dielectric material modeling as well. In comparison to other optimization schemes EAs are even able to deliver structural and temporal information of the device under optimization which is an important feature when targeting computer guided engineering and virtual design platforms. **[Vol. 15, No. 2 (2000), pp. 43-60]**

GENETIC-ALGORITHM OPTIMIZATION OF AN ARRAY FOR NEAR-FIELD PLANE WAVE GENERATION

Neil N. Jackson and Peter S. Excell

An alternative approach to the design of an array antenna to be used to generate plane waves in the near field is presented. The original array was designed on the basis of a triangular grid of seven elements arranged in a hexagon, to minimize the number needed to achieve approximately uniform illumination of the test zone, under the assumption of isotropic element radiation patterns. In the alternative approach, a genetic algorithm was used to discover more economical distributions of elements which could still generate acceptable approximations to a plane wave zone. It was found that considerable simplifications from the 'common sense' approach were possible. **[Vol. 15, No. 2 (2000), pp. 61-74]**

INCREASING GENETIC ALGORITHM EFFICIENCY FOR WIRE ANTENNA DESIGN USING CLUSTERING

D. S. Linden and R. MacMillan

The Genetic Algorithm (GA) is a very robust, powerful technique that is capable of optimizing designs in a very multimodal search spaces. However, it also requires significant numbers of simulations to perform such optimizations. If the simulations are expensive, as in the case of antenna design, GA's can be prohibitively expensive to use. A clustering technique has been investigated which cuts the required number of function calls 20-90% with minor or no degradation in the optimization quality. In this technique, a GA using real-valued genes is halted when the population has clustered around portions of the search space, and a local optimization technique completes the optimization quickly. This method has been applied to a variety of test functions and wire antenna designs, and the advantages of this technique seem to have broad applicability. **[Vol. 15, No. 2 (2000), pp. 75-86]**

A GENETIC APPROACH FOR THE EFFICIENT NUMERICAL ANALYSIS OF MICROWAVE CIRCUITS

Luciano Tarricone

The development of efficient and effective algorithms for sparse matrix bandwidth minimization is of paramount importance for the enhancement of many numerical techniques for the analysis of microwave circuits. The test of bandwidth reduction is computationally hard. Several approaches have already been proposed, but the problem is still open. In this paper, a genetic solution is proposed. The genetic algorithm is described, as well as its main characteristics (choice of chromosomes, genetic operations, etc.). Results demonstrate that the advantages of the genetic approach vanish because of the huge computational effort required. This severe limitation is removed thanks to the natural amenability of genetic algorithms to a parallel implementation. Results in the paper prove that a parallel genetic approach is a state-of-the-art solution to the problem of bandwidth reduction of sparse matrices encountered in electromagnetic numerical methods. **[Vol. 15, No. 3 (2000), pp. 87-93]**

OPTIMUM POPULATION SIZE AND MUTATION RATE FOR A SIMPLE REAL GENETIC ALGORITHM THAT OPTIMIZES ARRAY FACTORS

Randy L. Haupt and Sue Ellen Haupt

The population size and mutation rate of a genetic algorithm have great influence upon the speed of convergence. Most genetic algorithm enthusiasts use a large population size and low mutation rate due to the recommendations of several early studies. These studies were somewhat limited. This paper presents results that show a small population size and high mutation rate are actually better for many problems. **[Vol. 15, No. 2 (2000), pp. 94-102]**

A NOVEL PRECONDITIONING TECHNIQUE AND COMPARISON OF THREE FORMULATIONS FOR HYBRID FEM/MOM METHODS

Yun Ji, Hao Wang, and Todd H. Hubing

Hybrid FEM/MoM methods combine the finite element method (FEM) and the method of moments (MoM) to model inhomogeneous unbounded problems. These two methods are coupled by enforcing field continuity on the boundary that separates the FEM and MoM regions. There are three ways of formulating hybrid FEM/MoM methods: outward-looking formulations, inward-looking formulations and combined formulations. In this paper, the three formulations are compared in terms of computer-resource requirements and stability and four sample problem geometries. A novel preconditioning technique is developed for the outward-looking formulation. This technique greatly improves the convergence rate of iterative solvers for the type of problems investigated in this study. **[Vol. 15, No. 2 (2000), pp. 103-114]**

A NEW EXCITATION MODEL FOR PROBE-FED PRINTED ANTENNA ON FINITE SIZE GROUND PLANES

F. Tiezzi, A. Alvarez-Melcón, and Juan R. Mosig

This paper presents a new excitation model for probe-fed printed antennas on both infinite and finite size ground planes. The model has been developed within the general frame of the mixed potential integral equation (MPIE) and the method of moments (MoM). The technique is based on a delta-gap voltage model, and a special procedure is implemented inside the integral equation to effectively impose a voltage reference plane into a floating metallic plate which is acting as a ground plane. The present technique allows the accurate calculation of the input impedance of printed antennas, and the effects of finite size ground planes can be easily accounted for in the calculations. In addition, an efficient technique is present for the evaluation of the radiation patterns of printed antennas, taking also into account the presence of the finite size ground plane. Comparisons with measured results show that the new derived excitation method is indeed accurate, and can be used for the prediction of the backside radiation and sidelobe levels of real life finite ground plane printed antennas. **[Vol. 15, No. 2 (2000), pp. 115-125]**

A RANDOM-PHASE-ASSISTED RAY-TRACING TECHNIQUE FOR WIRELESS CHANNEL MODELING

Houtao Zhu, Jun-ichi Takada, Kiyomichi Araki, and Takehiko Kobayashi

A random-phase-assisted ray-tracing technique for predicting spatio-temporal wireless channel parameters is presented. A two dimensional-three dimensional (2D-3D) hybrid ray-tracing algorithm is implemented in code for the prediction of channel parameters in outdoor micro- and pico-cellular urban environments. Meanwhile, a Random Phase Approach (RPA) is applied in the ray-tracing algorithm. The application of the RPA is intended for two purposes: 1) to account for the effects of inaccurate antenna positions; 2) to predict the range of short-term fading fluctuation. Several measurements carried out in pico-cell environments confirm the calculation accuracy of this technique. It was found that measured fluctuation of path-loss and delay profiles are almost fully confined within the 90% confidence interval, providing that the approach can account for the effects mentioned above. In addition, the conventional verification of path-loss and delay profiles predicted by ray tracing was extended to include the verification of angle-of-arrival (AOA). The demonstrated calculation accuracy in spatial and temporal domain confirms the applicability of authors' technique to analyze system performance in real environments. **[Vol. 15, No. 3 (2000), pp. 126-134]**

NANOCELLS INTRASYSTEM INTERFERENCE REALISTIC WORST CASE ANALYSIS FOR OPEN SITE PERSONAL COMMUNICATION SCENARIOS

J. Gavan

The exponential growth in mobile communications is followed by the development of new generations of Personal Communication Systems (PCS). Numerous research activities and papers have been published on PCS but only a few deal with the Electromagnetic Interference (EMI) affecting those systems. This paper presents a realistic worst case analysis and computation of the PCS intrasystem interference effects on open site nanocell scenarios. The operation range is up to 200m, usually under Line of Sight (LOS) propagation conditions where intrasystem interfering signals are maximum. Analysis and computation results are provided for a typical second-generation cordless PCS CT-2 telephone (telepoint) operating in the 900 MHz frequency band. The computations show that for most cases of nanocell open site, intrasystem interference can be neglected, except for a few cases of single tone spurious. The good performance is due to PCS advanced Digital Signal Processing (DSP) technology advantages using Adaptive Power Control (APC) to optimize transmitter power requirements and to Dynamic Channel Assignment (DCA) electing the best signal to noise and interference channel available. **[Vol. 15, No. 3 (2000), pp. 135-151]**

DESIGNING EMBEDDED ANTENNAS FOR BLUETOOTH PROTOCOL

Ray Perez

In the near future, all kinds of portable devices ranging from laptops, PDAs, to cellular phones will be capable of communicating and inter-operate with each other using a new wireless technology networking protocol known as bluetooth. There are however, several hurdles that must be overcome. One of these hurdles is to provide a communication link that is mostly interference free. The design of an appropriate antenna is important in providing a good communication between devices. In this paper we present the outline of an embedded antenna using the method of moments. This work is also extended to address generally other design issues in bluetooth technology that can be addressed using computational electromagnetics. **[Vol. 15, No. 3 (2000), pp. 152-158]**

ANALYSIS AND DESIGN OF TAPERED MEANDER LINE ANTENNAS FOR MOBILE COMMUNICATIONS

Chun-Wen Paul Huang, Atef Z. Elsherbeni, and Charles E. Smith

Small printed antennas are becoming one of the most popular designs in personal wireless communications systems. In this paper, the characterization and design of a novel printed tapered meander line antenna are presented using the finite difference time domain technique. Experimental verifications are applied to ensure the effectiveness of the numerical model, and excellent agreement is found between numerical analysis and prototype measurements. A new design of this antenna features an operating frequency of 2.55 GHz with a 230 MHz bandwidth, which supports future generations of mobile communication systems. **[Vol. 15, No. 3 (2000), pp. 159-166]**

A COLE-COLE DIAGRAM REPRESENTATION OF MICROSTRIP STRUCTURE

S. Malisuwan, P. S. Neelakanta, and V. Ungvichian

A method for analyzing the performance of a microstrip line using the concept of Cole-Cole diagram is proposed. Analogous to dielectric relaxation considerations of Cole-Cole diagrams as applied to dielectric materials, a "reactive relaxation" concept is introduced to represent the frequency-dependent characteristics of a microstrip. Also, included in the algorithm are relevant considerations pertinent to the substrate dielectric and strip-line conductor losses. The dynamic permittivity of the microstrip structure (deduced via Cole-Cole diagram) leads to a convenient and modified Smith-chart representation that includes the frequency-dependent influence of the fringing field and the lossy characteristics of the line cohesively. The efficacy of the model is illustrated with an example concerning a microstrip patch antenna in ISM band. Relevant algorithms are useful in computer-aided designs (CADs). **[Vol. 15, No. 3 (2000), pp. 167-174]**

ENHANCEMENT OF NUMERICAL COMPUTATION METHODS USEFUL FOR RADIO COMMUNICATION ANTENNA SYSTEMS

H. Matzner, N. Amir, U. Mahlab, and J. Gavan

The radiation from a flanged parallel-plate waveguide is solved efficiently by the moment method, where the expansion functions contain the correct edge behavior of the fields. This computation method can be useful to optimize radiation of microwave transmitters and efficiency of receiver antenna and front-end circuits. It is shown that three appropriate expansion functions are sufficient for an excellent accuracy and convergence rate of the solution. **[Vol. 15, No. 3 (2000), pp. 175-185]**

TIME AND FREQUENCY DOMAIN WAVE PROPAGATORS

Funda Akleman and Levent Sevgi

In this paper, a new time-domain wave propagator (TDWP) that was recently introduced, is compared against a frequency-domain one that has been in use for more than a decade. The new time-domain wave propagator is built by a two-dimensional (2D) finite-difference time-domain (FDTD) algorithm. The frequency-domain wave propagator is the Split-step Parabolic Equation (SSPE), which is the solution of (one-way) wave equation in parabolic form. These two techniques can be both used for different kinds of 2D propagation problems. In this paper, ground wave problems, which are difficult to solve, have been taken into consideration in order to compare the methods and show their power. Assuming an azimuthal symmetry, ground wave propagation and surface and/or elevated ducts may be represented via transverse and/or longitudinal refractivity and boundary perturbations in 2D space. The 2D propagation space extends from x=0 (bottom) to $x \rightarrow \infty$ (top), vertically and from $z \rightarrow \infty$ (left) to $z \rightarrow \infty$ (right), horizontally. Pulse propagation is simulated in TDWP and while a moving window escorts the transmitted waveform from one end to the other end within the FDTD computation space, time histories are accumulated at chosen observation points. Any vertical and/or horizontal field profile at a desired frequency is extracted by applying off-line discrete Fourier transformation (DFT). On the other hand, a given vertical field profile is longitudinally propagated by moving back and forth between the transverse spatial and wavenumber domains in SSPE. The results of TDWP and SSPE are compared on different ducting and anti-ducting refractivity profiles and their agreement is presented. **[Vol. 15, No. 3 (2000), pp. 186-208]**

RAY-TRACING TECHNIQUES FOR MOBILE COMMUNICATIONS

O. Gutiérrez, F. Saez de Adana, I. González, J. Pérez, and M. F. Cátedra

In this paper an application for mobile communication of several ray-tracing techniques is presented. The techniques work in combination with deterministic propagation models based on GTD/UTD techniques. Several ray-tracing techniques are reviewed and some results applying one of them, the Angular Zeta Buffer (AZB) method for urban and indoor scenarios are shown, obtaining in all the cases good results comparing with measurements. **[Vol. 15, No. 3 (2000), pp. 209-231]**

ON THE FEASIBILITY OF THE MULTIPATH FINGERPRINT METHOD FOR LOCATION FINDING IN URBAN ENVIRONMENTS

Ivy Y. Kelly, Hai Deng, and Hao Ling

The feasibility of the multipath fingerprint method for wireless location finding in urban environments is examined using computational electromagnetics simulation. Fingerprints composed of time and angle of arrival data in urban environments are created using electromagnetic ray tracing. The fingerprints at specific locations within a simple four-by-four building model are studied to address issues including uniqueness of the fingerprints, repeatability due to environmental changes, and bandwidth limitations. A classifier based on template matching is also constructed using the simulation data from a 1-km city area of downtown Austin, Texas. Angle of Arrival (AOA) is found to be a stronger identifier than Time of Arrival (TOA). The classifier results demonstrate that good location-finding performance is achievable using both time of arrival and angle of arrival features. **[Vol. 15, No. 3 (2000), pp. 232-247]**

NEW DESIGNS FOR DUAL BAND ANTENNAS FOR SATELLITE MOBILE COMMUNICATIONS HANDSETS

S. M. Daddish, R. A. Abd-Alhameed, and P.S. Excell

The design of dual-band antennas for hand-held terminals (HHT) to be used in personal communications via a satellite network (SPCN) is investigated. The quadrifilar helical antenna (QHA) is selected as the optimum design for further study and a new design for a QHA is derived and optimized using a standard Moment-Method program. A dual L-S band design with an input VSWR in its two operating bands of between 1 and 2 was developed, incorporating external shorted turns to achieve the desired passbands. The design of the required hybrid feed phasing network is derived. Experiments with physical realizations of the optimum designs showed good performance and confirmed the computational predictions. **[Vol. 15, No. 3 (2000), pp. 248-258]**

VIEWS OF THE 2001 ACES ANNUAL REVIEW OF PROGRESS

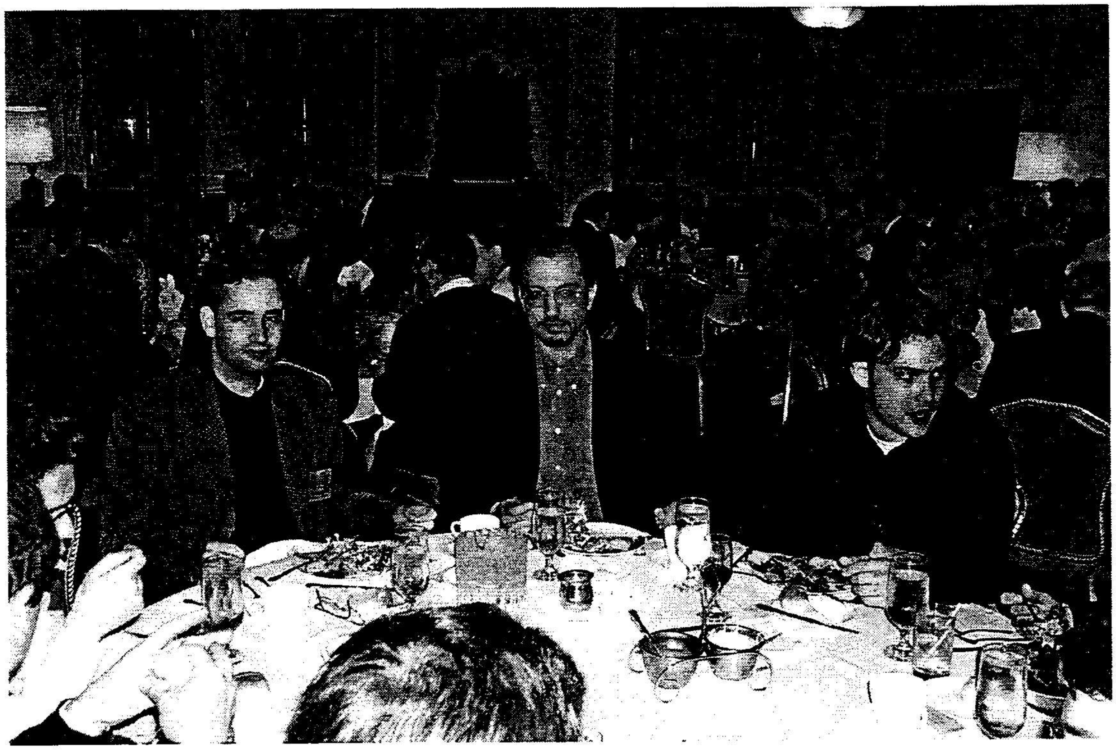

Costas Sarris, Manos Tentzeris, and Nathan Bushyager

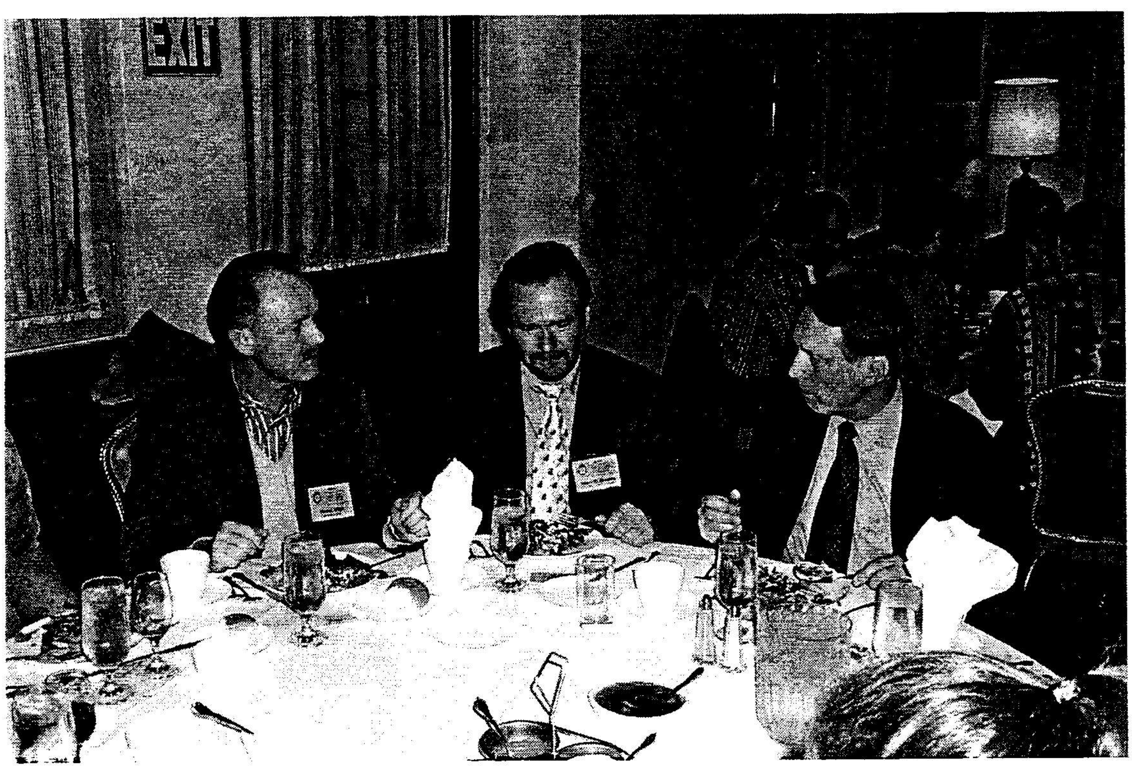

Heinz Wipf, Heinz Bruens, Herman Singer

VIEWS OF THE 2001 ACES ANNUAL REVIEW OF PROGRESS

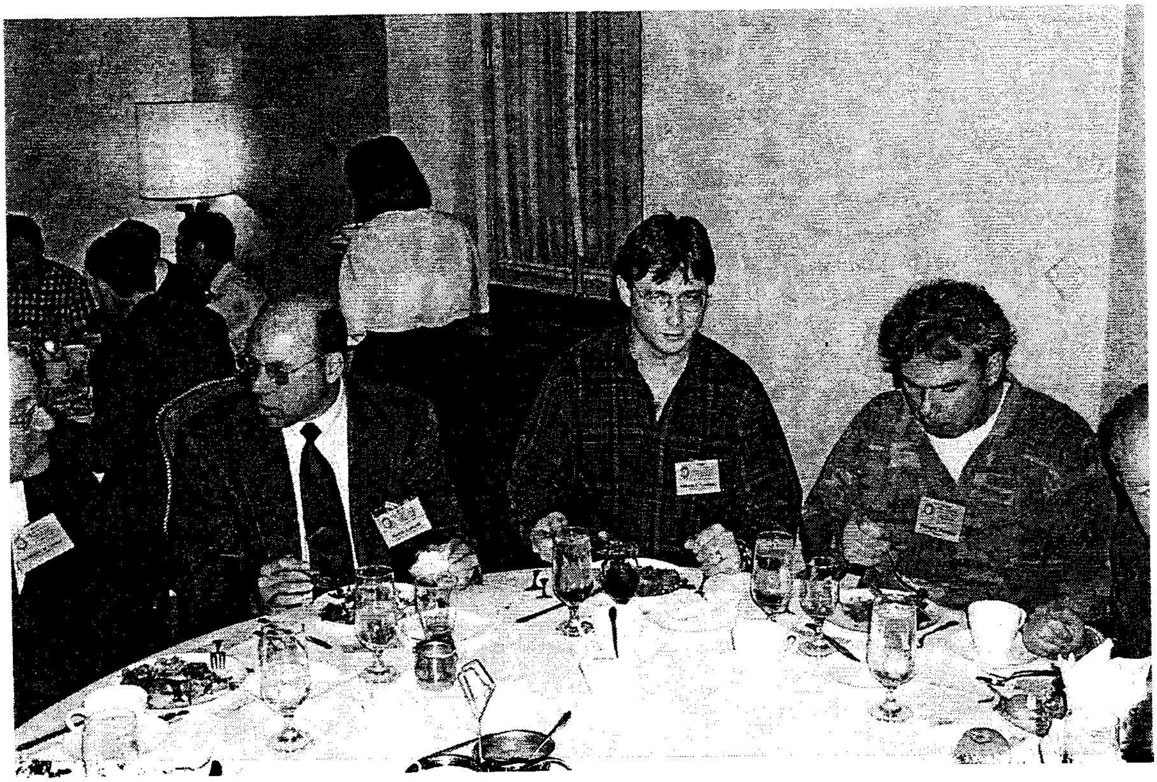

Keith Lysiak, Francis Lenning, Peter Rimbey

Pamela Markland, Christopher Trueman, Keith Lysiak

VIEWS OF THE 2001 ACES ANNUAL REVIEW OF PROGRESS

Allen Glisson, Thereza MacNamara, Perry Wheless

Ahmed Kishk, Masanori Koshiba, Atef Elsherbeni

VIEWS OF THE 2001 ACES ANNUAL REVIEW OF PROGRESS

Francisco Cabrera, Lynn and Alan Nott

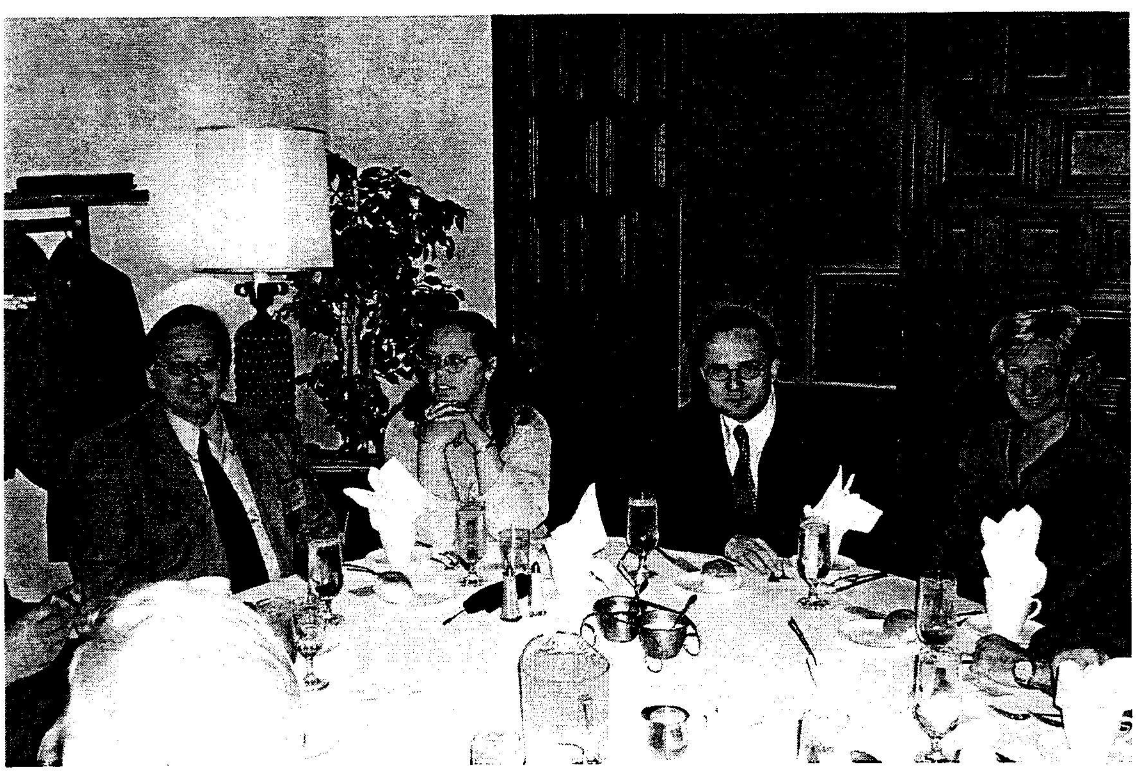

Andrew and Barbara Drozd, Jose Antonio and Lourdes Marcotegui

VIEWS OF THE 2001 ACES ANNUAL REVIEW OF PROGRESS

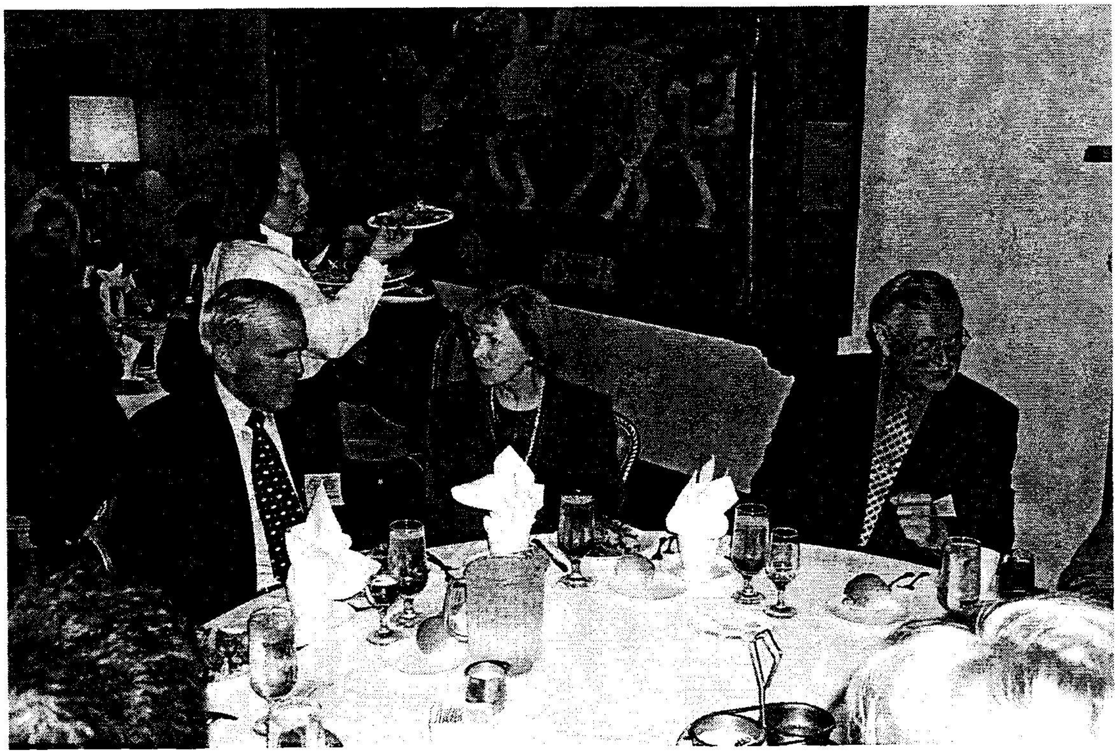

Gerald Burke, Lily and Stan Kubina

Ping Werner, Matt Bray, Mark Gingrich

VIEWS OF THE 2001 ACES ANNUAL REVIEW OF PROGRESS

Vladimir Machavariani, Rene Allard, Alkim Akyurtlu

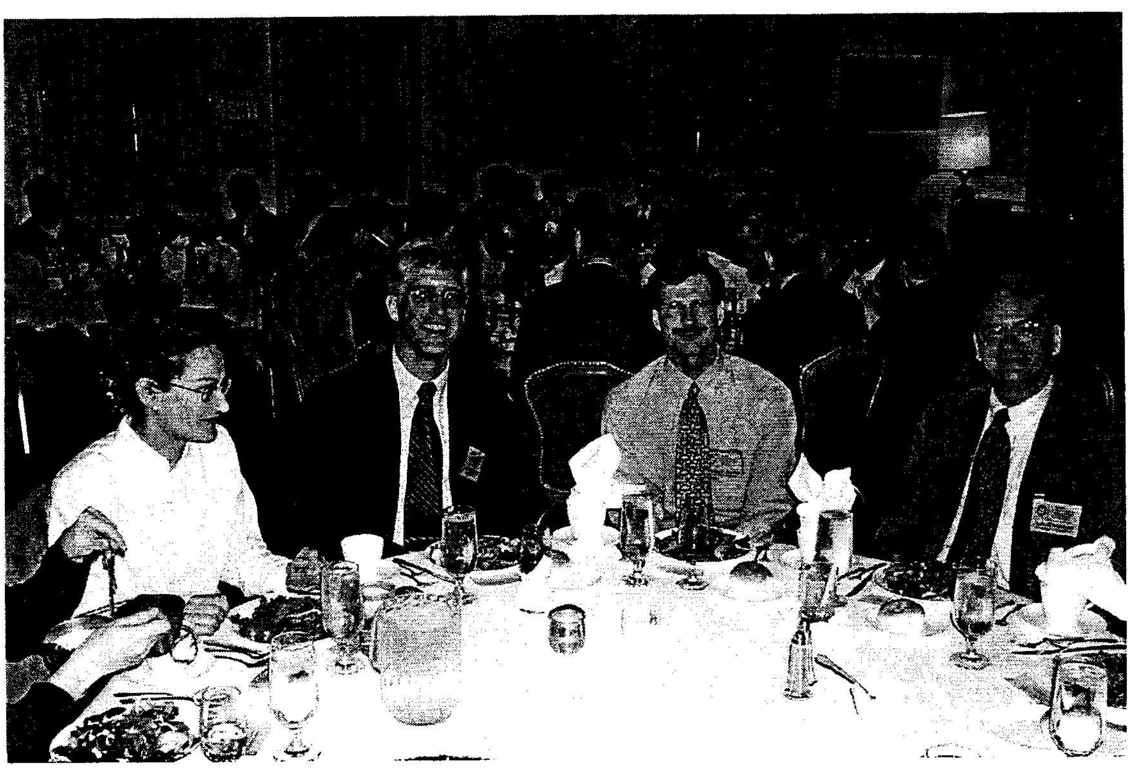

Amelia Bretones, Randy Haupt, Doug Werner, Leo Kempel

VIEWS OF THE 2001 ACES ANNUAL REVIEW OF PROGRESS

Jim, Jimmy and Aida Breakall

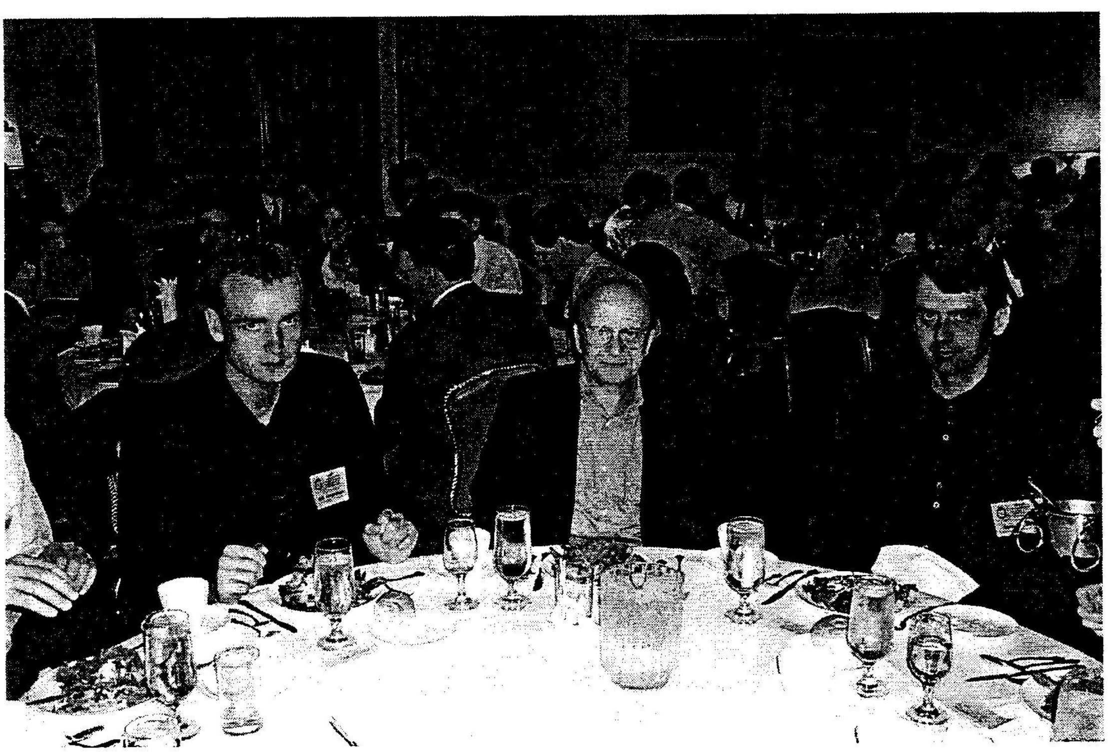

Erik Jorgensen, John Asvestas, Ione Lager

VIEWS OF THE 2001 ACES ANNUAL REVIEW OF PROGRESS

Thadeus Owoc, Bo Wastberg, Tomas Boman, Erik Jorgensen

Michael and Linda McKaughan, Pat and Dick Adler

VIEWS OF THE 2001 ACES ANNUAL REVIEW OF PROGRESS

John Shaeffer, Hal Buscher

James Cole, Tamami Maruyama, Michiko Kuroda

VIEWS OF THE 2001 ACES ANNUAL REVIEW OF PROGRESS

Ross Speciale, Margaret and Steve Inge

Richard Miller, Jeffrey Miller, Eliot Lebsack

VIEWS OF THE 2001 ACES ANNUAL REVIEW OF PROGRESS

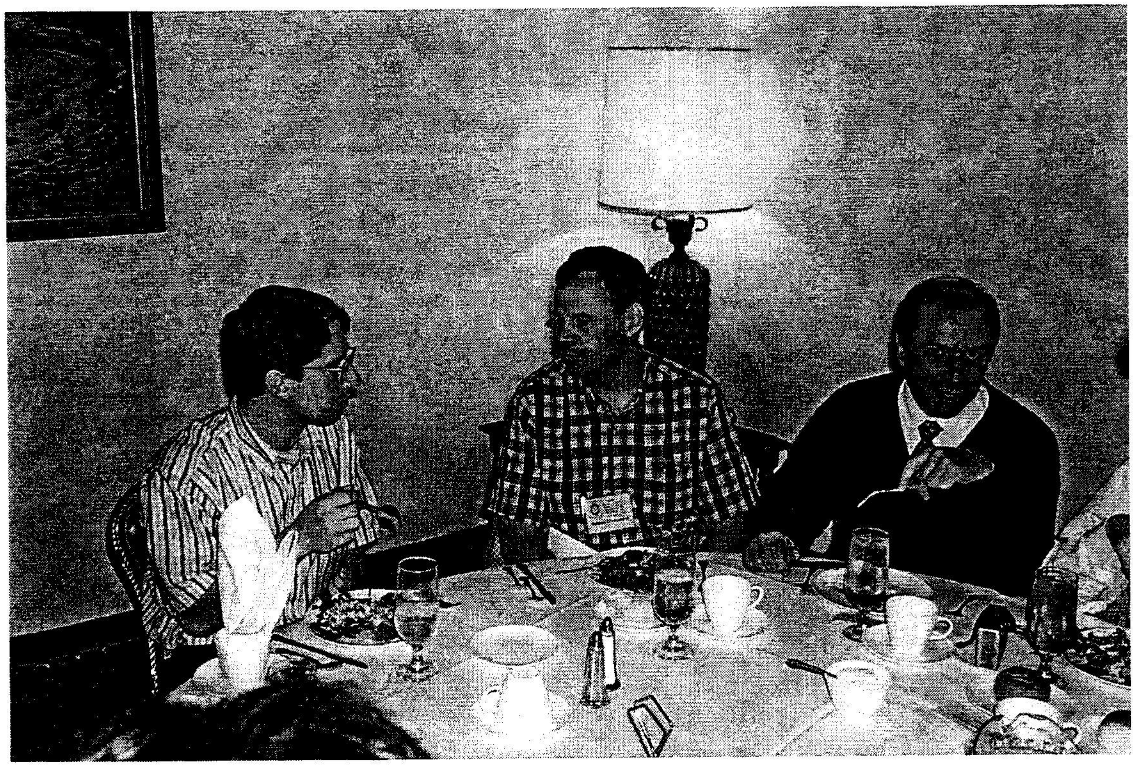

Darin Fowers, Nathan Champagne, Jean-Pierre Estienne

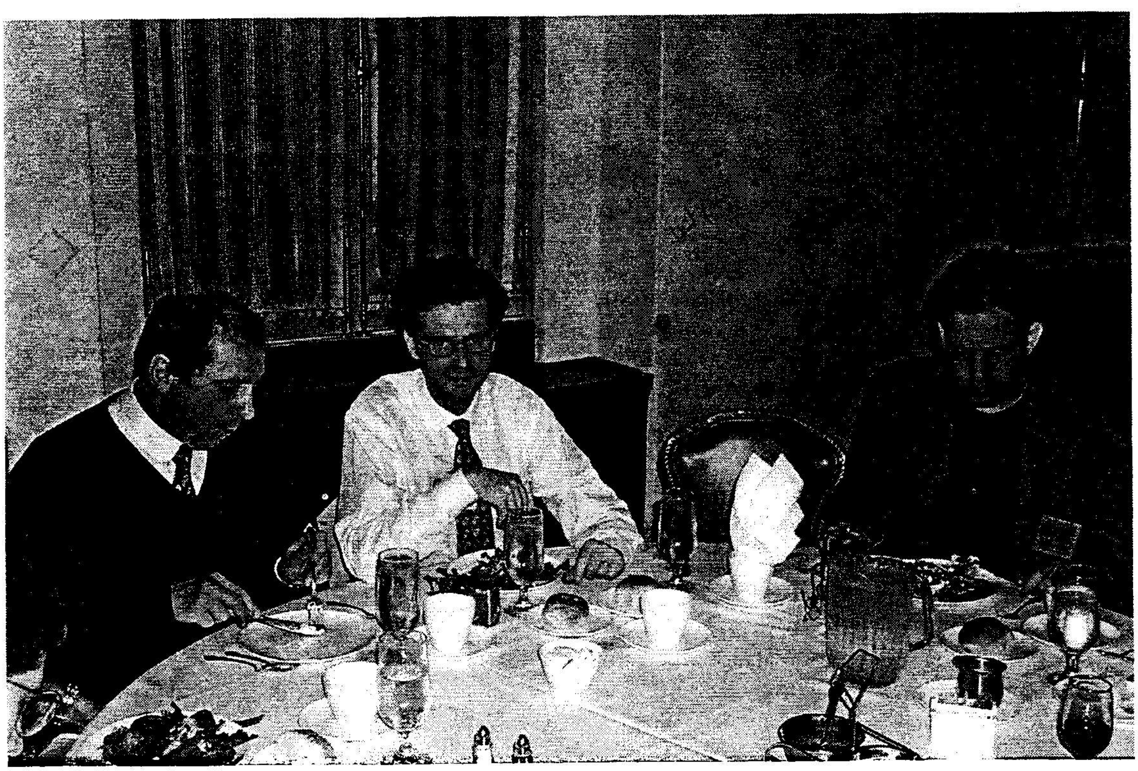

Jean-Pierre Estienne, Amaury Soubeyran, Costas Sarris

VIEWS OF THE 2001 ACES ANNUAL REVIEW OF PROGRESS

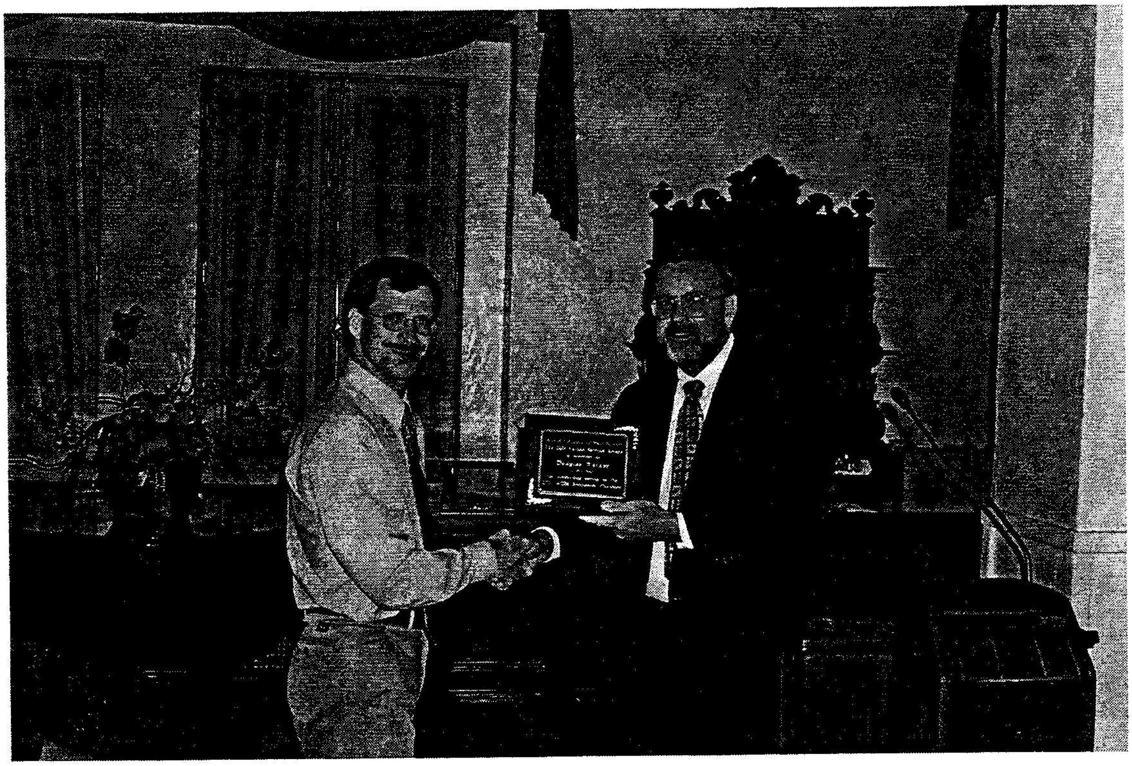

Doug Werner accepting the Valued Service Award from W. Perry Wheless, Jr.

Andrew Drozd accepting the 2001 Exemplary Service Award for continuous service as Newsletter Editor for theTechnical Feature Article

VIEWS OF THE 2001 ACES ANNUAL REVIEW OF PROGRESS

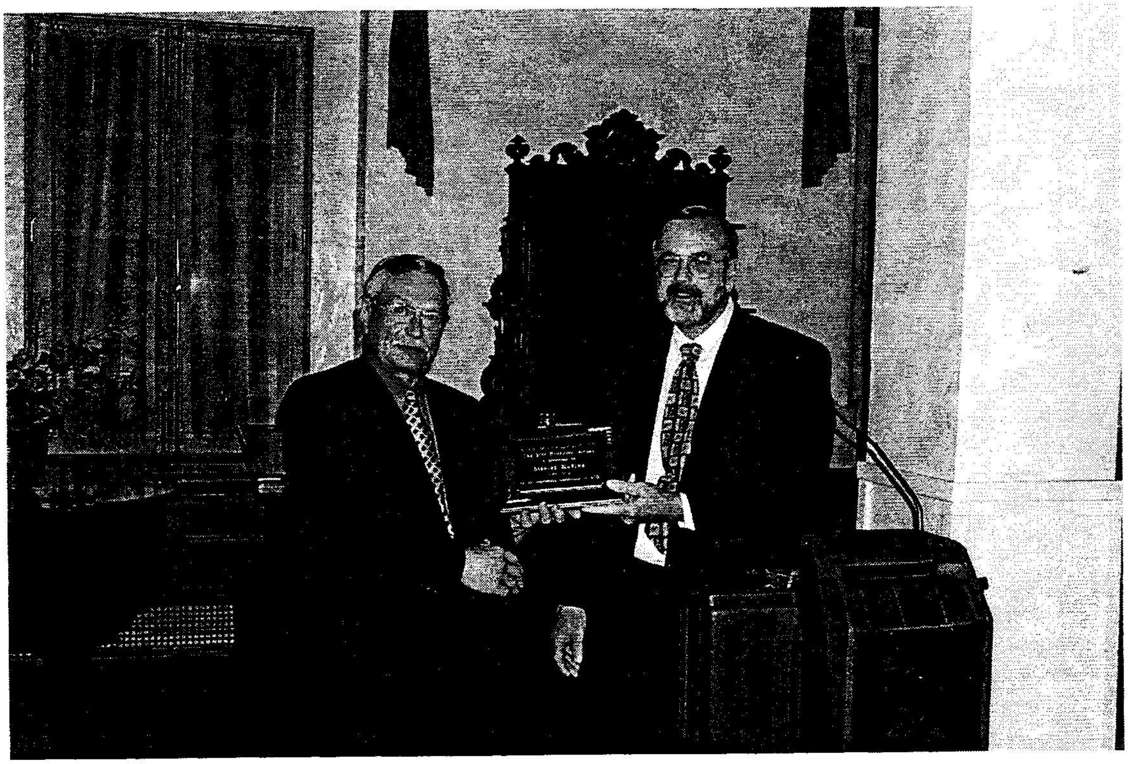

Stan Kubina accepting the 2001 Founder's Award for his long standing contributions to ACES.

Atef Elsherbeni accepting the 2001 Exemplary Service Award for leadership and contributions as Electronic Publications Managing Editor for 1999-2001

VIEWS OF THE 2001 ACES ANNUAL REVIEW OF PROGRESS

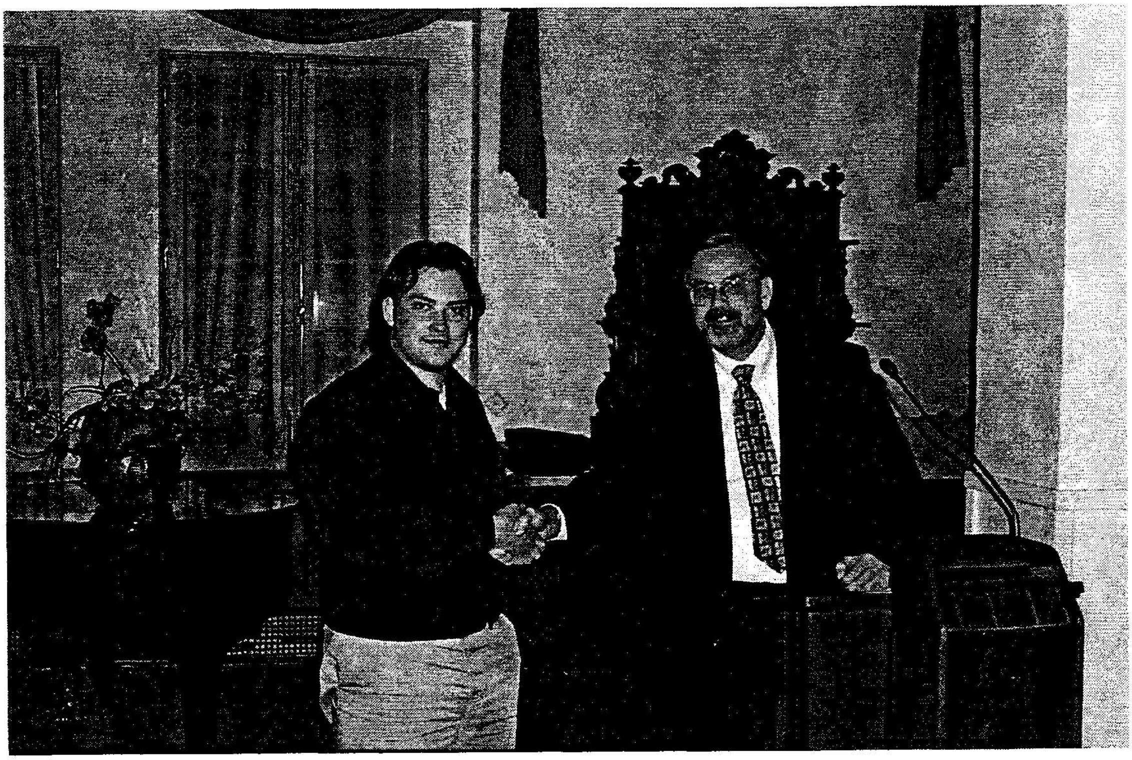

Nathan Bushyager accepting the Best Student Paper Award

OTHER AWARDS PRESENTED

(Not presented at the Awards Banquet]

2001 Founders Award presented to Robert Bevensee for long standing and steadfast support of ACES.

Winner of the ACES Conference (March 2001) Best Paper Award is Alfred R. Lopez of BAE Systems, NY. His paper is titled "Differential GPS Ground Reference Antenna for Aircraft Precision Approach Operations -- WIPL Design". This award includes a prize of $500.00

CALL FOR PAPERS

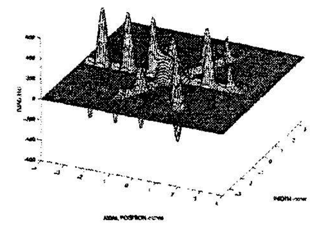

THE APPLIED COMPUTATIONAL ELECTROMAGNETICS SOCIETY

The 18TH Annual Review of Progress in Applied Computational Electromagnetics

March 18 - 22, 2002

Naval Postgraduate School, Monterey, California

Classical electromagnetic field theory is already a mature branch of Theoretical Physics. Quite to the contrary, the relatively new engineering discipline of Applied Computational Electromagnetics (CEM) is a very dynamic and evolving field. Indeed, research in CEM is continuously generating practical and efficient new solutions for the analysis, design, development and measurement problems posed by increasingly complex systems. The pace of evolution in applied computational electromagnetics is monotonically escalating, driven by the ever-increasing and unrelenting requirements of new applications in such fields as global *EM* communications, radar, remote sensing, high-power microwaves *(HPM)*, high-speed computers, and large-scale nuclear physics facilities.

The annual *ACES* Symposium has been also continuously evolving from its rather modest origins, and is now recognized as the most influential and authoritative international forum in the field of CEM, where leading scientists and engineers convene annually to present the results of their most recent research efforts, and to share those results with their peers worldwide.

The annual *ACES* Symposium combines high scientific level and practical engineering emphasis to present a review of the most recent developments. International participation by non-members is welcome and strongly encouraged. The annual *ACES* Symposium is indeed *the premier* forum where the dynamic, vibrant progress in Applied Computational Electromagnetics is extensively reviewed, reported, and documented for archival reference.

The following matrix of hot topics, applications, methods and computational tools is merely intended to exemplify the extent of ACES interests by listing some of the most popular session subjects:

Typical Hot Topics	Applications	Methods	Computational Tools
Fast Hybrid Methods	Antennas	FDFD	New Codes or Languages
Modal Expansions	Phased Arrays	FEFD	New Computers/WorkStations
Domain Decomposition Methods	Adaptive Arrays	FDTD	High-Speed Computer Clusters
Symmetry Analysis & Applications	Beam Forming Networks	FETD	Graphic Domain-Definition
High Performance Computing	Radar Tracking	Modal Expansions	Output Data Post-Processing
Unstructured Meshes	Radar Imaging	TLM/Wavelets	Parallel Processing
Multiple Parallel Processors	Radar cross section	Symplectic Integr.	Diff. Equation Techniques
Large Scale Microwave Structures	Microwave components	Diakoptics	Moment Methods
Generalized Scattering Matrix *(GSM)*	Communications systems	GTD	Object-Oriented Programming
Multi-Mode Analysis	Satellite Communications	Physical Optics	Visualizations
Inverse Scattering	Wireless Communications	Integral Eqns.	Virtual Reality in Elec. Mag.
Non-Commutative Symbolic Comp.	High Power Sources	EFIE/MFIE	Differential Algebra
High Power Microwave Sources	Particle Accelerators	Perturb. methods	Inv. of Structured Matrices
MIMIC Interconnect Technologies	Fiber Optics	Hybrid methods	Code Validation
Susceptibility & Survivability	Bio-Electromagnetics	Numerical Optim.	High Order Taylor Maps

SYMPOSIUM STRUCTURE: The annual ACES Symposium traditionally takes place during the third week of March, and includes, in addition to formal sessions for oral presentation of submitted papers: (1) a poster session, (2) a student paper competition, (3) numerous short courses (both *full-day* and *half-day*), (4) an awards banquet, (5) vendor exhibits, and (6) a wine and cheese social. The ACES Symposium also includes three Plenary Sessions, where illustrious invited speakers deliver original essay-like reviews of hot topics of their own choice.

EARLY REGISTRATION FEES

(for registration prior to March 1, 2002)

ACES member	$310	Student/Retired/Unemployed	$130 (no proceedings)
Non-member	$365	Student/Retired/Unemployed	$165 (includes proceedings)

Each conference registrant is entitled to publish two papers in the proceedings free of charge. Excess pages over the limit of eight (8) pages for each paper will be charged $25/page.

INSTRUCTIONS FOR AUTHORS

PAPER FORMATTING REQUIREMENTS

The recommended paper length is 6 pages, with 8 pages as a free maximum, including figures. The paper should be camera-ready (good resolution, clearly readable when later photo-reduced to the final proceedings format of 6x9-inch paper). The submitted papers should be formatted for printing on 8.5x11-inch U.S. standard paper, with 13/16 inch side margins, 1-1/16 inch top margin, and 1 inch margin at the bottom. On the first page, the title should be 1-1/2 inches from top with authors, affiliations, and e-mail addresses beneath the title. Use single line spacing, with 10-12 point font size. The entire text should be fully justified (flush left and flush right). No typed page numbers, but sequential page numbers must be inserted as *non printing Acrobat Annotations*. Electronic submission of full photo-ready finished papers is required, in Acrobat 4.0 or 5.0 format only (*.pdf). **Acrobat job options specifications and further crucial technical details are posted on the ACES Web Site at: http://aces.ee.olemiss.edu.** All papers must strictly conform at the time of submission to the detailed electronic format specifications described on the ACES Web Site.

SUBMISSION DEADLINE

Submission deadline is **November 16, 2001.** The signed ACES copyright-transfer form, and a payment covering the registration for at least the corresponding author must be provided at the time of paper submission. Authors of rejected papers, who choose not to attend the conference, will receive a refund of their registration fee.

Authors will be notified of acceptance on or about December 15, 2001.

$500 BEST-PAPER PRIZE

A $500 prize will be awarded to the authors of the best non-student paper accepted for the *18^{TH} Annual Review.*
Papers will be judged by a special ACES prize-paper committee, considering the following criteria:

1. EM/CEM theory and technical content correctness.
2. Reliable data.
3. Computational EM component and results.
4. Practical applications value.
5. Estimates of computational errors.
6. Significant new conclusions.

$300 BEST STUDENT PAPER CONTEST

This will be for the best student paper accepted for the *18^{TH} Annual Review.* Student presentation at conference is required. Submissions will be judged by three (3) members of the ACES Board of Directors. Prizes for the best student paper include: (1) one free *Annual Review* registration for the following year; (2) one full-day, or two half-day, free short course(s) taken during the 2002 or 2003 *Annual Review,* and (3) $300 cash.

Ross A. Speciale - Technical Program Chairman

Tel: (310) 375-1287

Fax: (714) 374-9826

E-mail: rspeciale@socal.rr.com

Personal Home Page: http://66.12.125.34/dr-ross.asp

ACES Web Site: http://aces.ee.olemiss.edu

2002 ACES Symposium Sponsored by: ACES, Naval Postgraduate School, Pennsylvania State University, University of Mississippi, Michigan State University, and South West Research Institute, in cooperation with: The IEEE Antennas and Propagation Society, The IEEE Electromagnetic Compatibility Society, and the United States National Committee of URSI.

Technical Program Chair
Ross A. Speciale

Symposium Co-Chairs
Leo C. Kempel
Michigan State University
Andrew F. Peterson
Georgia Institute of Technology

Electronic Publication Chair
Atef Elsherbeni
University of Mississippi

Symposium Administrator
Richard W. Adler
Naval Postgraduate School

Short Course Chair
John Schaeffer
Marietta Scientific

Publicity Chair
Keith A. Lysiak
Southwest Research Institute

APPLIED COMPUTATIONAL ELECTROMAGNETICS SOCIETY
RICHARD W. ADLER, EXECUTIVE OFFICER, ECE DEPARTMENT, CODE ECAB, NAVAL POSTGRADUATE SCHOOL, 833 DYER ROAD, RM 437, MONTEREY, CA 93943-5121, PHONE: 831-646-1111 FAX: 831-649-0300 EMAIL: RWA@ATTGLOBAL.NET

please print

LAST NAME FIRST NAME MIDDLE INITIAL

COMPANY/ORGANIZATION/UNIVERSITY DEPARTMENT/MAIL STATION
(PLEASE LIST THE ADDRESS YOU WANT USED FOR PUBLICATIONS BELOW)

MAILING ADDRESS

CITY PROVINCE/STATE COUNTRY ZIP/POSTAL CODE

TELEPHONE FAX AMATEUR RADIO CALL SIGN

E-MAIL ADDRESS E-MAIL ADDRESS CAN BE INCLUDED IN ACES DATABASE YES ☐ NO ☐
PERMISSION IS GRANTED TO HAVE MY NAME PLACED ON MAILING LISTS WHICH MAY BE SOLD YES ☐ NO ☐

CURRENT SUBSCRIPTION PRICES

AREA	INDIVIDUAL SURFACE MAIL	INDIVIDUAL AIRMAIL	ORGANIZATIONAL (AIRMAIL ONLY)
U.S., CANADA, MEXICO	( ) $60	( ) $60	( ) $110
W. EUROPE, ISRAEL, SCANDINAVIA, GREECE	( ) $63	( ) $73	( ) $110
ASIA, AFRICA, MIDDLE EAST, PACIFIC RIM, FORMER USSR, E EUROPE, BALKANS, CENTRAL & SO. AMERICA, TURKEY	( ) $63	( ) $80	( ) $110

FULL-TIME STUDENT/RETIRED/UNEMPLOYED RATE IS $25 FOR ALL COUNTRIES

Non-USA participants: Prices are in U.S. dollars. All currencies must be converted to U.S. dollars payable by banks with U.S. affiliates. (1) Bank Checks, must have U.S. address of bank; (2) Traveler's Checks (in U.S. $$); (3) U.S./International Money Order drawn in U.S. funds, payable in U.S., (4) Credit Cards: Visa, MasterCard, Amex and Discover.

PAYMENT METHOD: ALL CHECKS/TRAVELER'S CHECKS/MONEY ORDERS ARE PAYABLE TO "ACES"

☐ CHECK (PAYABLE TO ACES) ☐ TRAVELER'S CHECKS ☐ INTERNATIONAL MONEY ORDER

☐ CREDIT CARD ☐ VISA ☐ MASTERCARD ☐ AMEX ☐ DISCOVER

CREDIT CARD USERS

SIGNATURE AND ADDRESS OF CARD HOLDER IS MANDATORY.

IF YOU ARE PAYING VIA ANOTHER PERSONS CARD, HE/SHE MUST PRINT AND SIGN NAME AND ADDRESS.

PRINT CARD HOLDER NAME: ____________________

CREDIT CARD HOLDER SIGNATURE: ____________________

CREDIT CARD EXPIRATION DATE: ____/____

CREDIT CARD HOLDER ADDRESS: ____________________

CREDIT CARD ACCOUNT # ☐☐☐☐☐☐☐☐☐☐☐☐☐☐☐☐ 2001

ADVERTISING RATES

	FEE	PRINTED SIZE
Full page	$200.	7.5" x 10.0"
1/2 page	$100.	7.5" x 4.7" or 3.5" x 10.0"
1/4 page	$ 50	3.5" x 4.7"

All ads must be camera ready copy.

Ad deadlines are same as Newsletter copy deadlines.

Place ads with Ray Perez, Newsletter Editor, Martin Marietta Astronautics, MS 58700, PO Box 179, Denver, CO 80201, USA. The editor reserves the right to reject ads.

DEADLINE FOR THE SUBMISSION OF ARTICLES

Issue	Copy Deadline
March	January 13
July	May 25
November	September 25

For the ***ACES NEWSLETTER*** send copy to Bruce Archambeault in the following formats:

1. A hardcopy.
2. Camera-ready hardcopy of any figures.
3. If possible also send the full document; if not, send the text on a floppy disk. We can read any version of MICROSOFT WORD, PageMaker and PDF files on IBM disks. On IBM disks we can also read LATEX files but contact us first concerning the LATEX version. If any software other than MICROSOFT WORD has been used, contact the Managing Editor, Richard W. Adler **before** submitting a diskette.